Mathematical modelling of transmission dynamics of *Opisthorchis viverrini*

Inauguraldissertation

zur

Erlangung der Würde eines Doktors der Philosophie

vorgelegt der

Philosophisch-Naturwissenschaftlichen Fakultät

der Universität Basel

von

Christine Bürli

aus

Grosswangen LU

2021

Originaldokument gespeichert auf dem Dokumentenserver der Universität Basel

edoc.unibas.ch

Genehmigt von der Philosophisch-Naturwissenschaftlichen Fakultät auf Antrag von

Prof. Dr. Helmut Harbrecht (Fakultätsverantwortlicher)

PD Dr. Nakul Chitnis (Dissertationsleiter)

Prof. Dr. Roy Anderson (Korreferent)

Basel, den 17. September 2019

Prof. Dr. Martin Spiess

Contents

1. Abstract

The trematode liver fluke, *Opisthorchis viverrini*, is endemic in Thailand, Lao People's Democratic Republic (Lao PDR) and Cambodia. Its life cycle involves humans, dogs and cats as definitive hosts; and snails and fish as intermediate hosts. Humans get infected through the consumption of raw or undercooked fish. A severe infection of *O. viverrini* can lead to cholangiocarcinoma, a mostly fatal bile duct cancer. Control activities include treatment of humans and domestic pets, health education on food consumption and improved sanitation. Mathematical modelling can help us to understand this multi-host disease system, identify weak points in the transmission cycle and determine the effectiveness of combinations of interventions to provide rational advice for the planning of control activities.

Analysis and simulation of a series of mathematical models, ranging from deterministic ordinary differential equations models to stochastic individual-based models, calibrated to data from two islands in the Mekong river in Lao PDR, suggest that (i) mass drug administration is necessary for elimination of *O. viverrini* to be achieved as quickly as possible; (ii) sustainable education campaigns are as important as mass drug administration; and (iii) it is unlikely that cats and dogs are necessary for transmission to persist.

2. Acknowledgements

This dissertation would not have been possible with all the people being part of my life for the last few years. Firstly, my thanks goes to my two supervisors Nakul Chitnis and Helmut Harbrecht. Thank you for the support and believing in me, the advices and feedbacks you always had ready for me to bring me further and all the other things I could learn from the two of you. Besides my supervisors I thank Peter Odermatt for introducing my to the fascinating world of parasitology and Somphou Sayasone for showing me his beautiful country, and to both of you for answering all my question concerning biology or Laos. My thank goes to the Swiss National Science Foundations for funding this project and so giving me the opportunity to write this dissertation. Another thank goes to all my colleagues and friends from the infectious Disease Modelling Unit for being part of my time at the Swiss Tropical and Public Health Institute. Especially thank you Mirjam Laager for all the discussion and the feedback and Tamsin Lee for proofreading part of my thesis. Finally my thank goes to my family and my husband for supporting and encouraging me to do this PhD. Thank you

3. Contribution

Chapters 5 and 6 are based on the publication [38], where I contributed the section 'Opportunities and challenges for mathematical disease modelling of transmission dynamics'. Chapter 8 is based on the publication [19] while Chapter 9 is based on the publication [18]. Chapter 10 is based on the submitted paper [15]. Chapter 11 is already in preparation as a paper [16]. Chapters 12 and 13 are the basis for a paper [17].

We derive all the definitions in the thesis by explicit calculations using Mathematica 10.0.2. The numerical calculations were performed in Matlab R2017a or at sciCORE (http://scicore.unibas.ch) scientific computing center at University of Basel using Matlab R2016a.

4. Abbreviations

CASCAP	cholangiocarcinoma screening and care program
CCA	cholangiocarcinoma
DALYs	disability-adjusted life years
EPG	eggs per gram
FBT	food-borne trematode
Lao PDR	Lao People's Democratic Republic
MDA	mass drug administration
MLE	maximum likelihood estimation
NTD	neglected tropical disease
ODE	ordinary differential equation
PDE	partial differential equation
PRCC	partial rank correlation coefficient
WHO	World Health Organization

5. Introduction

The liver fluke *Opisthorchis viverrini* belongs to the food-borne trematodes (FBT) and is endemic in South East Asia where it is a public health issue. *O. viverrini* is transmitted through consumption of raw or undercooked fish. The transmission is further promoted when there is inadequate sanitation and outdoor defecation [57]. Besides humans, the definitive hosts of *O. viverrini* are dogs and cats. The intermediate hosts are *Bythnia* snails and fish in the Cyprinidae family [54].

5.1 Mathematical modelling of disease transmission dynamics

Reducing the prevalence and burden of food-borne trematodiases requires rational planning of interventions. Mathematical modelling and analysis is well placed to clarify parasite transmission dynamics, and compare the effectiveness of different control strategies. Mathematical models have been useful in planning for the control and elimination of many diseases, from providing qualitative inputs on how best to interrupt disease life cycles [92, 106] and determining optimal vaccination strategies [46], to providing quantitative predictions to disease eradication programmes [44].

To date, besides this work on modelling the transmission dynamics of *O. viverrini*, only one other model of FBT transmission dynamics exists. A two stage catalytic (linear ordinary differential equation with constant coefficients) model of *Clonorchis sinensis* is used to estimate the egg positive rate from age prevalence data [107]. However, there are models which focus on the environmental aspect of the life cycle of *O. viverrini* for example a spatial model, including water flow, to investigate environmental drivers of transmission [67]. Another example is that of Partumchart *et al.* [86] which simulates the distribution of *Bythnia* snails in Thailand to predict the occurrence of snails and link it to the prevalence of Opisthorchiasis .

The development of these first disease transmission models largely followed earlier efforts on schistosomiasis, a related trematodiasis. Schistosomes have a similar life cycle as *O. viverrini*, but do not have the additional stage in secondary aquatic hosts. Therefore, by adding state variables for the secondary hosts, schistosomiasis models could be expanded to models of other FBT transmission dynamics. As such, the following is a brief overview of relevant schisosomiasis models from the past fourty years: extensions of population-based models which include schistosome larval population dynamics [133], the latent period in snails [133, 6], snail population dynamics [133], heterogeneity in human exposure [133, 6, 132, 131], human age structure [47, 129, 130], acquired immunity in

humans [6, 130], the existence of reservoir mammalian hosts [133, 47, 129, 2], and the effects of control interventions [47, 129, 134]; a model with age-structure for schistosomiasis which simulates different treatment strategies with mass drug administration (MDA) to determine which age group should be targeted

Of note, in general, macroparasite mean-burden models, such as those based on Nåsell and Hirsch [79], are more appropriate than prevalence-based models for human FBT infection because, unlike microparasites, trematodes cannot reproduce within humans. Consequently, morbidity effects and onward infection to snails is strongly dependent on the intensity of infection within each human. However, the main drawback of these models is that they do not include prevalence of infection in humans, and additional sets of assumptions are required to estimate prevalence from model outputs on intensity of infection. These models have ignored dependence of worm burden in humans and human age, which affects the impact of age-specific interventions, such as the intermittent treatment of school children, and potential biases caused by MDA campaigns achieving lower coverage in working age adults.

Different studies on age-related patterns in *O. viverrini* infection show that the mean worm burden and the prevalence is the lowest in young children (< 5 years). From here, all studies show an increase in prevalence as children became school-age. Some studies show a decrease in the elderly age group, which is common in helminth infections [115]. Additionally, these models are inappropriate for evaluating the effectiveness of strategies that selectively target infected populations.

Individual-based models may overcome these problems because they can track the number of worms in each person at each time, thereby simultaneously capturing infection intensities and prevalences. However, they are difficult to analyse mathematically and, unlike simpler population-based models, less frequently provide deeper insights into disease transmission. Individual-based models also contain more parameters and require more comprehensive data sets for model calibration.

Prevalence-based susceptible-infected dynamics, as currently used in schistosomiasis snail infection models, could also be applied to model FBT snail infections. Essential model adaptations would have to consider infection of secondary aquatic hosts and the force of infection from these secondary hosts to human and other animal hosts. Extensions to capture more details of the secondary hosts could include (seasonal) population dynamics, a latent period of the parasites, and the relationship between parasite infection and likelihood of being eaten by humans or animals. Similar models would then need to be developed to also include infection in paratenic, reservoir, and definitive animal hosts. However, at the moment, the very limited data available is probably still the biggest challenge for mathematically modelling FBT, and thus *O. viverrini*.

5.2 Aims and objectives

The goal of this thesis is to understand which factors have the most influence on the life cycle of *O. viverrini*, and compare the effectiveness of intervention strategies in reducing parasite burden. The specific aims are

- **to identify the role of reservoir hosts**,
- **to determine the weakest point in the life cycle of *O. viverrini***, and
- **to see the effect of different intervention strategies**.

We created four population-based models and an individual based model of *O. viverrini*, calibrated to data from Lao People's Democratic Republic (Lao PDR), descpribed in Chapter 7. (i) The first population-based model (basic model) is a simple one, (ii) the second one (model with reservoir hosts) is used to determine the role of reservoir hosts in maintaining transmission, (iii) the third one (model with intervention) enables to define the optimal combination of interventions and (iv) the fourth one (model depending on age) allows to analyse the worm burden depending on age. The individual-based model simulates the worm burden in humans individually and is used to measure mortality.

In Chapter 8, the model simulates the mean worm burden of *O. viverrini* in the definitive hosts (humans and the reservoir hosts, dogs and cats) and the prevalence in the intermediate hosts (snails and fish). There are few geographical regions with comprehensive data on infection prevalence in all intermediate and definitive hosts that allow for these more detailed models. We calibrate the model with the available data from Lao PDR. The only unknown parameters are the infection rate of a parasite from one host to the next. These parameters have to be calibrated with help of the data. We use a Bayesian sampling resampling approach and maximum likelihood estimation. We calculate the basic reproduction number and perform sensitivity analysis, determining the sensitivity index and the Partial Rank Correlation Coefficient (PRCC), on this crucial indicator to identify weak points in the parasite's life cycle for the first model. We also calculate the steady state of the mean worm burden in humans, and identify potential targets for interventions to reduce parasite burden in humans. To analyse the importance of the reservoir hosts, host-specific reproduction numbers were computed, which describe whether those hosts can sustain transmission or not [80]. The analysis suggests that it is likely that humans can maintain transmission, and interventions only targeted at humans could interrupt transmission of the parasite in this part of Lao PDR.

In Chapter 9, the model includes three different interventions. The first intervention is the use of education campaigns to change people's eating habits so that they stop eating raw or undercooked fish, which reduces new infections in humans. The second one is improved sanitation, which prevents outdoor defecation. We assume that this intervention is perfect, that means no egg is able to reach the environment and be ingested

by snails when people are using the latrine. The last intervention is treatment. We look at the coverage levels of people that need to be treated, with the assumption that the drugs are completely efficacious. We are also interested in the optimal frequency of drug distribution. The optimal coverage of each intervention has been defined to reach the goal of elimination as a public health problem of *O. viverrini* within 20 years [141].

In Chapter 10, age-dependency in the worm burden of humans is included. We develop two new model extensions, presenting a partial differential equation (PDE) model of the age-specific worm burden of the human population, assuming continuous age, and an age-structured ordinary differential equation (ODE) model, which assumes discrete age groups. We use these models to (i) define the basic reproduction number, which provides a threshold condition for the persistence of transmission, (ii) evaluate the steady state solution of the system with a fixed point iteration, and (iii) estimate model parameters using data from Lao PDR. We built different scenarios of MDA campaigns to compare their effectiveness in reducing the mean worm burden in humans when targeting different age groups.

In Chapter 11, we created an individual-based model. It simulates the individual worm burden in humans depending on their characteristics such as sex, age and eating habits. The worm burden of the reservoir hosts is modelled as a pool of worms, and the intermediate hosts are distributed into a susceptible and an infected group. This model lays the basis for individual-based models of *O. viverrini*. We are now able to capture the heterogeneity. The individual modelling of the worm burden allows to measure morbidity and mortality. We implement different interventions strategies to determine the effect on mortality.

6. Epidemiology and burden

Opisthochris viverrini belongs to the food-borne trematodiases, which are some of the most neglected of the so-called neglected tropical diseases. They are caused by digenetic trematodes, which live in the biliary duct of their host animal [54]. Food-borne trematodes (FBT) are transmitted to humans via the ingestion of contaminated food. Depending on their target organ in the definitive host, FBT are also called liver, lung, or intestinal flukes [35, 36]. Only some FBT species are considered to be of public health relevance, among the liver flukes these are *Clonorchis sinensis*, *Fasciola gigantica*, *Fasciola hepatica*, *Opisthorchis felineus* and *Opisthorchis viverrini*; among the other FBT, the lung flukes are *Paragonimus* species pluralis (spp) and the intestinal flukes are *Echinostoma* spp, *Fasciolopsis buski*, *Gynmophalloides seoi*, *Haplorchis* spp, *Heterophyes* spp and *Metagonimus* spp [35, 36, 37, 104]. The disease opisthorchiasis is caused by the worm parasites *Opisthorchis viverrini* and *Opisthorchis felineus*.

6.1 Life cycle and transmission

Figure 6.1 shows the life cycle of *O. viverrini* (and correspondingly of *O. felineus*). A wide range of animals serve as definitive hosts for liver flukes besides humans. Infections with *O. viverrini* are also frequently found in cats, dogs and pigs [104].

After sexual reproduction in the definitive hosts, the adult worm of *O. viverrini* pro-

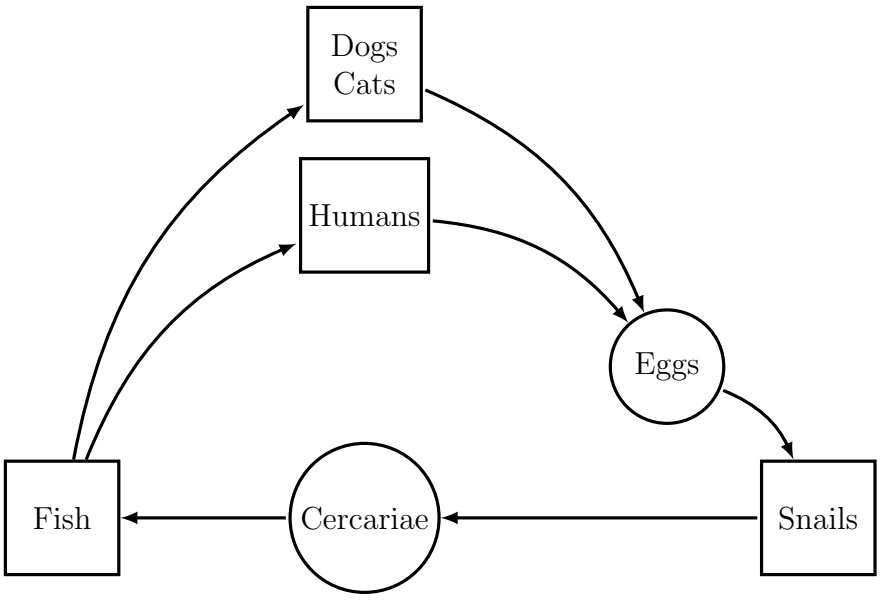

Figure 6.1: Schematic of the life cycle of *O. viverrini*.

duces fertilised eggs. The daily output of infected humans ranges between 3,000 and 36,000 eggs per gram of stool [102, 121]. However, density dependent effects within the host such as parasite overcrowding can lead to a reduction in per capita parasite egg production [100, 28, 124]. The parasite eggs are released via the hosts' faeces. The eggs need to encounter suitable environmental conditions, including appropriate levels of humidity, temperature and oxygen, and must reach water bodies, which are populated by aquatic snails, the first intermediate hosts. The first intermediate hosts of *O. viverrini* are snails of the genus *Bithynia* [33]. Eggs of *O. viverrini* are usually directly ingested by the intermediate host snails and miracidia hatch only within the snails [36, 56, 70]. Within the snails, miracidia reproduce and multiply asexually developing into sporocyst, rediae, and cercariae over several weeks [36, 56].

Cercariae are released from the intermediate host snails either by passive extrusion or active escape [56]. The free-swimming cercariae penetrate through the skin of the second intermediate hosts, Cyprinidae fish [121], and become fully infective metacercariae after 21 days [54].

Definitive hosts, including humans, become infected when ingesting viable metacercariae by consuming contaminated food [36, 56, 70, 137]. Sufficiently high or low temperature kills the metacercariae and hence, properly cooked or deep-frozen food is considered safe. The inhibition of metacercariae infectivity by means of other food processing methods (e.g. acidification, disinfection, drying, irradiation, pressure treatment, salting, smoking, or washing) remains questionable [35, 137, 41, 99]. In the definitive host, metacercariae excyst in the intestine and the hermaphroditic juvenile flukes migrate to the liver where they mature, mate, and start producing eggs, thereby completing their life cycles [35, 36, 56]. The life span of *O. viverrini* in humans is around ten years. The whole life cycle of *O. viverrini* has a duration of four months [102, 121].

6.2 Epidemiology

The epidemiology of liver flukes is governed by complex interactions between ecological, socioeconomic, and behavioural factors. Together, these factors need to allow the different parasite stages to survive and reach susceptible intermediate and definitive hosts. Environmental factors such as air temperature, vegetation, rainfall, water current, water quality, and water temperature influence the population dynamics of host species and therefore the possibility for liver flukes to establish their life cycles. Other socioeconomic developments such as the exponential growth of aquacultural production and the implementation of irrigation systems, coupled with often still inadequate sanitary facilities at less wealthy production sites, have favoured the spread of the disease [74, 56, 99, 58, 59]. Demographic changes such as human population growth, increasing urbanisation and mobility, together with expanding food distribution networks, have led to the occurrence of human liver flukes in locations distant from naturally endemic areas. This effect has been

amplified by the increasing wealth and associated lifestyle changes, which have led to the increased consumption of exotic foods [36, 9, 56, 68]. However, the main behavioural driver behind human liver fluke infections is probably still the ingestion of undercooked or pickled aquatic products because of their high ethnic, cultural, and nutritional value [36, 56]. Hence, most human infections still occur in distinct areas, where the parasites successfully sustain their life cycles and people consume certain traditional food dishes [137, 97]. In Thailand and Laos such traditional food include uncooked and fermented small- or medium-sized fish (*koi pla, lab pla, pla ra, pla som*) [104, 137, 109, 55].

Probably because of differing traditions and eating habits, men suffer from opisthorchiasis more often. For instance, men may consume more risky food during certain traditional festivities or – as a patient's perspective from Laos demonstrates [35] – may more frequently engage in recreational fishing with friends and subsequently consume raw or undercooked catch [104, 37, 56, 99].

Age-prevalence curves demonstrate that young children are already at risk of liver fluke infections and the age-specific prevalence rates usually steadily increase until plateauing in the middle age groups. Often, liver fluke infections are sustained by the longevity of the parasites and by continuous re- and super-infection due to unchanged eating habits. [104, 37, 73, 56, 99, 102, 121, 24]. However, gender- and age-specific prevalence profiles may vary locally as changes in the interplay between ecological, socioeconomic, and behavioural factors, and effects of disease control efforts over the past years may alter local epidemiological situations [36, 9, 37, 56, 137, 68].

6.3 Clinical signs and symptoms

Most people infected with *O. viverrini* are asymptomatic, and when symptoms occur they are often non-specific. Among the clinical symptomatic group, severity is associated with worm burden, typically measured by faecal egg counts, and the duration of infection. Clinical presentations depend on the affected organs [35] and as the human liver flukes *O. viverrini* inhabit the biliary system, the pathogenesis of opisthorchiasis is confined to the hepatobiliary region.

The primary pathogenesis occurs in the bile duct epithelial tissue and is caused by irritation and damage due to mechanical, chemical, and/or immune-mediated effects [94, 110, 48, 89]. Mechanical injury is caused by the suckers of feeding and migrating flukes and contributes to biliary ulceration. Chemical irritation arises from metabolic products from the liver flukes' tegument and excretory openings.

As a result, an increased susceptibility to cholangiocarcinoma (CCA) is the most severe clinical aspect of liver fluke infection (Figure 6.2a–d). CCA is a primary malignancy of the biliary tract and patients usually have very poor prognosis resulting in death [83]. In Asia, liver flukes *O. viverrini* is a main risk factors for CCA, while further to the west, CCA

is mainly associated with primary sclerosing cholangitis and other gall bladder diseases [103, 60, 45].

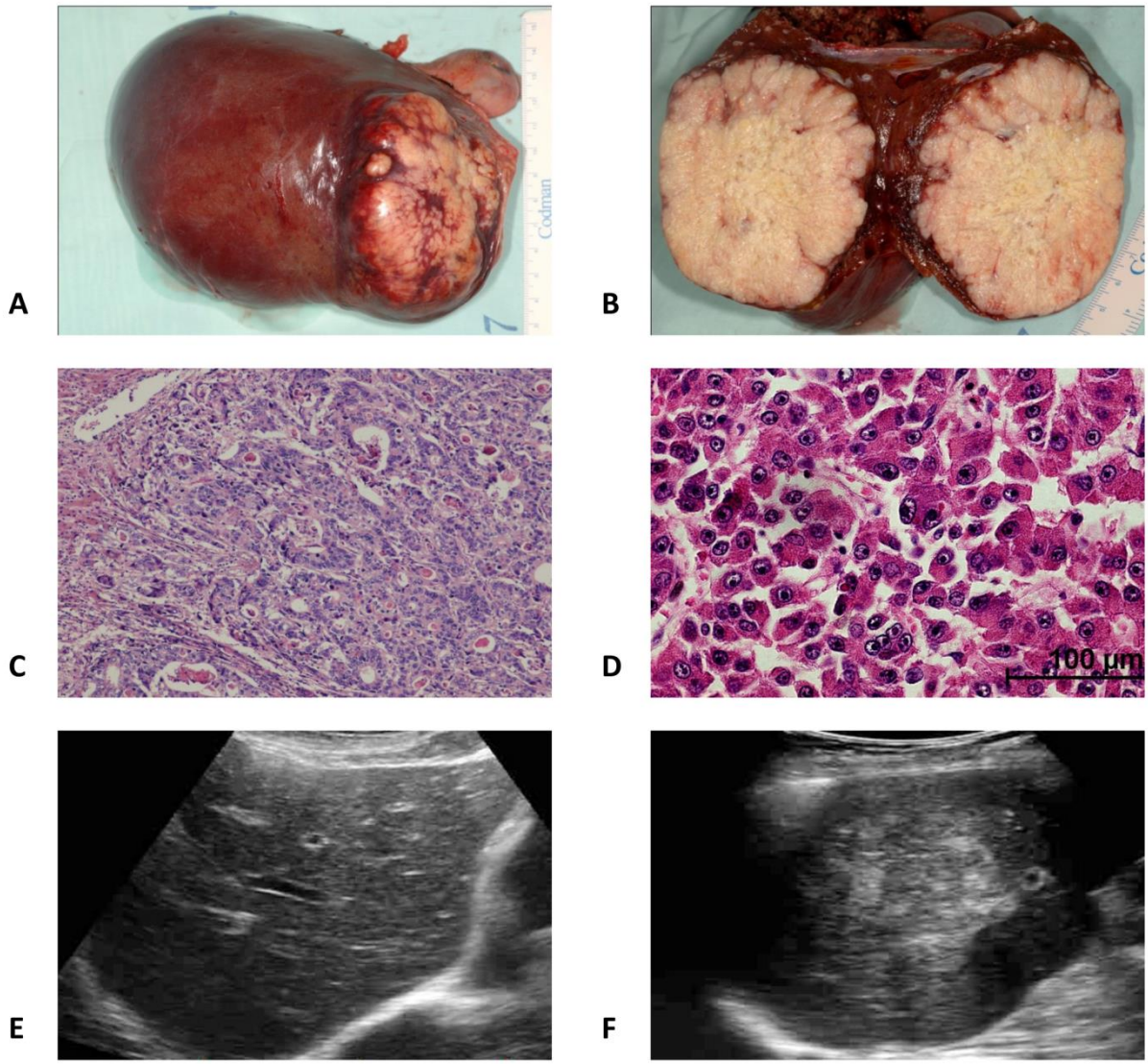

Figure 6.2: Clinical manifestations of liver fluke induced cholangiocarcinoma. Gross specimen from a liver resection from a cholangiocarcinoma patient (A, B); histology section of cholangiocarcinoma at low (10x; C) and high (40x; D) magnification; and ultrasonogram of periportal fibrosis (E) and cholangiocarcinoma (F). (source: Profs. Puangrat Yongvanit, Narong Khuntikeo, and Paiboon Sithithaworn).

People with chronic *O. viverrini* infections usually present with few specific signs and symptoms. An increased frequency of palpable liver may be diagnosed, but biochemical and haematological tests remain unremarkable [89, 29]. Furthermore, patients presenting with opisthorchiasis may suffer from loss of appetite, fullness, indigestion, diarrhoea, pain in the right upper quadrant, lassitude, weight loss, ascites, and oedema [89, 87]. Cholangitis, obstructive jaundice, intra-abdominal mass, cholecystitis, and gallbladder or intrahepatic stones may occur as complications [87, 90]. Ultrasonography is used for screening high risk groups with biliary fibrosis and other hepatobiliary diseases such as gallbladder enlargement, sludge, gallstones and poor function (Figure 6.2e–f) [29, 81, 25, 71]. Even CCA patients usually present with non-specific signs and symptoms such as fever,

anorexia, and dyspepsia and only a few may experience hepatomegaly and obstructive jaundice until progression of cancer [123, 78].

6.4 Diagnosis

Currently available diagnostic methods for FBT are unsatisfactory and diagnostic problems commonly occur for patients with light and mixed species infections. An affordable, rapid and simple to use diagnostic approach with high sensitivity and specificity is urgently needed to improve individual patient care, monitoring and evaluation of disease control programmes, disease surveillance, and burden estimation [51]. The most widely used diagnostic method for liver flukes is based on the microscopic detection of parasite eggs in patients' faeces. Techniques used for faecal examination include the formalin-ether concentration, Kato-Katz thick smear, and Stoll's dilution egg count. Depending on the available facilities, direct smear or sedimentation techniques may also be used. Repeated stool examinations are necessary to provide sufficient sensitivity particularly with regard to the confirmation of low-intensity infections [52]. However, multiple sample collection can be difficult in practice and costly. Morphological similarity of eggs from different trematodes, frequently occurring co-infections, low egg production by some FBT, crowding effects, obstruction in hosts' organs, and uneven distribution of eggs in samples further complicate the diagnosis [35, 53, 116, 118, 84, 10]. Occasionally, adult flukes in faeces or their identification during surgery facilitate the direct parasitological diagnosis. Complementary tools in well-equipped institutions include ultrasound, X-ray, computer tomography, and magnetic resonance imaging [35, 104, 9, 74, 56, 137, 99].

6.5 Treatment

A single dose of praziquantel of 40 mg/kg body weight (mg/kg) is effective against opisthorchiasis and is the treatment of choice in large-scale treatment programmes [99, 58]. However, experience from East Asia indicates that higher dosages such as 25 mg/kg three times per day for two days have to be administered to cure heavy *Opisthorchis* infections. Side effects occur frequently but are transient and rarely severe and may include dizziness, vomiting, and abdominal pain [99]. If treated in time, most pathological changes in the gallbladder are also reversed by elimination of the parasites [99, 88]. A recent randomised trial conducted in Laos found that a single dose of 200 mg (age below 14 years) or 400 mg (age above 14 years) tribendimidine results in a 99% egg reduction rate in individuals with opisthorchiasis, which is equivalent to praziquantel [108]. Furthermore, artesunate and artemether showed relatively high efficacy against *O. viverrini* in rodent models [57].

6.6 Current distribution and burden estimates

Human food-borne trematodiases are currently considered a cluster of emerging infectious diseases [56, 59]. The most recent Global Burden of Disease Study 2016 (GBD 2016) extrapolated the total global number of people infected by FBT at 74.7 million and the global burden at 1.8 million disability-adjusted life years (DALYs) lost due to human food-borne trematodiases in 2016 [39, 50].

Currently, most human FBT infections and the majority of the respective disease burden are reported from East and Southeast Asia [37, 41, 50]. *O. viverrini* is mainly endemic in East and particularly Southeast Asia [14], mainly in Thailand, Lao People's Democratic Republic (Lao PDR) and Cambodia [102]. Worldwide 9–10 million people are infected with *O. viverrini* [102, 56] and 67.3 million are at risk of infection. Another opisthorchiidae species, *O. felineus*, occurring only further to the North and West in Central, Northern, and Western Eurasia. Of note, the highest incidence of CCA occurs in Northeast Thailand, where the carcinogenic *O. viverrini* is endemic, with an estimated 20,000+ deaths due to CCA annually [14].

6.7 *O. viverrini* as a veterinary and economic issue

Liver flukes are also of veterinary importance as they infect aquacultural animals, domestic pets and wildlife. Besides reductions in animal wellbeing, animal infections result in economic losses to livestock and are an important issue for human disease control and prevention [36, 37, 56, 137, 99, 82]. As in humans, animal morbidity and mortality depends on susceptibility, the pathogenicity of the parasite species, and the intensity and duration of infection [82].

Aquacultural production and trade has been rapidly growing over the past decades with a particularly focus in Asia and it has become an important source of animal proteins, minerals and essential fatty acids in many parts of the world [56, 137, 1, 11]. However, in endemic liver fluke regions, aquaculture may expand the habitat of first (i.e. snails) and second intermediate hosts (i.e. fish). In combination with the lack of clean water and poor sanitation, wastewater and excreta use as nutrient sources, and inadequate aquacultural management allowing agricultural, domestic, and wild animals to access ponds, this may favour the spread of liver flukes [56, 11, 138]. Hence, while the increased aquacultural production opens new domestic and international markets, potential economic losses from contaminated products may be substantial [137, 11]. Unfortunately, the aquacultural production loss due to liver flukes is still largely unknown, although most recent laboratory studies suggest that liver flukes infections are associated with an increased mortality in some aquaculture fish species [62].

Liver fluke infections of domestic cats and dogs appear to be common in endemic areas [5]. However, arguably the most important aspect of liver flukes in domestic pets is the

potential for contamination of watercourses by faeces containing trematode eggs. This can result in the establishment or maintenance of the liver fluke life cycle and ultimately the contamination of food considered for human consumption. Thus, the control of liver fluke infection in cats and dogs is also an important aspect for human disease control and prevention [4, 26].

Besides the losses in animal production, the economic costs of human liver flukes infections and associated morbidity, absenteeism, reduced productivity, and health care can be considerable. In the 1990s, the annual cost due to *O. viverrini* in Thailand was estimated at US$ 65 million for lost wages and an additional US$ 19 million for direct medical care [137, 69]. Also considering only lost wages and cost of direct medical care, a more recent opinion piece from 2008 provided an annual estimate of US$ 120 million due to human opisthorchiasis and opisthorchiasis-induced CCA in Thailand [3]. Of note, all these estimates include only some selected categories of the total societal costs [20].

6.8 Control and prevention

Currently, the mainstay of human liver fluke control is drug-based morbidity control [99]. However, only a few endemic countries such as Thailand run larger-scale control programmes specifically targeting all FBT infections [75, 111]. Data for the World Health Organization (WHO) Western Pacific Region from 2006 indicate that a meagre 0.03% of the population at risk for FBT infections is covered by a specific preventive chemotherapy programme. And even when considering positive spill-over effects from other helminth control programmes, this coverage increases only to 0.3% [75]. Furthermore, the previously described complexities in the parasites' life cycles ask for more integrated interventions as the many non-human definitive hosts may maintain disease transmission in the environment [99, 34, 102, 121, 111, 49]. In fact, several studies found high human reinfection rates after solely drug-based interventions [24, 22, 122, 7].

The non-specific clinical manifestations and diagnostic challenges further complicate FBT control and prevention as patients may present late or infections may remain completely unnoticed. As part of its response, Thailand recently initiated the cholangiocarcinoma screening and care program (CASCAP). The programme utilises ultrasonography as a tool to screen cancer risk groups. As of 2014, the programme has screened up to 40,000 high risk individuals in Northeast Thailand and diagnosed ca. 1% positive for CCA. Thanks to the programme, many CCA cases could be identified at an early stage with better chances for curative surgery [81].

In the future, more integrated control and preventive efforts may complement individual-based chemotherapy, mass deworming and mass screening. In order to reduce or even completely interrupt disease transmission, additional interventions should adopt an ecosystem and one health perspective and consider intermediate, paratenic, reservoir, and definitive host control, sanitary improvements, and food inspections [111]. The development of ani-

mal vaccines is underway to reduce disease transmission and economic losses [35, 99, 8, 30]. Furthermore, information, communication, and education campaigns should promote safe food processing and behaviour change [35, 104, 9, 74, 56, 137, 99, 89, 139, 111].

Provided that sufficient data is available, mathematical modelling may not only help to better estimate disease burden and transmission dynamics in the future, but also to select optimal parasite- and location-specific interventions. In order to tackle all these formidable challenges and more closer to sustainable food-borne trematodiases control, prevention, or even elimination, collaborations within the health sector and also with non-health sectors (e.g. environmental, agricultural, and educational sector) may be essential [35, 137, 139, 75, 111, 77].

7. Data

The data used in this thesis was collected during an ecohealth study on two Mekong islands in Southern Lao PDR and published in [126].

7.1 Study area

The data were collected during a cross-sectional study between October 2011 and August 2012 on two islands. These two islands Done Khon and Done Som are situated in Champasack Province in the Southern Lao PDR, see Figure 7.1. The islands belong to the island district Khong with an estimated population of 100,000 people. *O. viverrini* is endemic in this district. Done Khon and Done Som belong to the biggest islands and are popular tourist destinations. In this thesis we assume that the data from the two islands represent one place. There are around 640 households with a total of 4000 people on the islands.

(a) Lao PDR (Source: Google Map).

(b) Khong District with the study site Done Som and Done Khon (Source: Google Map).

Figure 7.1: Study site of the data collection from October 2011 and August 2012 on Done Khon and Done Som islands in Khong district, Campasack Province, Lao PDR [126].

7.2 Data collection

994 individuals were part of the study from two selected villages on each islands. Reservoir hosts present during the study were also examined. They collected intermediate hosts of *O. viverrini*, snails and fish, and tested them for infection. We use the following field data in this thesis,

- population sizes of humans
- eggs per gram in stool of humans and their characteristics (sex, age,...), see Figure 7.2,
- population level data on eating behaviour, see Figure 7.3, and latrine usage habits, see Figure 7.4,
- number of infected fish, snails, cat and dog, see Tables 7.1 and 7.2,
- number of eggs per gram in dogs and cats, see Table 7.2.

Variable	Description	Value
n_h	number of tested humans	994
p_h	number of positive tested humans	603
n_d	number of tested dogs	68
p_d	number of positive tested dogs	17
n_c	number of tested cats	64
p_c	number of positive tested cats	34
n_s	number of tested snails	3102
p_s	number of positive tested snails	9
n_f	number of tested fish	628
p_f	number of positive tested fish	169

Table 7.1: Total number tested and positive hosts from two islands in Lao PDR [126].

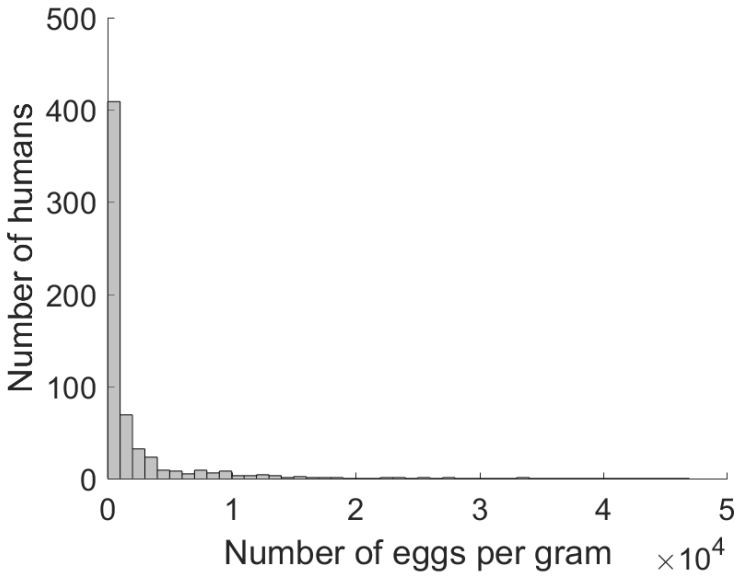

Figure 7.2: Histogram of eggs per gram of human stool.

The number of eggs per gram in dogs and cats was not available for the parameter fitting of the population-based models, we use it for the fitting of the individual-based model in Chapter 11.

Host	Prevalence P	Mean worm burden w
Humans	0.6066	32.2884
Dogs	0.2500	3.7905
Cats	0.5313	25.9234
Snails	0.0029	
Fish	0.2691	

Table 7.2: Prevalence of all hosts from the two islands in Lao PDR [126] and the mean worm burden of the definitive hosts transformed from the eggs per gram of human stool by the equation (7.1).

7.3 Results

60.7% of the study participants were infected with *O. viverrini* in 2012. The infection of *O. viverrini* on Done Som was almost two times higher than on Done Khon. The Prevalence of infection seems to be acquired at a young age and increases with age. Most of the infections are classified as light infection, between 1 and 999 eggs per gram (EPG).

Infection prevalence in reservoir hosts was highest in cats with 53.1% followed by dogs (25%) and 0.9% of pigs were infected. We neglected the infection of pigs in our models, as the prevalence is so low.

The infection rate of the intermediate hosts snails was 0.3% and 26.9% in fish. Only fish of the species *Cyprinoid* where infected with *O. viverrini* and the average metacercariae burden was 228.7 per fish.

Multivariate analysis showed that illiteracy and a lower socio-economic status increases the risk of infection with *O. viverrini*. The age group from 10 to 16 years and the ones having a latrine available are less likely of having an *O. viverrini* infection.

7.4 Data assumptions

We assume a population size of 15,000 humans, the accuracy of the assumption can be ignored because the population size is multiplied by the infection rates in the population-based models. Further, we assume that there are as half dogs as humans and one third cats as humans. We do not know the populations sizes of fish and snails, so we assume that there are much more snails than fish.

Additional parameters are set by using literature reviews or reasonable assumptions. If some of this data is not available we will conduct sensitivity analysis around reasonable parameter values derived from literature and experts opinion.

We convert the eggs per gram in human faeces to mean worm burden as we are interested in the worm burden. We use the pre-calculated relationship from literature,

$$y = x^2 + 2x \tag{7.1}$$

to convert the eggs per gram in stool, y, into mean worm burden, x, [28]. Firstly, we assume in the population-based models a Poisson distribution as shown in Figure 7.5. Later in the individual-based model we assume that the mean worm burdens remains high at a certain level as fewer people eat raw or undercooked fish, see Figure 7.6. We use the maximum likelihood method (MLE)[1] for the fittings.

[1]Matlab R2017a: Distribution Fitting App

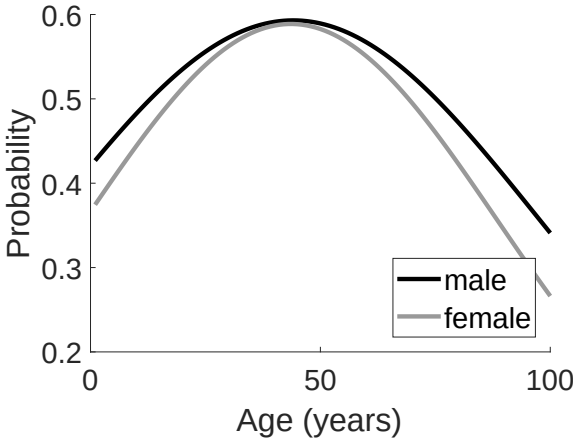

Figure 7.3: Exponential distribution of the probability to eat raw fish over age, $0.9884 \cdot \exp\left(\left(\frac{\text{age in years}-44.1}{75.15}\right)^2\right) \cdot 0.6$ for men and $0.9813 \cdot \exp\left(\left(\frac{\text{age in years}-43.59}{63.32}\right)^2\right) \cdot 0.6$ for women.

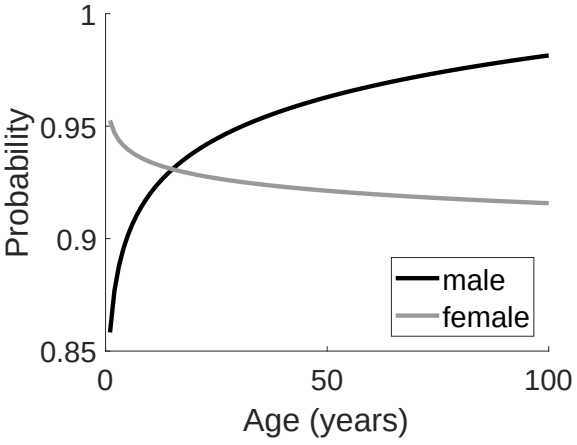

Figure 7.4: Logarithm distribution of the probability to use the latrine if available, $-0.02674 \cdot \log(\text{age in yrs}) + 0.1417$ for men and $0.007993 \cdot \log(\text{age in yrs}) + 0.04745$ for women.

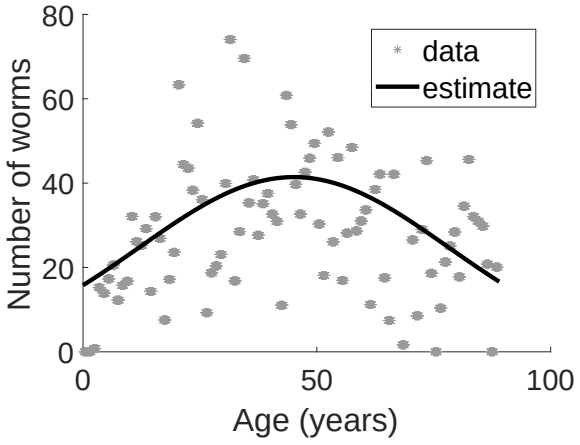

Figure 7.5: Estimate of the number of eggs per gram of stool from humans per age fitted to a Gaussian distribution: $f(\text{age}) = 1799 \cdot \exp\left(-\left(\frac{\text{age}-45.1}{33.1}\right)^2\right)$, and transformed to the number of worms in humans, see equation (7.1). This distribution is used in the model with age-dependency in Chapter 10.

Figure 7.6: Distribution of number of worms over age fitted to a logarithmic distribution, $5.503 \cdot \log(\text{age in yrs}) + 0.3164$ for men and $8.284 \cdot \log(\text{age in yrs}) - 7.201$ for women. This distribution is used in the individual-based model in Chapter 11.

8. Basic model and model with reservoir hosts

To create a basis for the mathematical modelling of FBT we develop two different population-based models without interventions. We first develop a simple model that only includes infection in fish, snails and humans. We then develop a second model that also includes infection in cats and dogs. These models allow us to better understand the role of domestic pets in the transmission dynamics of *O. viverrini*.

For these models, we define the equilibrium points, the basic reproduction number and the host-specific type-reproduction numbers. We then use data from Lao PDR described in Chapter 7. to estimate reasonable distributions for the parameter values of the models. We conduct sensitivity analysis using these distributions on the equilibrium points and the reproduction numbers for both models to determine weak points in the parasite's life cycle and the role of each mammalian host in maintaining transmission.

8.1 Basic transmission model

In the basic transmission model we assume that only fish, snails and humans are involved in the life cycle of *O. viverrini*, ignoring the reservoir hosts: cats and dogs. We model the mean worm burden in human and the prevalences of infected snails and fish. The deterministic population-based ODE model represents the base transmission dynamics of *O. viverrini*. It is given by

$$\frac{\mathrm{d}w_h}{\mathrm{d}t} = \beta_{hf} N_f i_f - \mu_{ph} w_h, \tag{8.1a}$$

$$\frac{\mathrm{d}i_s}{\mathrm{d}t} = \beta_{sh} N_h w_h (1 - i_s) - \mu_s i_s, \tag{8.1b}$$

$$\frac{\mathrm{d}i_f}{\mathrm{d}t} = \beta_{fs} N_s i_s (1 - i_f) - \mu_f i_f, \tag{8.1c}$$

with the state variables shown in Table 8.1 and the parameters shown in Table 8.2.

Variable	Description
w_h	Mean worm burden per human host
w_d	Mean worm burden per dog host
w_c	Mean worm burden per cat host
i_s	Proportion of infectious snails
i_f	Proportion of infectious fish

Table 8.1: State variables of the opisthrochiasis models.

The mean worm burden per human host w_h increases with the consumption of infected fish. This depends on the number of fish, the proportion of infectious fish and the

Parameter	Description	Dimension
N_h	Population size of humans	Animals
N_d	Population size of dogs	Animals
N_c	Population size of cats	Animals
N_s	Population size of snails	Animals
N_f	Population size of fish	Animals
μ_{ph}	Per capita death rate of adult parasites in humans (includes additional mortality due to death of humans)	1/Time
μ_{pd}	Per capita death rate of adult parasites in dogs (includes additional mortality due to death of dogs)	1/Time
μ_{pc}	Per capita death rate of adult parasites in cats (includes additional mortality due to death of cats)	1/Time
μ_s	Per capita death rate of snails	1/Time
μ_f	Per capita death rate of fish including mortality through fishing by humans	1/Time
β_{hf}	Transmission rate from infectious fish to humans per person per fish	1/(Time × Animals)
β_{df}	Transmission rate from infectious fish to dogs per dog per fish	1/(Time × Animals)
β_{cf}	Transmission rate from infectious fish to cats per cat per fish	1/(Time × Animals)
β_{sd}	Infection rate of snails per parasite in a dog host	1/(Time × Animals)
β_{sc}	Infection rate of snails per parasite in a cat host	1/(Time × Animals)
β_{sh}	Infection rate of snails per parasite in a human host	1/(Time × Animals)
β_{fs}	Infection rate of fish per snail	1/(Time × Animals)

Table 8.2: Parameters of the opisthorchiasis model.

transmission rate of parasites to humans per fish, $\beta_{hf}N_f i_f$, and decreases with the death of parasites, $\mu_{ph}w_h$. The proportion of infectious snails i_s, depends on the total adult worm population and the eggs they produce that enter the aquatic environment and the proportion of snails that are susceptible, $\beta_{sh}N_h w_h(1-i_s)$. Snails are infected until they die at a total rate, $\mu_s i_s$. The proportion of infectious fish has similar dynamics. Their rate of infection depends on the number of infectious snails and the snails' rate of releasing cerceriae and the proportion of susceptible fish, $\beta_{fs}N_s i_s(1-i_f)$. The fish remain infected until they die at a total rate, $\mu_f i_f$.

This model ignores the intensity of infection in fish, as well as the distribution of intensity in humans. We assume negative binomial distribution for the intensity of infection in humans but ignore additional heterogeneities, and that all infected fish and snails are

equal with regards to within- and between-species transmission, and assume no assortative mixing. We also ignore density-dependent effects in hosts such as acquired immunity and Allee effects.

Existence and uniqueness of the solution

The system with the equations (8.1) is well-posed and epidemiologically relevant in the strip $S \subset \mathbb{R}^3$. The strip S is defined by the boundaries of the solutions of the system (w_h, i_s, i_f),

$$S = \left[0, \frac{N_f \beta_{hf}}{\mu_{ph}}\right] \times [0,1]^2 .$$

The right hand side of the ODE system (8.1) is continuous with continuous partial derivatives in S. Assuming that an initial condition exists in the strip S, we can show that a solution of the system cannot leave this strip S:

(i) If $w_h = 0$, then

$$\frac{\mathrm{d}w_h}{\mathrm{d}t} = \beta_{hf} N_f i_f - \mu_{ph} \cdot 0 \geq 0,$$

and, if $w_h = \frac{N_f \beta_{hf}}{\mu_{ph}}$, then

$$\frac{\mathrm{d}w_h}{\mathrm{d}t} = \beta_{hf} N_f i_f - \mu_{ph} \cdot \frac{N_f \beta_{hf}}{\mu_{ph}} \leq 0.$$

(ii) If $i_s = 0$, then

$$\frac{\mathrm{d}i_s}{\mathrm{d}t} = \beta_{sh} N_h w_h \cdot 1 - \mu_s \cdot 0 \geq 0,$$

and, if $i_s = 1$, then

$$\frac{\mathrm{d}i_s}{\mathrm{d}t} = \beta_{sh} N_h w_h \cdot 0 - \mu_s \cdot 1 \leq 0.$$

(iii) If $i_f = 0$, then

$$\frac{\mathrm{d}i_f}{\mathrm{d}t} = \beta_{fs} N_s i_s \cdot 1 - \mu_{fs} \cdot 0 \geq 0,$$

and, if $i_f = 1$, then

$$\frac{\mathrm{d}i_f}{\mathrm{d}t} = \beta_{fs} N_s i_s \cdot 0 - \mu_{fs} \cdot 0 \leq 0.$$

It finally follows with the Picard-Lindelöf theorem that a unique solution exists for the ODE system (8.1) in the strip S.

Equilibrium points

Definition 1 (Disease free equilibrium point)**.** *The disease free equilibrium, also called trivial equilibrium point, is the steady state solution with no disease in the population.*

Definition 2 (Endemic equilibrium point)**.** *The endemic equilibrium point is the steady state solution with all state variables positive, where the disease persists in the population.*

Setting the derivatives equal to zero, the equilibrium points are given as the solution of

$$\begin{aligned} 0 &= \beta_{hf} N_f i_f^* - \mu_{ph} w_h^*, \\ 0 &= \beta_{sh} N_h w_h^* (1 - i_s^*) - \mu_s i_s^*, \\ 0 &= \beta_{fs} N_s i_s^* (1 - i_f^*) - \mu_f i_f^*. \end{aligned}$$

The system has two solutions, the disease free and the endemic equilibrium point. The disease free equilibrium point is characterized by $E_0^{BM} = (w_h^*, i_s^*, i_f^*) = (0, 0, 0)$. The endemic equilibrium point $E_e^{BM} = (w_h^*, i_s^*, i_f^*)$ corresponds to

$$w_h^* = \frac{\beta_{hf}\beta_{sh}\beta_{fs}N_s N_h N_f - \mu_{ph}\mu_s\mu_f}{\beta_{sh}N_h\mu_{ph}(\beta_{fs}N_s + \mu_f)}, \tag{8.2a}$$

$$i_s^* = \frac{\beta_{hf}\beta_{sh}\beta_{fs}N_s N_h N_f - \mu_{ph}\mu_s\mu_f}{\beta_{fs}N_s(\beta_{hf}\beta_{sh}N_h N_f + \mu_{ph}\mu_s)}, \tag{8.2b}$$

$$i_f^* = \frac{\beta_{hf}\beta_{sh}\beta_{fs}N_s N_h N_f - \mu_{ph}\mu_s\mu_f}{\beta_{hf}\beta_{sh}N_h N_f(\beta_{fs}N_s + \mu_f)}, \tag{8.2c}$$

which is in the interior of S if $\beta_{hf}\beta_{sh}\beta_{fs}N_s N_h N_f > \mu_{ph}\mu_s\mu_f$.

Basic reproduction number

Definition 3 (Basic reproduction number)**.** *The basic reproduction number $\mathcal{R}_0$ is the average number of new cases of an infection (or number of parasite offspring) caused by one typical infected individual (or one parasite), from one generation to the next, in a population with no pre-existing infections.*

To determine $\mathcal{R}_0$, we define the next-generation matrix (NGM) $\mathbf{K}$. This matrix relates the number of newly infected individuals or number of adult parasites in consecutive generations. $\mathcal{R}_0$ is then defined as the spectral radius of $\mathbf{K}$.

The linearised infection subsystem describes the production of newly infected individuals and changes in the states of already infected individuals. To derive the next-generation matrix $\mathbf{K}$, we decompose the matrix, which describes the linearised model, into two matrices, $\mathbf{T}$ and $\mathbf{\Sigma}$. $\mathbf{T}$ describes transmission: the production of new infections; and $\mathbf{\Sigma}$ describes transition: the changes in state. $\mathbf{K}$ is defined as the product of $-\mathbf{T}$ and $\mathbf{\Sigma}^{-1}$ and $\mathcal{R}_0$ is the spectral radius, ρ, of $\mathbf{K}$. Therefore, $\mathcal{R}_0 = \rho(-\mathbf{T}\mathbf{\Sigma}^{-1})$.

The interpretation of the (i,j)-th entry of $\mathbf{\Sigma}^{-1}$ is the expected time that an individual, who presently has the infected state j, will spend in the infected state i. The (i,j)-th entry of $\mathbf{T}$ is the rate at which an individual in the infected state j produces individuals with the infected state i. Therefore, the (i,j)-th entry of the NGM $\mathbf{K}$ is the expected number of the infected offspring with the state i who are infected by an individual currently in infected state j [27].

The transmission matrix is

$$\mathbf{T} = \begin{bmatrix} 0 & 0 & \beta_{hf} N_f \\ \beta_{sh} N_h & 0 & 0 \\ 0 & \beta_{fs} N_s & 0 \end{bmatrix},$$

and the transition matrix is

$$\mathbf{\Sigma} = \begin{bmatrix} -\mu_{ph} & 0 & 0 \\ 0 & -\mu_s & 0 \\ 0 & 0 & -\mu_f \end{bmatrix}.$$

The next-generation matrix of the basic model is therefore

$$\mathbf{K} = -\mathbf{T}\mathbf{\Sigma}^{-1} = \begin{bmatrix} 0 & 0 & \frac{\beta_{hf} N_f}{\mu_f} \\ \frac{\beta_{sh} N_h}{\mu_{ph}} & 0 & 0 \\ 0 & \frac{\beta_{fs} N_s}{\mu_s} & 0 \end{bmatrix}.$$

The eigenvalues of the next-generation matrix $\mathbf{K}$ are

$$\lambda_1 = \sqrt[3]{\frac{\beta_{hf}\beta_{sh}\beta_{fs} N_h N_s N_f}{\mu_{ph}\mu_s\mu_f}},$$

$$\lambda_2 = -(-1)^{\frac{1}{3}} \sqrt[3]{\frac{\beta_{hf}\beta_{sh}\beta_{fs} N_h N_s N_f}{\mu_{ph}\mu_s\mu_f}},$$

$$\lambda_3 = (-1)^{\frac{2}{3}} \sqrt[3]{\frac{\beta_{hf}\beta_{sh}\beta_{fs} N_h N_s N_f}{\mu_{ph}\mu_s\mu_f}}.$$

All eigenvalues have the same modulus, so the (not strictly) dominant eigenvalue is λ_1, the only real and positive eigenvalue of $\mathbf{K}$. Hence, it follows that

$$\mathcal{R}_0 = \sqrt[3]{\frac{\beta_{hf}\beta_{sh}\beta_{fs} N_h N_s N_f}{\mu_{ph}\mu_s\mu_f}}. \tag{8.3}$$

The ecological definition of the basic reproduction number is the number of offspring adult worms produced by a single adult worm in its life time, in the absence of density-dependence. This number corresponds to the cube of $\mathcal{R}_0$ defined in (8.3) to include all life stages of the parasite. When $\mathcal{R}_0 = 1$, $\mathcal{R}_0^3 = 1$ so both definitions provide the same threshold conditions.

Stability of the equilibrium points

The basic reproduction number provides a threshold condition for the stability of the disease free equilibrium point. If $\mathcal{R}_0 < 1$, then the disease free equilibrium point is locally asymptotically stable, and if $\mathcal{R}_0 > 1$ it is unstable. We calculate the eigenvalues of the Jacobian matrix of the model at the disease free equilibrium and show with Descartes' rule of sign that not all real parts of the eigenvalues are negative. It follows that the diseases free equilibrium is locally asymptotically unstable. We conjecture that the disease free equilibrium point is globally asymptotically stable if $\mathcal{R}_0 \leq 1$ because we do not expect any non-equilibrium asymptotic dynamics but we do not have a proof for this.

The endemic equilibrium exists if and only if $\beta_{hf}\beta_{sh}\beta_{fs}N_hN_sN_f > \mu_{ph}\mu_s\mu_f$, that is $\mathcal{R}_0 > 1$. To investigate the local stability of the endemic equilibrium point, we use the Routh-Horwitz Criterion (Proposition 3 in Appendix A) to determine the signs of the real parts of the eigenvalues of the Jacobian matrix.

The Jacobian matrix of the basic model at the endemic equilibrium point is

$$\begin{aligned}\mathbf{J} &= \begin{bmatrix} -\mu_{ph} & 0 & \beta_{hf}N_f \\ \beta_{sh}N_h(1-i_s^*) & -(\beta_{sh}N_hw_h^* + \mu_s) & 0 \\ 0 & \beta_{fs}N_s(1-i_f^*) & -(\beta_{fs}N_si_s^* + \mu_f) \end{bmatrix} \\ &=: \begin{bmatrix} -j_{1,1} & 0 & j_{1,3} \\ j_{2,1} & -j_{2,2} & 0 \\ 0 & j_{3,2} & -j_{3,3} \end{bmatrix},\end{aligned}$$

for w_h^*, i_s^* and i_f^*, defined in (8.2). The eigenvalues of the Jacobian matrix are calculated by setting the characteristic polynomial $p(\lambda) = \det(\mathbf{J} - \lambda\mathbf{E})$ to zero. This leads to the equation

$$\begin{aligned}\lambda^3 + \lambda^2(j_{1,1} + j_{2,2} + j_{3,3}) + \lambda(j_{1,1}j_{2,2} + j_{1,1}j_{3,3} + j_{2,2}j_{3,3}) \\ + j_{1,1}j_{2,2}j_{3,3} - j_{1,3}j_{2,1}j_{3,2} \stackrel{!}{=} 0.\end{aligned}$$

We can determine the a_i of the Routh-Horwitz criterion in Proposition 3 (in Appendix A) for $i = 0, 1, 2, 3$:

$$\begin{aligned}a_0 &= 1, \\ a_1 &= j_{1,1} + j_{2,2} + j_{3,3}, \\ a_2 &= j_{1,1}j_{2,2} + j_{1,1}j_{3,3} + j_{2,2}j_{3,3}, \\ a_3 &= j_{1,1}j_{2,2}ij_{3,3} - j_{1,3}j_{2,1}j_{3,2}.\end{aligned}$$

With all the a_i's at hand, we can calculate the T_k's for $k = 0, 1, 2$ and see if they are

positive or negative:

$$
\begin{aligned}
&T_0 = a_0 = 1 > 0,\\
&T_1 = a_1 > 0,\\
&T_2 = \det \begin{bmatrix} a_1 & a_0 \\ a_3 & a_2 \end{bmatrix} > 0 \Leftrightarrow \beta_{hf}\beta_{sh}\beta_{fs}N_hN_sN_f > \mu_{ph}\mu_s\mu_f \Leftrightarrow \mathcal{R}_0 > 1.
\end{aligned}
$$

From the Routh-Hurwitz criterion it follows that the roots of the characteristic polynomial $p(\lambda)$ and thus the eigenvalues of $\mathbf{J}$ have negative real parts. This means that the endemic equilibrium is locally asymptotically stable whenever $\mathcal{R}_0 > 1$.

8.2 Model with reservoir hosts

In the second transmission model we add cats and dogs as reservoir hosts to the basic transmission model. We extend the basic model (8.1) by including two additional variables: the mean number of adult parasites per hosts in dogs (w_d) and cats (w_c) with similar dynamics for cats and dogs as for humans. This leads to

$$
\begin{aligned}
\frac{\mathrm{d}w_h}{\mathrm{d}t} &= \beta_{hf}N_f i_f - \mu_{ph}w_h, && \text{(8.4a)}\\
\frac{\mathrm{d}w_d}{\mathrm{d}t} &= \beta_{df}N_f i_f - \mu_{pd}w_d, && \text{(8.4b)}\\
\frac{\mathrm{d}w_c}{\mathrm{d}t} &= \beta_{cf}N_f i_f - \mu_{pc}w_c, && \text{(8.4c)}\\
\frac{\mathrm{d}i_s}{\mathrm{d}t} &= (\beta_{sh}N_h w_h + \beta_{sd}N_d w_d + \beta_{sc}N_c w_c)(1 - i_s) - \mu_s i_s, && \text{(8.4d)}\\
\frac{\mathrm{d}i_f}{\mathrm{d}t} &= \beta_{fs}N_s i_s(1 - i_f) - \mu_f i_f. && \text{(8.4e)}
\end{aligned}
$$

The additional state variables are given in Table 8.1 and the additional parameters are given in Table 8.2.

Existence and uniqueness of the solution

The existence and the uniqueness of the solution $(w_h, w_d, w_c, i_s, i_f)$ of the ODE system (8.4) follows in complete analogy to Section 8.1 in the strip $S \subset \mathbb{R}^5$ given by

$$
D = \left[0, \frac{N_f\beta_{hf}}{\mu_{ph}}\right] \times \left[0, \frac{N_f\beta_{df}}{\mu_{pd}}\right] \times \left[0, \frac{N_f\beta_{cf}}{\mu_{pc}}\right] \times [0,1]^2 .
$$

Equilibrium points

For the model with reservoir hosts (8.4) we solve the following system

$$
\begin{aligned}
0 &= \beta_{hf} N_f i_f^* - \mu_{ph} w_h^*, \\
0 &= \beta_{df} N_f i_f^* - \mu_{pd} w_d^*, \\
0 &= \beta_{cf} N_f i_f^* - \mu_{pc} w_c^*, \\
0 &= (\beta_{sh} N_h w_h^* + \beta_{sd} N_d w_d^* + \beta_{sc} N_c w_c^*)(1 - i_s^*) - \mu_s i_s^*, \\
0 &= \beta_{fs} N_s i_s^* (1 - i_f^*) - \mu_f i_f^*,
\end{aligned}
$$

to determine the equilibrium points. We see that $E_0^{RM} = (w_h^*, w_d^*, w_c^*, i_s^*, i_f^*) = (0, 0, 0, 0, 0)$ is the disease free equilibrium point and show the existence of at most one endemic equilibrium point. We calculated an analytic expression for this endemic equilibrium but do not present it here because of its length.

Basic reproduction number

To define the reproduction number of the model with reservoir hosts (8.4), we use the same method as for the basic model before. Hence, we obtain the transmission matrix

$$
\mathbf{T} = \begin{bmatrix}
0 & 0 & 0 & 0 & \beta_{hf} N_f \\
0 & 0 & 0 & 0 & \beta_{df} N_f \\
0 & 0 & 0 & 0 & \beta_{cf} N_f \\
\beta_{sh} N_h & \beta_{sd} N_d & \beta_{sc} N_c & 0 & 0 \\
0 & 0 & 0 & \beta_{fs} N_s & 0
\end{bmatrix}
$$

and the transition matrix

$$
\mathbf{\Sigma} = \begin{bmatrix}
-\mu_{ph} & 0 & 0 & 0 & 0 \\
0 & -\mu_{pd} & 0 & 0 & 0 \\
0 & 0 & -\mu_{pc} & 0 & 0 \\
0 & 0 & 0 & -\mu_s & 0 \\
0 & 0 & 0 & 0 & -\mu_f
\end{bmatrix}.
$$

The next-generation matrix is thus defined as

$$
\mathbf{K} = -\mathbf{T}\mathbf{\Sigma}^{-1} = \begin{bmatrix}
0 & 0 & 0 & 0 & \frac{\beta_{hf} N_f}{\mu_f} \\
0 & 0 & 0 & 0 & \frac{\beta_{df} N_f}{\mu_f} \\
0 & 0 & 0 & 0 & \frac{\beta_{cf} N_f}{\mu_f} \\
\frac{\beta_{sh} N_h}{\mu_{ph}} & \frac{\beta_{sd} N_d}{\mu_{pd}} & \frac{\beta_{sc} N_c}{\mu_{pc}} & 0 & 0 \\
0 & 0 & 0 & \frac{\beta_{fs} N_s}{\mu_s} & 0
\end{bmatrix}.
$$

The eigenvalues of the next-generation matrix $\mathbf{K}$ are the roots of the characteristic polynomial:

$$\det(\mathbf{K}-\lambda\mathbf{E}) =$$
$$-\lambda^5+\lambda^2\frac{\beta_{fs}N_s}{\mu_s}\left(\frac{\beta_{cf}N_f}{\mu_f}\frac{\beta_{sc}N_c}{\mu_{pc}}+\frac{\beta_{sd}N_d}{\mu_{pd}}\frac{\beta_{df}N_f}{\mu_f}+\frac{\beta_{hf}N_f}{\mu_f}\frac{\beta_{sh}N_h}{\mu_{ph}}\right)\stackrel{!}{=}0$$

Straightforward calculation yields:

$$\begin{aligned}
\lambda_1 &= \lambda_2 = 0,\\
\lambda_3 &= \sqrt[3]{\frac{\beta_{fs}N_s}{\mu_s}}\sqrt[3]{\frac{\beta_{cf}N_f}{\mu_f}\frac{\beta_{sc}N_c}{\mu_{pc}}+\frac{\beta_{sd}N_d}{\mu_{pd}}\frac{\beta_{df}N_f}{\mu_f}+\frac{\beta_{hf}N_f}{\mu_f}\frac{\beta_{sh}N_h}{\mu_{ph}}},\\
\lambda_4 &= -(-1)^{\frac{1}{3}}\sqrt[3]{\frac{\beta_{fs}N_s}{\mu_s}}\sqrt[3]{\frac{\beta_{cf}N_f}{\mu_f}\frac{\beta_{sc}N_c}{\mu_{pc}}+\frac{\beta_{sd}N_d}{\mu_{pd}}\frac{\beta_{df}N_f}{\mu_f}+\frac{\beta_{hf}N_f}{\mu_f}\frac{\beta_{sh}N_h}{\mu_{ph}}},\\
\lambda_5 &= (-1)^{\frac{2}{3}}\sqrt[3]{\frac{\beta_{sf}N_s}{\mu_s}}\sqrt[3]{\frac{\beta_{cf}N_f}{\mu_f}\frac{\beta_{sc}N_c}{\mu_{pc}}+\frac{\beta_{df}N_f}{\mu_f}\frac{\beta_{sd}N_d}{\mu_{pd}}+\frac{\beta_{hf}N_f}{\mu_f}\frac{\beta_{sh}N_h}{\mu_{ph}}}.
\end{aligned}$$

Since λ_4 and λ_5 are complex numbers, λ_3 is the dominant real eigenvalue of $\mathbf{K}$, and the reproduction number is

$$\mathcal{R}_0 = \sqrt[3]{\frac{\beta_{fs}N_s}{\mu_s}}\sqrt[3]{\frac{\beta_{cf}N_f}{\mu_f}\frac{\beta_{sc}N_c}{\mu_{pc}}+\frac{\beta_{sd}N_d}{\mu_{pd}}\frac{\beta_{df}N_f}{\mu_f}+\frac{\beta_{hf}N_f}{\mu_f}\frac{\beta_{sh}N_h}{\mu_{ph}}}.$$

The endemic equilibrium point exists if and only if $\mathcal{R}_0 > 1$. We expect that is locally asymptotically stable for $\mathcal{R}_0 > 1$ but did not prove this.

Type reproduction numbers

To determine the role of cats and dogs in maintaining transmission, we analyse host-specific type-reproduction numbers. They are given by the spectral radii of the next-generation matrices leaving out one or more host types [91]. U_i is the host-specific and Q_j is the host excluded reproduction number, which are defined as

$$\begin{aligned}
U_i &= \rho(\mathbf{K}_i),\\
Q_j &= \rho(\mathbf{K}-\mathbf{K}_j+\mathbf{K}_{fs}),
\end{aligned}$$

where $\mathbf{K}_i$ is the next-generation matrix of only including host i and $\mathbf{K}_{fs}$ the next-generation matrix of the transmission from snails to fish. In this multi-host population with n types of hosts, the reservoir community is defined as the minimum set of hosts with $U > 1$. A maintenance host is the minimum of m ($m \leq n$) different hosts which satisfy $U > 1$ and $Q < 1$ [80]. With the type reproduction number, we can define the reservoir community and subdivide the hosts into maintenance and non-maintenance hosts. Transmission is not possible without snails and fish, so we always

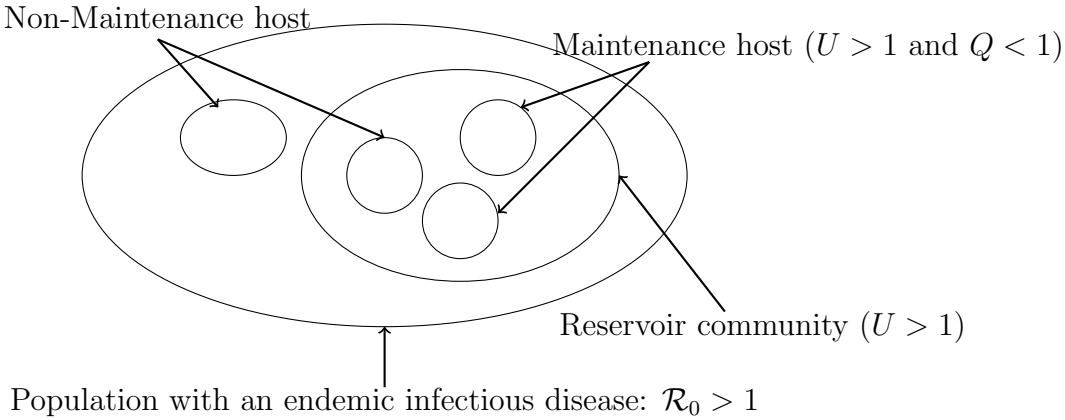

Figure 8.1: Definition of reservoir, maintenance, and non-maintenance hosts in a population with an endemic infectious disease, figure based on [80, Figure 3].

include them in the model while determining the role of the three mammalian hosts, that means $i \in \{\text{humans } (h), \text{dogs } (d), \text{cats } (c)\}$.

The different next-generation matrices and their spectral radii are given by

$$U_h(= Q_{d,c}) = \rho(\mathbf{K}_h) = \rho\left(\begin{bmatrix} 0 & 0 & 0 & 0 & \frac{\beta_{hf}N_f}{\mu_f} \\ 0 & 0 & 0 & 0 & 0 \\ 0 & 0 & 0 & 0 & 0 \\ \frac{\beta_{sh}N_h}{\mu_{ph}} & 0 & 0 & 0 & 0 \\ 0 & 0 & 0 & \frac{\beta_{fs}N_s}{\mu_s} & 0 \end{bmatrix}\right) = \sqrt[3]{\frac{N_f N_h N_s \beta_{hf}\beta_{sh}\beta_{fs}}{\mu_f \mu_{ph} \mu_s}},$$

$$U_d(= Q_{h,c}) = \rho(\mathbf{K}_d) = \rho\left(\begin{bmatrix} 0 & 0 & 0 & 0 & 0 \\ 0 & 0 & 0 & 0 & \frac{\beta_{df}N_f}{\mu_f} \\ 0 & 0 & 0 & 0 & 0 \\ 0 & \frac{\beta_{sd}N_d}{\mu_{pd}} & 0 & 0 & 0 \\ 0 & 0 & 0 & \frac{\beta_{fs}N_s}{\mu_s} & 0 \end{bmatrix}\right) = \sqrt[3]{\frac{N_f N_s N_d \beta_{df}\beta_{fs}\beta_{sd}}{\mu_f \mu_{pd} \mu_s}},$$

$$U_c(= Q_{h,d}) = \rho(\mathbf{K}_c) = \rho\left(\begin{bmatrix} 0 & 0 & 0 & 0 & 0 \\ 0 & 0 & 0 & 0 & 0 \\ 0 & 0 & 0 & 0 & \frac{\beta_{cf}N_f}{\mu_f} \\ 0 & 0 & \frac{\beta_{sc}N_c}{\mu_{pc}} & 0 & 0 \\ 0 & 0 & 0 & \frac{\beta_{fs}N_s}{\mu_s} & 0 \end{bmatrix}\right) = \sqrt[3]{\frac{N_f N_s N_c \beta_{cf}\beta_{fs}\beta_{sc}}{\mu_f \mu_{pc} \mu_s}},$$

$$Q_h(=U_{d,c}) = \rho(\mathbf{K}_{d,c}) = \rho\left(\begin{bmatrix} 0 & 0 & 0 & 0 & 0 \\ 0 & 0 & 0 & 0 & \frac{\beta_{df}N_f}{\mu_f} \\ 0 & 0 & 0 & 0 & \frac{\beta_{cf}N_f}{\mu_f} \\ 0 & \frac{\beta_{sd}N_d}{\mu_{pd}} & \frac{\beta_{sc}N_c}{\mu_{pc}} & 0 & 0 \\ 0 & 0 & 0 & \frac{\beta_{fs}N_s}{\mu_s} & 0 \end{bmatrix}\right)$$
$$= \sqrt[3]{\frac{N_s\beta_{fs}}{\mu_s}\left(\frac{N_fN_d\beta_{df}\beta_{sd}}{\mu_f\mu_{pd}} + \frac{N_fN_c\beta_{cf}\beta_{sc}}{\mu_f\mu_{pc}}\right)},$$

$$Q_c(=U_{h,d}) = \rho(\mathbf{K}_{h,d}) = \rho\left(\begin{bmatrix} 0 & 0 & 0 & 0 & \frac{\beta_{hf}N_f}{\mu_f} \\ 0 & 0 & 0 & 0 & \frac{\beta_{df}N_f}{\mu_f} \\ 0 & 0 & 0 & 0 & 0 \\ \frac{\beta_{sh}N_h}{\mu_{ph}} & \frac{\beta_{sd}N_d}{\mu_{pd}} & 0 & 0 & 0 \\ 0 & 0 & 0 & \frac{\beta_{fs}N_s}{\mu_s} & 0 \end{bmatrix}\right)$$
$$= \sqrt[3]{\frac{N_s\beta_{fs}}{\mu_s}\left(\frac{N_fN_h\beta_{hf}\beta_{sh}}{\mu_f\mu_{ph}} + \frac{N_fN_d\beta_{df}\beta_{sd}}{\mu_f\mu_{pd}}\right)},$$

and

$$Q_d(=U_{h,c}) = \rho(\mathbf{K}_{h,c}) = \rho\left(\begin{bmatrix} 0 & 0 & 0 & 0 & \frac{\beta_{hf}N_f}{\mu_f} \\ 0 & 0 & 0 & 0 & 0 \\ 0 & 0 & 0 & 0 & \frac{\beta_{cf}N_f}{\mu_f} \\ \frac{\beta_{sh}N_h}{\mu_{ph}} & 0 & \frac{\beta_{sc}N_c}{\mu_{pc}} & 0 & 0 \\ 0 & 0 & 0 & \frac{\beta_{fs}N_s}{\mu_s} & 0 \end{bmatrix}\right)$$
$$= \sqrt[3]{\frac{N_s\beta_{fs}}{\mu_s}\left(\frac{N_fN_h\beta_{hf}\beta_{sh}}{\mu_f\mu_{ph}} + \frac{N_fN_c\beta_{cf}\beta_{sc}}{\mu_f\mu_{pc}}\right)}.$$

8.3 Sensitivity analysis

Sensitivity analysis describes what happens to some dependent variables when one or more independent parameters are changed [21]. Thus, we can see the influence of the different parameter to the basic reproduction number, the host-specific type-reproduction number and the endemic equilibrium point.

Data and parameter values

We use data on prevalence of infection in cats, dogs, snails, and fish; and on intensity of infection in humans from the two islands Done Khon and Done Som, Champasack province, Lao PDR, described in Chapter 7. We assume that this data represents an equilibrium solution, which we use to estimate the unknown parameters. The number of hosts tested and found positive is shown in Table 7.1 [126].

We assume triangular distributions as prior distributions for the model parameters and estimate ranges and modes from the data, literature, and expert opinions, as shown in Tables 8.3 and 8.4. We assume that the mean life span of parasite in humans (μ_{ph}) is 10 years, mean life span of a snail (μ_s) is 1 year and of a fish (μ_f) is 2.5 years [13]. We assume that parasites in cats (μ_{pc}) and dogs (μ_{pd}) die after 4 years, which is the average life span of cats and dogs in the area. We use the adapted population sizes of 15,000 humans. From discussions with local village chiefs, We assume that there are half as many dogs as humans and a third as many cats as humans. We further expect that there are a lot more snails than fish. We calculate the modes of the transmission parameters (β) by assuming $\beta_{sh} = \beta_{sd} = \beta_{sc}$ and solving the system of equations (8.4) of the endemic equilibrium point for the data given in Table 7.1 (after converting the mean worm burden in humans, cats, and dogs to prevalence as described in equation (8.6)). For the basic model (8.1), we multiply β_{sh} from the reservoir model by three to account for increased transmission from humans in the absence of reservoir hosts. We estimate wide ranges for the transmission parameters and the population sizes of snails and fish because we have little data on these values. Since the transmission parameters and population sizes only appear as product in the equations, the individual rates do not matter — only the product — does matter.

Variable	Mode	Range	Unit
N_h	14542	$[1454.2, 29084]$	Animals
N_s	20000	$[2000, 40000]$	Animals
N_f	8000	$[800, 16000]$	Animals
μ_{ph}	$\frac{1}{10\times365}$	$\left[\frac{1}{20\times365}, \frac{1}{1\times365}\right]$	1/Days
μ_s	$\frac{1}{1\times365}$	$\left[\frac{1}{2\times365}, \frac{1}{0.1\times365}\right]$	1/Days
μ_f	$\frac{1}{2.5\times365}$	$\left[\frac{1}{5\times365}, \frac{1}{0.25\times365}\right]$	1/Days
β_{hf}	4.898×10^{-5}	$[4.898 \times 10^{-6}, 9.795 \times 10^{-5}]$	1/(Animal x Day)
β_{sh}	9.160×10^{-11}	$[9.160 \times 10^{-12}, 1.832 \times 10^{-10}]$	1/(Animal x Day)
β_{fs}	3.477×10^{-5}	$[3.477 \times 10^{-6}, 6.954 \times 10^{-5}]$	1/(Animal x Day)

Table 8.3: Parameter values and ranges of the basic model (8.1) assuming triangular distribution.

Sample construction and maximum likelihood estimation

We use a Bayesian sampling resampling approach to better estimate parameter distributions. We first draw 100,000 sample sets of parameter values, for both the basic and the reservoir hosts models, from the prior triangular distributions with modes and ranges described in Tables 8.3 and 8.4. We filter out samples that correspond to values of $\mathcal{R}_0 < 1$. In the basic model 92,758 (93%) parameter sets correspond to $\mathcal{R}_0 > 1$ and in the reservoir hosts model 84,548 (85%) correspond to $\mathcal{R}_0 > 1$.

Variable	Mode	Range	Unit
N_h	14542	$[7271, 21813]$	Animals
N_d	7271	$[3635.5, 10906.5]$	Animals
N_c	4847	$[2423.5, 7270.5]$	Animals
N_s	20000	$[2000, 40000]$	Animals
N_f	8000	$[800, 16000]$	Animals
μ_{ph}	$\frac{1}{10\times365}$	$\left[\frac{1}{20\times365}, \frac{1}{1\times365}\right]$	1/Days
μ_{pd}	$\frac{1}{4\times365}$	$\left[\frac{1}{8\times365}, \frac{1}{0.4\times365}\right]$	1/Days
μ_{pc}	$\frac{1}{4\times365}$	$\left[\frac{1}{8\times365}, \frac{1}{0.4\times365}\right]$	1/Days
μ_s	$\frac{1}{1\times365}$	$\left[\frac{1}{2\times365}, \frac{1}{0.1\times365}\right]$	1/Days
μ_f	$\frac{1}{2.5\times365}$	$\left[\frac{1}{5\times30}, \frac{1}{0.25\times365}\right]$	1/Days
β_{hf}	4.898×10^{-5}	$[4.898 \times 10^{-6}, 9.795 \times 10^{-5}]$	1/(Animal x Day)
β_{df}	4.110×10^{-6}	$[4.110 \times 10^{-7}, 8.220 \times 10^{-6}]$	1/(Animal x Day)
β_{cf}	4.414×10^{-5}	$[4.414 \times 10^{-6}, 8.829 \times 10^{-5}]$	1/(Animal x Day)
β_{sh}	3.053×10^{-11}	$[3.053 \times 10^{-12}, 6.107 \times 10^{-11}]$	1/(Animal x Day)
β_{sd}	3.053×10^{-11}	$[3.053 \times 10^{-12}, 6.107 \times 10^{-11}]$	1/(Animal x Day)
β_{sc}	3.053×10^{-11}	$[3.053 \times 10^{-12}, 6.107 \times 10^{-11}]$	1/(Animal x Day)
β_{fs}	3.477×10^{-5}	$[3.477 \times 10^{-6}, 6.954 \times 10^{-5}]$	1/(Animal x Day)

Table 8.4: Parameter values and ranges of the model with reservoir hosts (8.4) assuming triangular distribution.

For the resampling, we calculate probabilities from the likelihood that the solution of the equations is at the equilibrium point corresponding to the data in Table 8.6 (and the eggs per gram in each human tested). We define the likelihood function L of the model with reservoir hosts (8.4) as

$$L = L_h L_d L_c L_s L_f,$$

and of the basic model (8.1) as

$$L = L_h L_s L_f,$$

where

$$L_h = \frac{n_h!}{p_h!(n_h - p_h)!} (i_h^*)^{p_h} (1 - i_h^*)^{(n_h - p_h)}, \tag{8.5a}$$

$$L_d = \frac{n_d!}{p_d!(n_d - p_d)!} (i_d^*)^{p_d} (1 - i_d^*)^{(n_d - p_d)}, \tag{8.5b}$$

$$L_c = \frac{n_c!}{p_c!(n_c - p_c)!} (i_c^*)^{p_c} (1 - i_c^*)^{(n_c - p_c)}, \tag{8.5c}$$

$$L_s = \frac{n_s!}{p_s!(n_s - p_s)!} (i_s^*)^{p_s} (1 - i_s^*)^{(n_s - p_s)}, \tag{8.5d}$$

$$L_f = \frac{n_f!}{p_f!(n_f - p_f)!} \left(i_f^*\right)^{p_f} (1 - i_f^*)^{(n_f - p_f)}, \tag{8.5e}$$

assuming that the equilibrium prevalences i_h^*, i_d^*, i_c^*, i_s^*, and i_f^* are binomially distributed. For the three mammalian hosts we need to convert the mean worm burden at the endemic equilibrium into prevalence of infection. For humans we have data on both prevalence and

intensity of infection (eggs per gram in stool for each human). We use the pre-calculated relationship from literature, $y = x^2 + 2x$ to convert the eggs per gram in stool, y, into mean worm burden, x, [28]. We assume a negative binomial distribution for the number of worms per person, leading to the relation between mean number of eggs per person (M) and the prevalence (P) [43],

$$P = 1 - \left(1 + \frac{M}{k}\right)^{-k}. \tag{8.6}$$

We assume that cats and dogs have the same relationship between mean worm burden and eggs per gram in stool and the same distribution for the number of worms per host as humans. The prevalence of infection in humans is $P = 0.6066$ (see Table 7.2) and the mean number of eggs per person is $M = 1108.2$, so from equation (8.6), $k = 0.10020566$. It follows that the prevalences in cats and dogs are

$$i_c^* = 1 - \left(1 + \frac{(w_c^*)^2 + 2w_c^*}{k}\right)^{-k},$$
$$i_d^* = 1 - \left(1 + \frac{(w_d^*)^2 + 2w_d^*}{k}\right)^{-k}.$$

We resample 2,000 sets of parameter values with probability proportional to the likelihood function with replacement[1] [105, 114].

To optimize all the infection rates (β), we maximize[2] the logarithm of the likelihood function starting from the resampled parameter set with the highest likelihood [76, 143]. The maximum likelihood estimates are shown in Table 8.5.

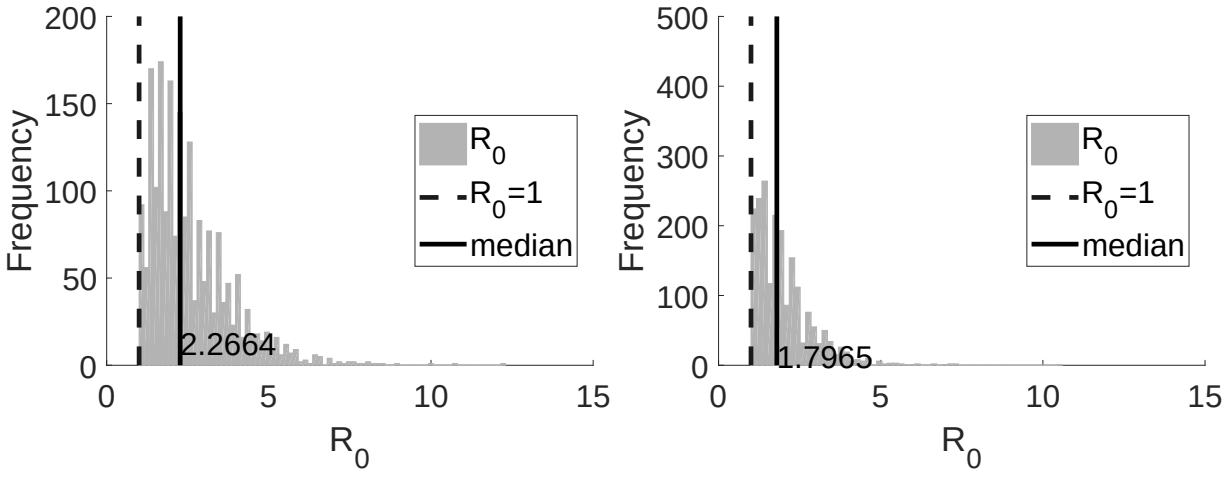

(a) Basic model. (b) Model with reservoir hosts.

Figure 8.2: Distributions of the basic reproduction number $\mathcal{R}_0$ of the basic (8.1) and the model with reservoir hosts (8.4) calculated for the resampled parameter distributions from Section 8.3.

[1] MatlabR2017a: bootstrp
[2] MatlabR2017a: fminsearch

	Basic model	Model with reservoir hosts
Parameter	MLE	MLE
β_{hf}	3.4891×10^{-5}	1.6850×10^{-5}
β_{df}	—	1.2733×10^{-6}
β_{cf}	—	1.1851×10^{-5}
β_{sh}	5.6002×10^{-11}	3.3575×10^{-11}
β_{sd}	—	5.2889×10^{-11}
β_{sc}	—	7.5833×10^{-12}
β_{fs}	4.1682×10^{-5}	2.5073×10^{-5}
N_h	$12,231$	$15,143$
N_d	—	$6,236$
N_c	—	$6,220$
N_s	$18,862$	$6,261$
N_f	$6,969$	$6,824$
μ_{ph}	$\frac{1}{1.3526\times365}$	$\frac{1}{2.8603\times365}$
μ_{pd}	—	$\frac{1}{0.7424\times365}$
μ_{pc}	—	$\frac{1}{1.6392\times365}$
μ_s	$\frac{1}{0.3580\times365}$	$\frac{1}{0.4600\times365}$
μ_f	$\frac{1}{0.4479\times365}$	$\frac{1}{2.2044\times365}$
Reproduction number		
$\mathcal{R}_0$	1.1112	1.1112

Table 8.5: Maximum likelihood estimation (MLE) and the corresponding basic reproduction number ($\mathcal{R}_0$). Units are provided in Table 8.4.

Threshold conditions

The basic reproduction number $\mathcal{R}_0$ calculated for each of these 2,000 samples is shown in Figure 8.2. Note that values of $\mathcal{R}_0 < 1$ are excluded because we assume the existence of the endemic equilibrium point. For this equilibrium point, we numerically show that all eigenvalues of the Jacobian matrix have negative real parts so it is locally asymptotically stable.

We calculate the distributions of the type reproduction numbers from the resampled distributions of the parameter values (Figure 8.3). Humans, snails, and fish belong to the reservoir community because their host-specific type-reproduction number is likely bigger than 1 ($U > 1$) and their host excluded type-reproduction number is likely smaller than 1 ($Q < 1$). Humans, snails, and fish are also maintenance-hosts, because they are the minimum set which satisfies $U > 1$. The host specific type-reproduction number of cats and dogs is smaller than 1 ($U_d, U_c < 1$), so they are non-maintenance hosts.

The host-specific type-reproduction numbers, calculated with the parameter values in

Table 8.5 from the maximum likelihood estimation, are

$$\begin{aligned} U_h &= 1.0935, & Q_h &= 0.4016, \\ U_d &= 0.2548, & Q_d &= 1.1067, \\ U_c &= 0.3640, & Q_c &= 1.0981. \end{aligned}$$

Local sensitivity analysis

The local sensitivity index is the ratio of the relative change in the variable to the relative change in the parameter. Hence, we define the normalized forward sensitivity index of a variable u and the parameter p as, see [23],

$$\Upsilon_p^u := \frac{\mathrm{d}u}{\mathrm{d}p} \times \frac{p}{u}. \tag{8.7}$$

We first use the formula in (8.7) to calculate the sensitivity index of $\mathcal{R}_0$ in the basic model (8.1) with respect to β_{hf}:

$$\begin{aligned} \Upsilon_{\beta_{hf}}^{\mathcal{R}_0} &= \frac{\mathrm{d}\mathcal{R}_0}{\mathrm{d}\beta_{hf}} \times \frac{\beta_{hf}}{\mathcal{R}_0} = \frac{1}{3\beta_{hf}^{\frac{2}{3}}} \sqrt[3]{\frac{\beta_{sh}\beta_{fs}N_hN_sN_f}{\mu_{ph}\mu_s\mu_f}} \times \frac{\beta_{hf}}{\sqrt[3]{\frac{\beta_{hf}\beta_{sh}\beta_{fs}N_hN_sN_f}{\mu_{ph}\mu_s\mu_f}}} \\ &= \frac{1}{3}. \end{aligned}$$

The calculation is similar for the sensitivity indices of $\mathcal{R}_0$ with respect to β_{sh},β_{fs},N_h,N_s and N_f. For the sensitivity indices of $\mathcal{R}_0$ with respect to μ_{ph}, μ_s and μ_f we have, for example,

$$\begin{aligned} \Upsilon_{\mu_{ph}}^{\mathcal{R}_0} &= \frac{\mathrm{d}\mathcal{R}_0}{\mathrm{d}\mu_{ph}} \times \frac{\mu_{ph}}{\mathcal{R}_0} = -\frac{1}{3\mu_{ph}^{\frac{4}{3}}} \sqrt[3]{\frac{\beta_{hf}\beta_{sh}\beta_{fs}N_hN_sN_f}{\mu_s\mu_f}} \times \frac{\mu_{ph}}{\sqrt[3]{\frac{\beta_{hf}\beta_{sh}\beta_{fs}N_hN_sN_f}{\mu_{ph}\mu_s\mu_f}}} \\ &= -\frac{1}{3}. \end{aligned}$$

Therefore if, for example, β_{hf} increases by 100%, then $\mathcal{R}_0$ increases by 33%. If μ_{ph} increases by 100%, then $\mathcal{R}_0$ decreases by 33%. Since the sensitivity index of $\mathcal{R}_0$ is independent of any other parameters, it is valid locally and globally. Due to the same absolute value of the sensitivity index, all parameters are equally important for $\mathcal{R}_0$. This is shown in Figure 8.4.

The sensitivity index of the state variables at the endemic equilibrium of the basic model is for example

$$\begin{aligned} \frac{\mathrm{d}w_h^*}{\mathrm{d}\beta_{hf}} \times \frac{\beta_{hf}}{w_h^*} &= \frac{\beta_{sh}\beta_{fs}N_hN_fN_s}{\beta_{sh}N_h\mu_{ph}(\beta_{fs}N_s+\mu_f)} \times \beta_{hf}\frac{\beta_{sh}N_h\mu_{ph}(\beta_{fs}N_s+\mu_f)}{\beta_{hf}\beta_{sh}\beta_{fs}N_hN_fN_s-\mu_{ph}\mu_s\mu_f} \\ &= \frac{\beta_{hf}\beta_{sh}\beta_{fs}N_hN_fN_s}{\beta_{hf}\beta_{sh}\beta_{fs}N_hN_fN_s-\mu_{ph}\mu_s\mu_f}. \end{aligned}$$

Figure 8.5 (a) shows the sensitivity index of w_h^* for the parameter values from Table 8.3.

The local sensitivity analysis for the model with reservoirs host (8.4) is performed as described in formula (8.7). we got analytical expressions with similar calculations to those for the basic model, but they are not shown here due to their length. The results for $\mathcal{R}_0$ are shown in Figure 8.4 (b) and the results for w_h^* are shown in Figure 8.5 (b).

Global sensitivity analysis and numerical simulation

We use partial rank correlation coefficients (PRCC) to analyse the sensitivity globally and to compare the influence of the parameters on $\mathcal{R}_0$ and on the endemic equilibrium point. To calculate the PRCC, we used the Matlab implementation of the PRCC function developed in [72][3]. The function was run on the 2,000 samples from Section 8.3.

Figures 8.4 (c) and (d) show, from the top to the bottom, the influence of the change in the parameter on $\mathcal{R}_0$ and Figures 8.5 (c) and (d) show the influence on w_h^* in the basic model (8.1) and in the model with reservoir hosts (8.4). The closer the absolute value is to one, the more influence the parameter has on the output.

In the basic model (8.1), the death rate of snails (μ_s) has the most global influence on $\mathcal{R}_0$, followed by the death rate of parasites in humans (μ_{ph}) and the death rate of fish (μ_f). However there is little difference between the parameter values, so the basic model is not able to differentiate between the sensitivity of the parameters on $\mathcal{R}_0$. For the model with reservoir hosts (8.4), the death rates of snails and fish (μ_s, μ_f), followed by death rate of parasites in humans (μ_{ph}) have the most global influence on $\mathcal{R}_0$.

The death rate of parasites in humans (μ_{ph}) has the most global influence on the mean worm burden of humans at the endemic equilibrium point w_h^* in both models, followed by the fish to human transmission rate (β_{hf}) and the number of fish (N_f).

In Figure 8.6 we show two dimensional sensitivity analysis of $\mathcal{R}_0$ (of both models) to the population sizes of the five hosts with all other parameters as in Table 8.5. Figure 8.6 (a) shows the dependence of $\mathcal{R}_0$ of the basic model (8.1) when the numbers of snails (N_s) and fish (N_f) are varied. $\mathcal{R}_0$ depends more strongly on the population size of snails than of fish. The sensitivity of $\mathcal{R}_0$ for the model with reservoir hosts (8.4) is presented in Figures 8.6 (b)–(d). Figure 8.6 (b) shows the variation of $\mathcal{R}_0$ to the number of snails (N_s) and fish (N_f). Similar to the basic model, $\mathcal{R}_0$ increases faster with more snails faster than with more fish. In Figure 8.6 (c), we see that $\mathcal{R}_0$ increases faster with the number of dogs (N_d) than with the number of cats (N_c). Figure 8.6 (d) shows that when the numbers of humans (N_h) and cats (N_c) are varied, $\mathcal{R}_0$ increases more rapidly with the number of cats.

We show numerical simulations of the basic model (8.1) and of the model with reservoir hosts (8.4) in Figure 8.7. For both models the parameter values are given in Table 8.5 and the initial conditions are $w_h = 1$, $w_d = 1$, $w_c = 1$, $i_s = 0$ and $i_f = 0$. We use the

[3]http://malthus.micro.med.umich.edu/lab/usanalysis.html (24.10.2016)

Dormand-Prince method [4] to integrate over the time interval $[0, 70000]$, which corresponds to a time period of 190 years.

[4] MatlabR2017a: ode45

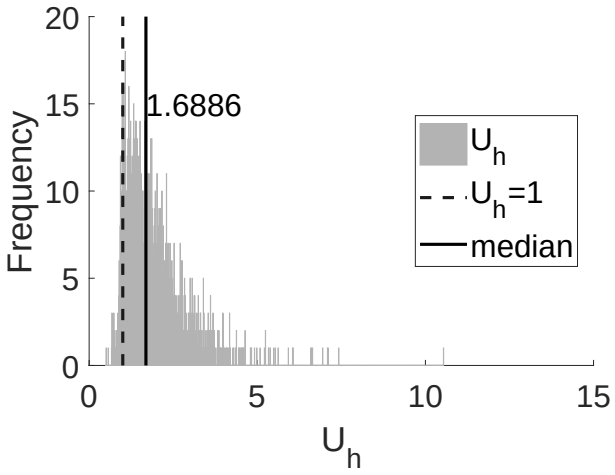

(a) $U_{h,s,f} = Q_{c,d}$; $P(U_h > 1) = 0.92$

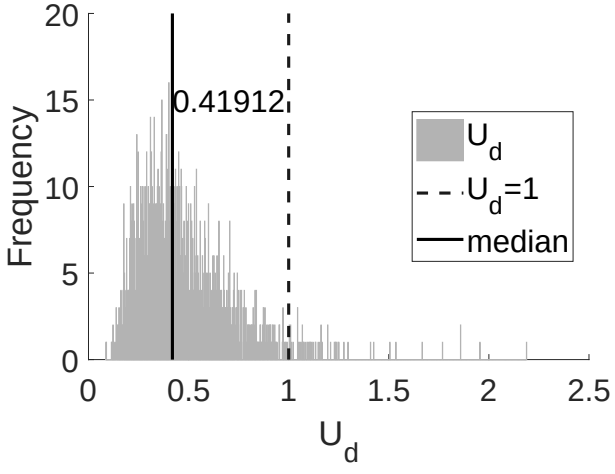

(b) $U_{d,s,f} = Q_{h,c}$; $P(U_d > 1) = 0.28$

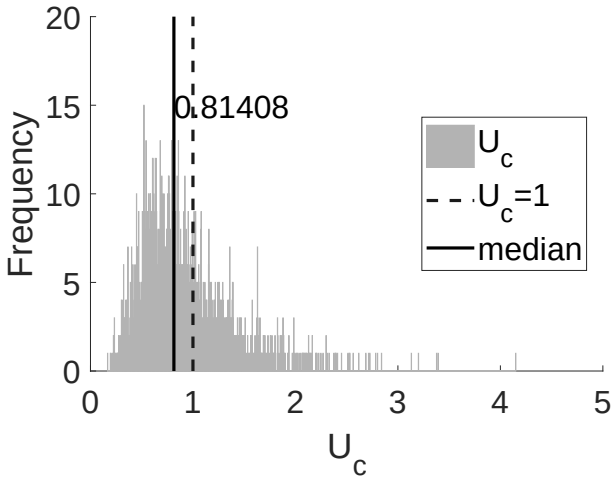

(c) $U_{c,s,f} = Q_{h,d}$; $P(U_c > 1) = 0.33$

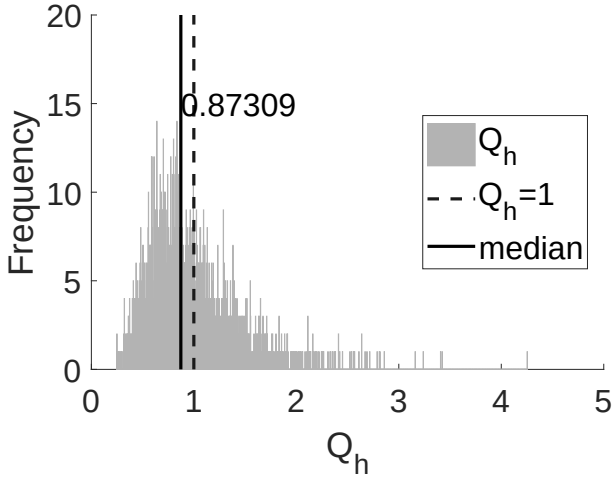

(d) $Q_h = U_{c,d,s,f}$; $P(Q_h > 1) = 0.38$

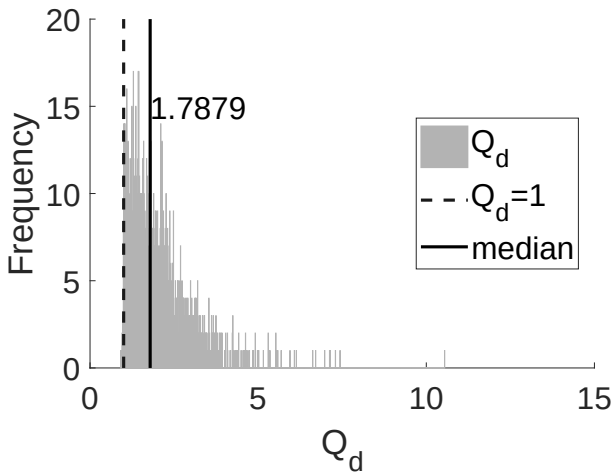

(e) $Q_d = U_{h,c,s,f}$; $P(Q_d > 1) = 0.99$

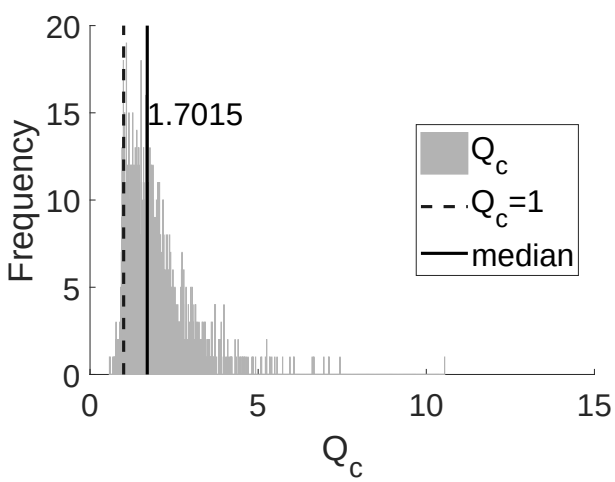

(f) $Q_c = U_{h,d,s,f}$; $P(Q_c > 1) = 0.94$

Figure 8.3: Distributions of the host-specific type-reproduction numbers of the model with reservoir hosts (8.4) calculated from the resampled parameter distributions from Section 8.3 and the probability that the number is above 1.

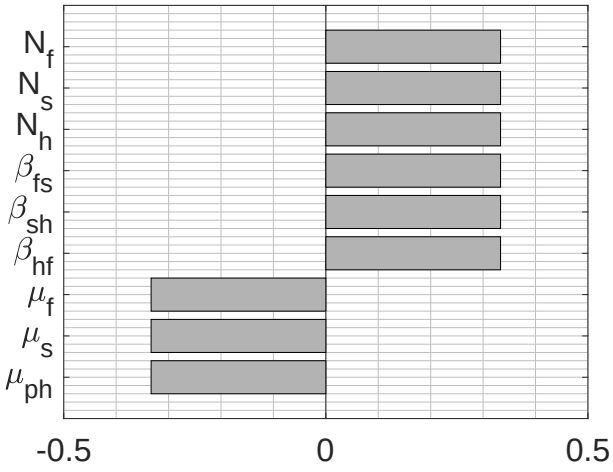

(a) Basic model: Sensitivity index.

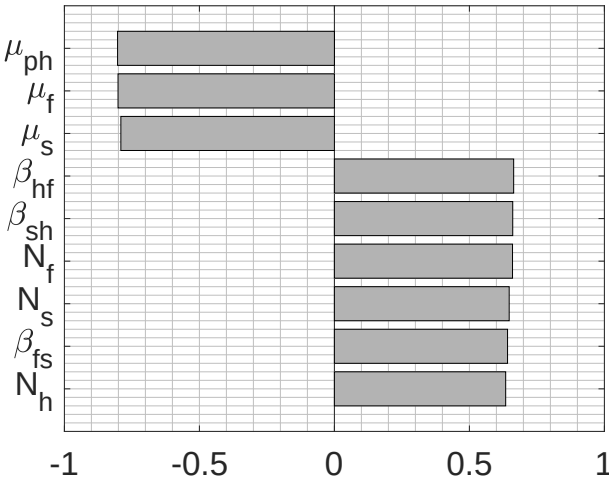

(c) Basic model: PRCC.

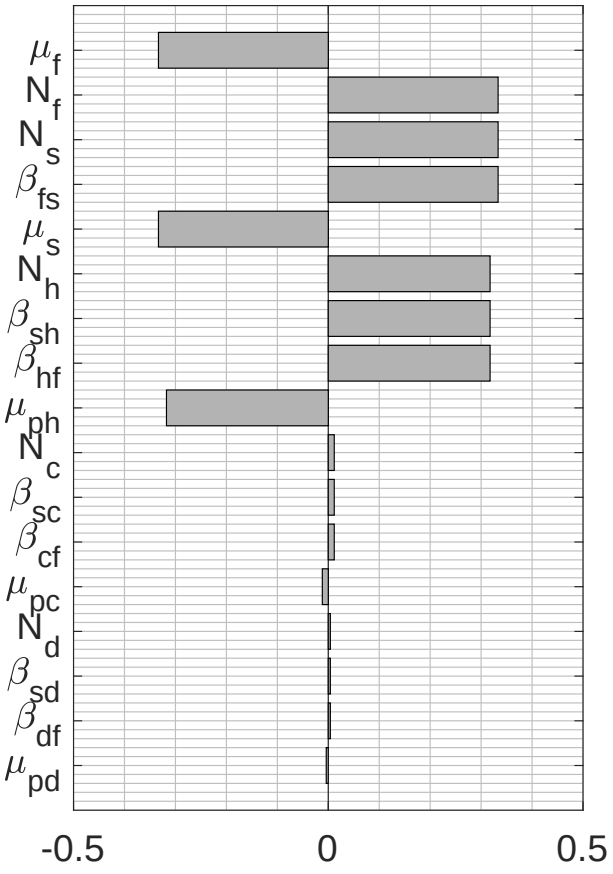

(b) Model with reservoir hosts: Sensitivity index.

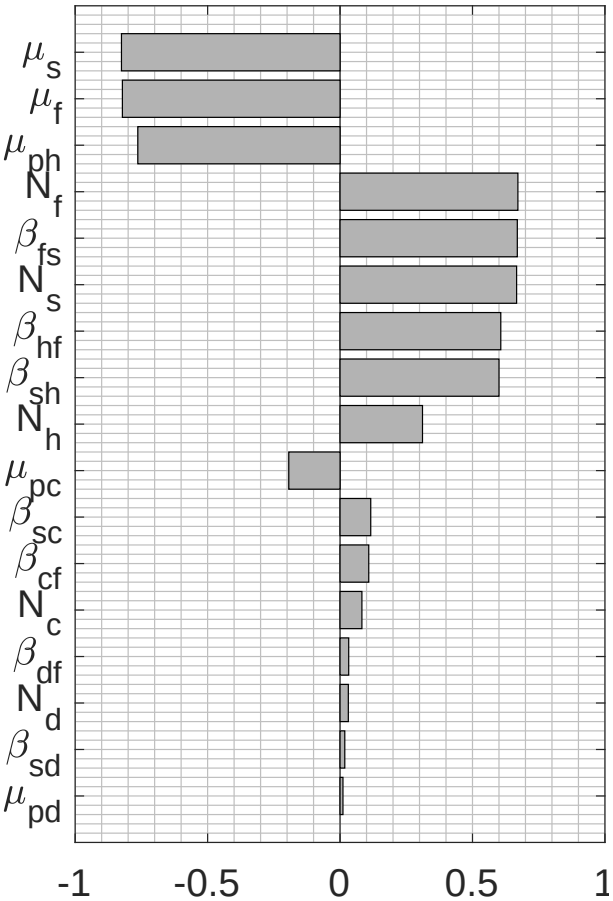

(d) Model with reservoir hosts: PRCC.

Figure 8.4: Local sensitivity indices and partial rank correlation coefficients (PRCC) of the basic reproduction number $\mathcal{R}_0$ for the basic model (8.1) and the model with reservoir hosts (8.4).

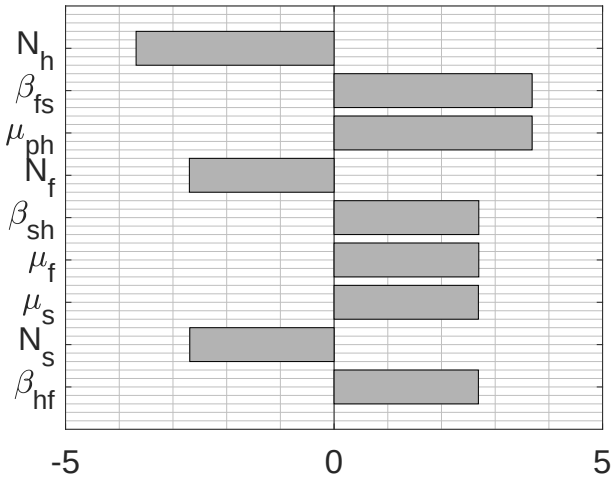

(a) Basic model: Sensitivity index.

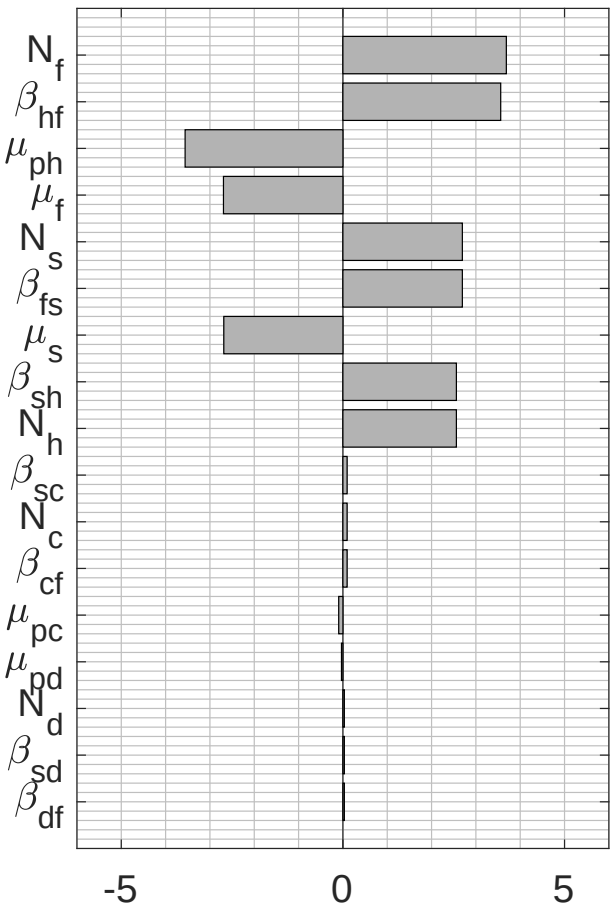

(b) Model with reservoir hosts: Sensitivity index.

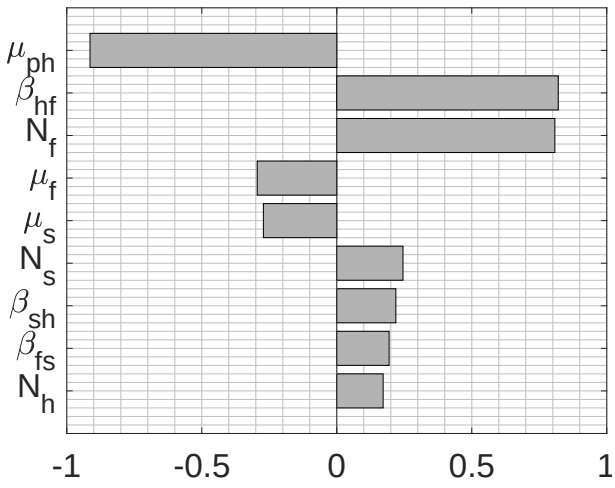

(c) Basic model: PRCC.

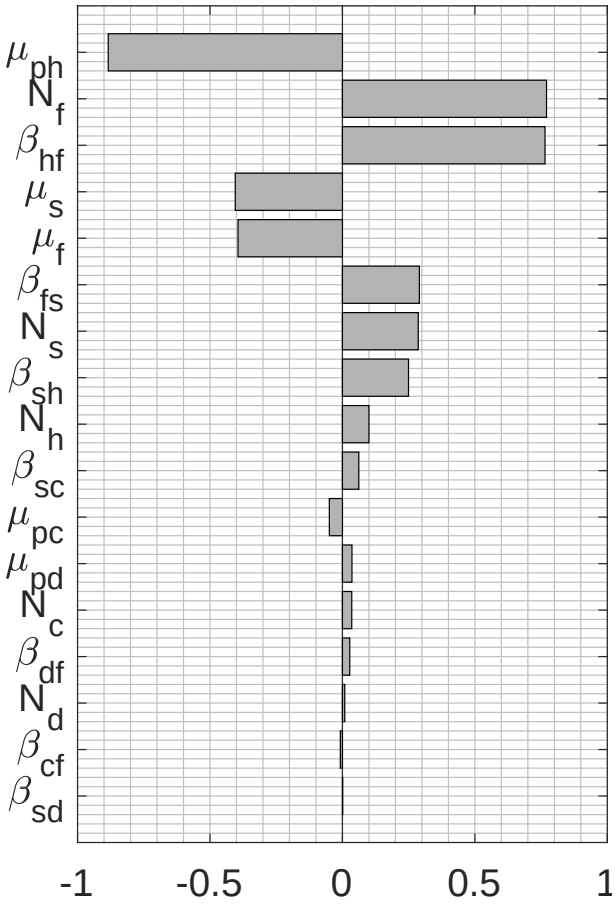

(d) Model with reservoir hosts: PRCC.

Figure 8.5: Local sensitivity indices and partial rank correlation coefficients (PRCC) of mean worm burden in humans at the endemic equilibrium point w_h^* of the basic model (8.1) and the model with reservoir hosts (8.4).

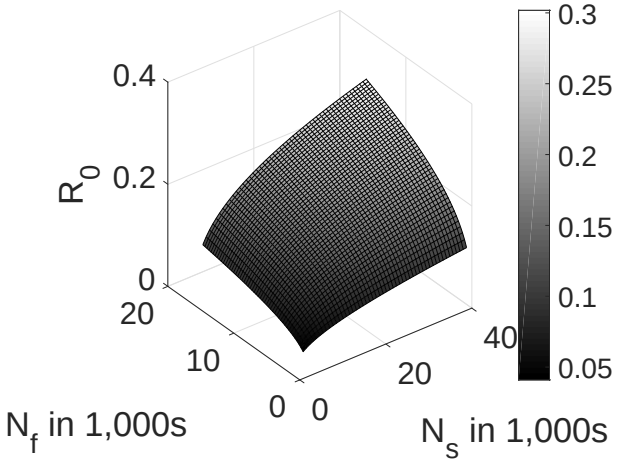

(a) Basic model: N_s and N_f.

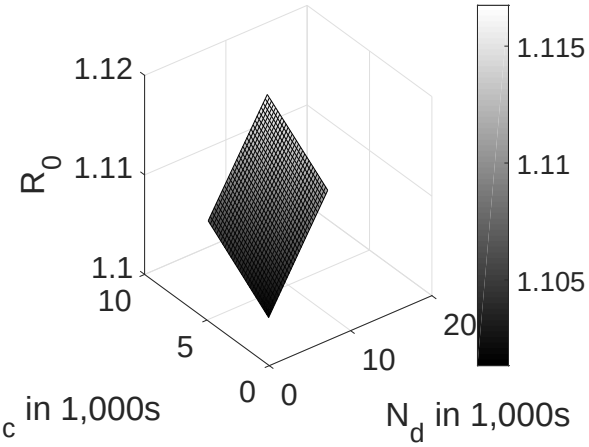

(c) Model with reservoir hosts: N_d and N_c.

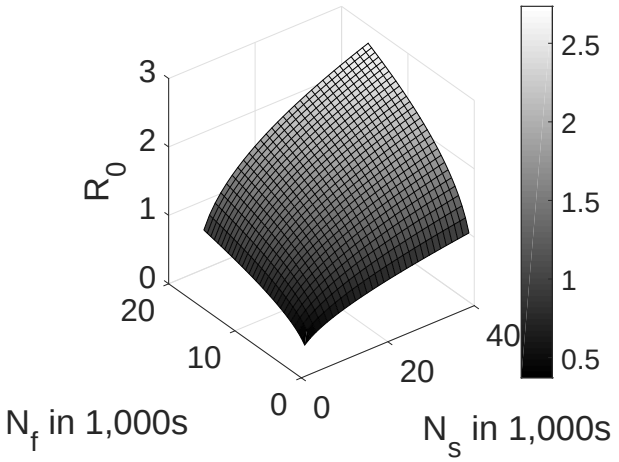

(b) Model with reservoir hosts: N_s and N_f.

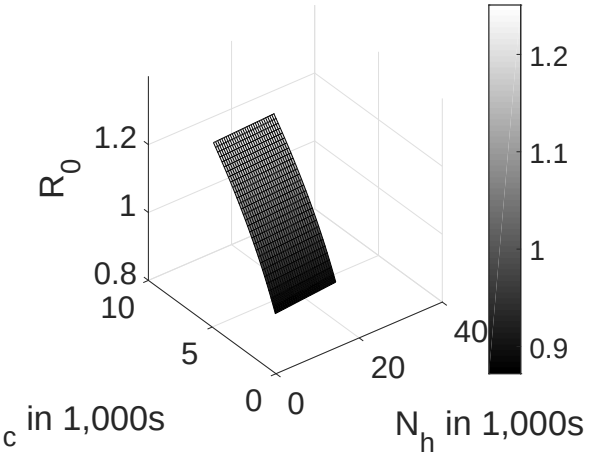

(d) Model with reservoir hosts; N_h and N_c.

Figure 8.6: Basic reproduction number $\mathcal{R}_0$ for the basic model (8.1) and the model with reservoir hosts (8.4) varying population sizes of two hosts with all other parameters as in Table 8.5.

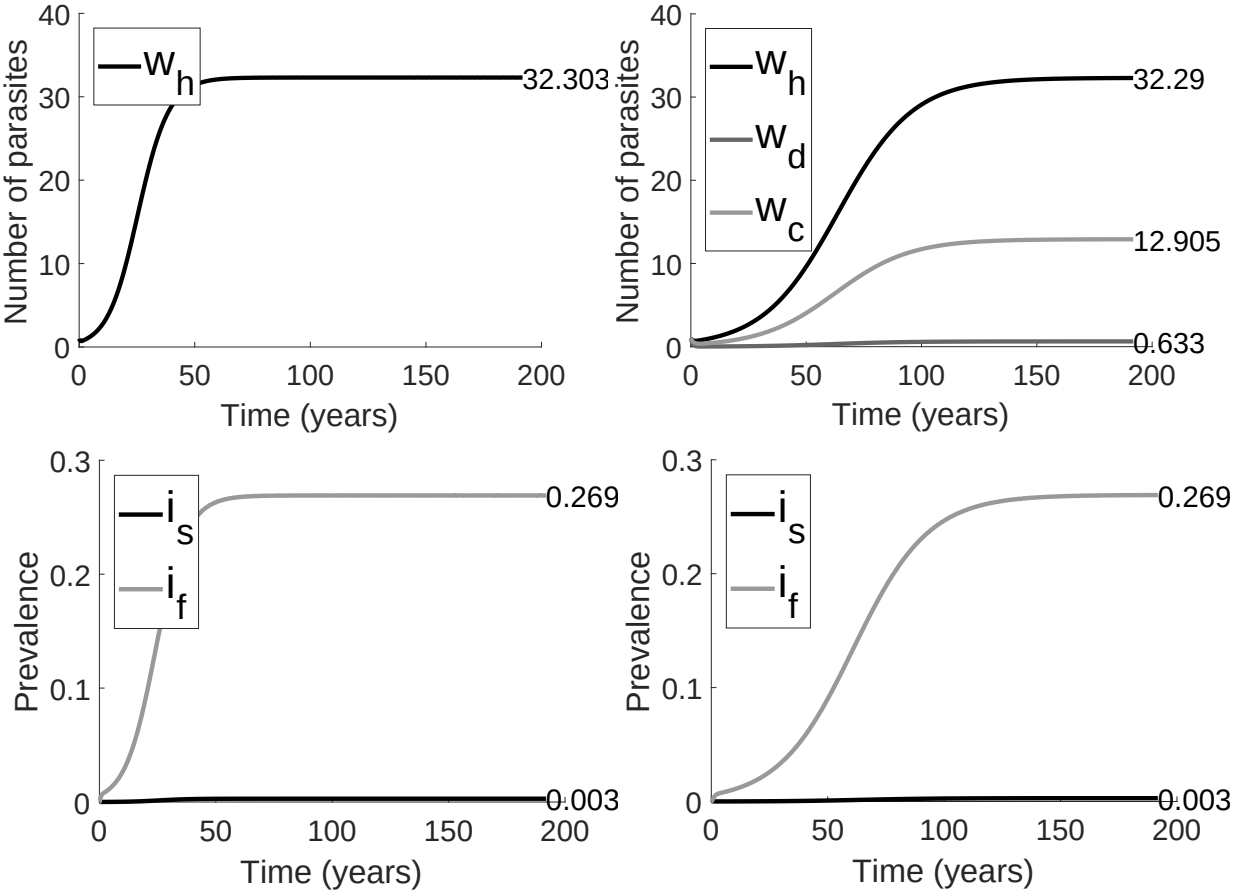

(a) Basic model.

(b) Model with reservoir hosts.

Figure 8.7: Numerical simulations of the opisthorchiasis models (8.1) and (8.4) with the Dormand-Prince method over a time line of 70,000 days. The initial values are 1 for the worm burdens and 0 for the prevalences. The parameter values are in Table 8.5.

9. Model with interventions

The model with interventions includes humans, dogs and cats as definitive hosts and snails and fish as intermediate hosts. We simulate the mean worm burden in humans, dogs and cats and the prevalence of infection in fish and snails. After developing the model, we estimate the unknown parameters using data from Lao PDR, see Chapter 7. Distributions of unknown parameters of this model were estimated by a Bayesian sampling resampling approach and point estimates with maximum likelihood estimation using data collected from the two islands in Lao PDR analogous to Section 8.3. We define the basic as well as the control reproduction numbers of the model. This helps us to determine the minimum coverage of each intervention. Then, we optimise targeted coverage levels with the optimal control method. Finally we investigate the elimination potential of interventions by estimating the time to and probability of achieving elimination as a public health problem of *O. viverrini* in 20 years.

9.1 General mathematical model with interventions

We extend the previous model with reservoir hosts of *O. viverrini* (8.4) to include the effects of interventions. We model the interventions as

(i) education campaigns to reduce the consumption of raw or undercooked fish: we let I_e denote the coverage successfully achieved by the education campaign, that is, the proportion of people who do not get further infected by eating raw or undercooked fish.

(ii) improved sanitation to stop transmission from humans to snails: we let I_d denote the coverage of improved sanitation, that is the proportion of people who stop defecating outdoors because of the improved sanitation.

(iii) mass drug administration: we let I_m denote the proportion of people treated annually (except for campaigns at lower frequencies as described later).

Assuming γ is the rate per unit time of treating people, then

$$\exp(-\gamma \times T_\gamma) = 1 - I_m$$

is the proportion of untreated humans with T_γ as the time interval of treatment in days [12]. It follows that the treatment rate is

$$\gamma = \frac{-\log(1 - I_m)}{T_\gamma}.$$

The full model is given by the ODE system,

$$\frac{\mathrm{d}w_h(t)}{\mathrm{d}t} = \beta_{hf} N_f i_f(t)(1 - I_e) - \left(\mu_{ph} - \frac{\log(1 - I_m(t))}{T_\gamma}\right) w_h(t), \tag{9.1a}$$

$$\frac{\mathrm{d}w_d(t)}{\mathrm{d}t} = \beta_{df} N_f i_f(t) - \mu_{pd} w_d(t), \tag{9.1b}$$

$$\frac{\mathrm{d}w_c(t)}{\mathrm{d}t} = \beta_{cf} N_f i_f(t) - \mu_{pc} w_c(t), \tag{9.1c}$$

$$\frac{\mathrm{d}i_s(t)}{\mathrm{d}t} = (\beta_{sh} N_h w_h(t)(1 - I_d) + \beta_{sd} N_d w_d(t) + \beta_{sc} N_c w_c(t))(1 - i_s(t)) - \mu_s i_s(t), \tag{9.1d}$$

$$\frac{\mathrm{d}i_f(t)}{\mathrm{d}t} = \beta_{fs} N_s i_s(t)(1 - i_f(t)) - \mu_f i_f(t), \tag{9.1e}$$

where the state variables are shown in Table 8.1 and the parameters in Table 8.2 and Table 9.1.

We model the mean worm burden per human host, w_h, assuming a negative binomial distribution for the distribution of worms in humans. We assume no correlation between the worm burden of an individual and the probability of being influenced by the education campaign to stop eating raw fish, so the transmission rate from fish to humans is proportionally reduced by $(1 - I_e)$. The worms die naturally in humans, $\mu_{ph} w_h$, or because of treatment, $\frac{-\log(1-I_m(t))}{T_\gamma} w_h$. We make the implicit assumption that there is no correlation between worm burden and the likelihood of being treated. Hence, the proportion of people getting treated (with the assumption that treatment is perfect) is equal to killing this proportion of worms in humans. The infection rate of snails depends on the proportion of people who have access to a latrine and do not defecate outdoors. Making the implicit assumption that access to a latrine is not correlated with worm burden, improved sanitation proportionally reduces the transmission from humans to snails by $(1 - I_d)$.

Parameter	Description	Dimension
I_e	Proportion of people who stop eating raw fish due to intervention	Dimensionless
I_d	Proportion of people who stop defecating outdoors due to intervention	Dimensionless
$I_m(t)$	Proportion of people getting treatment (medication) at time t	Dimensionless
T_γ	Interval of drug distribution	Time

Table 9.1: Addditional internvention parameters of the opisthorchiasis model with interventions.

We use the data in Chapter 7 from the Champasack province, Lao PDR (see Table 7.1).

To get a distribution of uncertainty, we estimate the parameters with a different number of sample. To estimate $\beta = (\beta_{hf}, \beta_{df}, \beta_{cf}, \beta_{sd}, \beta_{sc}, \beta_{sh}, \beta_{fs})$, we followed the Bayesian resampling approach in Section 8.3 with the same parameter ranges as in Table 8.4 and no intervention $I_e = I_d = I_m = 0$, followed by the maximum likelihood estimation (MLE) method. We sample 50,000 parameter sets and resample 500 of them in the Bayesian

resampling approach. The final estimate with MLE is found in Table 9.2. Due to the re-estimation we got slightly different values for the parameters.

We simulate the ODE system (9.1) with the Runge-Kutta 4 method with the initial value I estimate from the data, $(w_h(0), w_d(0), w_c(0), i_s(0), i_f(0)) = (33, 3, 13, 0.003, 0.3)$, and time steps in days up to 20 years. The numerical results of the model with parameter values from the MLE are presented in Figure 9.1. To show the uncertainty of the parameter sets, we also illustrate the median, the mean and the standard deviation of the 500 parameter sets in Figure 9.1.

Variable	MLE
N_h	15705
N_d	8437
N_c	6098
N_s	31019
N_f	9701
μ_{ph}	$\frac{1}{4.8\times365}$
μ_{pd}	$\frac{1}{2.2\times365}$
μ_{pc}	$\frac{1}{1.5\times365}$
μ_s	$\frac{1}{1\times365}$
μ_f	$\frac{1}{1.5\times365}$
β_{hf}	5.9785×10^{-6}
β_{df}	3.2337×10^{-7}
β_{cf}	2.9608×10^{-6}
β_{sh}	1.0210×10^{-11}
β_{sd}	2.8635×10^{-11}
β_{sc}	4.7734×10^{-12}
β_{fs}	1.2900×10^{-5}

Table 9.2: Parameter estimations with the maximum likelihood method, units are shown in Table 8.4.

9.2 Model with continuous treatment

We first assume continuous treatment with I_m constant throughout the year and $T_\gamma = 365$ days in the model, which refers to a daily treatment rate while coverage is defined as the proportion of people treated within one year (as described above). We model continuous treatment, as it allows us to calculate the basic and the control reproduction number and to determine the threshold value of coverage where the control reproduction number is equal to one.

Basic and control reproduction number

The basic reproduction number $\mathcal{R}_0$ is the average number of new offspring per parasite in the next step of the life cycle assuming no density dependence and no interventions.

It is calculated as the spectral radius of the next-generation matrix [27]. The cubic spectral radius is equal to the number of adult offspring in mammalian hosts from one adult worm in a mammalian host. It follows that, when the basic reproduction number is below one ($\mathcal{R}_0 < 1$), the parasite cannot produce enough offspring to persist. The control reproduction number $\mathcal{R}_c$ includes the impact of interventions on the reproduction number. The next-generation matrix $\mathbf{K}$ of the model (9.1), with constant I_m, is given by

$$\mathbf{K} = \begin{bmatrix} 0 & 0 & 0 & 0 & \frac{\beta_{hf} N_f (1-I_e)}{\mu_f} \\ 0 & 0 & 0 & 0 & \frac{\beta_{df} N_f}{\mu_f} \\ 0 & 0 & 0 & 0 & \frac{\beta_{cf} N_f}{\mu_f} \\ \frac{\beta_{sh} N_h (1-I_d)}{\mu_{ph} - \frac{\log(1-I_m)}{T_\gamma}} & \frac{\beta_{sd} N_d}{\mu_{pd}} & \frac{\beta_{sc} N_c}{\mu_{pc}} & 0 & 0 \\ 0 & 0 & 0 & \frac{\beta_{fs} N_s}{\mu_s} & 0 \end{bmatrix},$$

assuming that treatment is distributed continuously. Its spectral radius, and therefore the control reproduction number of the model, is given by the expression,

$$\mathcal{R}_c = \left(\frac{N_s N_f \beta_{fs} (\mu_{ph} T_\gamma - \log(1-I_m))(N_d \beta_{df} \beta_{sd} \mu_{pc} + N_c \beta_{cf} \beta_{sc} \mu_{pd})}{(\mu_{ph} T_\gamma - \log(1-I_m)) \mu_{pd} \mu_{pc} \mu_s \mu_f} + \frac{N_s N_f \beta_{fs} (1 - I_d - I_e + I_d I_e)(T_\gamma N_h \beta_{hf} \beta_{sh} \mu_{pd} \mu_{pc})}{(\mu_{ph} T_\gamma - \log(1-I_m)) \mu_{pd} \mu_{pc} \mu_s \mu_f} \right)^{\frac{1}{3}}.$$

The basic reproduction number,

$$\mathcal{R}_0 = \left(\frac{N_s N_f \beta_{fs} (N_d \beta_{df} \beta_{sd} \mu_{pc} + N_c \beta_{cf} \beta_{sc} \mu_{pd} + N_h \beta_{hf} \beta_{sh} \mu_{pd} \mu_{pc})}{\mu_{ph} \mu_{pd} \mu_s \mu_f} \right)^{\frac{1}{3}},$$

is equal to the control reproduction number $\mathcal{R}_c$ if the coverage of all interventions is 0 (no interventions in the population). The basic reproduction number is $\mathcal{R}_0 = 1.1351$ with the MLE parameter values given in Table 9.2.

The control reproduction number depends on the type and coverage of the intervention. Figure 9.2, shows the impact of coverage of each intervention applied singly on the control reproduction number for parameter values determined by MLE and $T_\gamma = 365$ days. The control reproduction number $\mathcal{R}_c$ has a similar dependence on the level of coverage of education campaigns (I_e) and improved sanitation (I_d). The coverage needs to be at least 34% for either of these two interventions for $\mathcal{R}_c$ to be below 1. The coverage of the mass drug administration (I_m) has a much stronger effect on the control reproduction number than the coverage of the education campaign (I_e) and improved sanitation (I_d). The control reproduction number for mass drug administration decreases below 1 at the low coverage of 10%. Figure 9.2 also shows that the incremental effectiveness of the interventions in reducing $\mathcal{R}_c$ increases with coverage for improved sanitation and education campaign but decreases for mass treatment. Therefore, programmes should try to achieve a coverage of education campaigns and improved sanitation as high as possible, but a moderate coverage of mass treatment may be sufficient.

The possible combination of the interventions I_e and I_d (without I_m) which are successful in achieving $\mathcal{R}_c < 1$, for MLE parameter values, are shown in Figure 9.3. The minimum combination such that $\mathcal{R}_c < 1$ is $I_e = I_d = 0.2025$.

9.3 Model with pulsed treatment

We also develop a model with pulsed treatment applied at a fixed frequency. This model takes into account the fact that the number of worms increases in humans in between mass drug administration campaigns. For example, treatment once a year, conducted over one day, is modelled by,

$$I_m(t) = \begin{cases} I_m, & t \mod 365 = 1, \\ 0, & \text{else}, \end{cases}$$

with $T_\gamma = 1$ day.

This model allows us to additionally consider the effect of frequency of the mass drug administration campaigns on the probability of elimination and time to elimination. We also calculate the optimal coverage of the mass drug administration and education campaigns using optimal control theory.

Effectiveness of interventions

The minimum levels of coverage we calculated with continuous treatment, where $\mathcal{R}_c = 1$, are not sufficient to reach a low mean worm burden in humans in 20 years. Hence, we simulate reasonably achievable coverage levels of $I_e \in \{0.2, 0.4, 0.6\}$ and $I_d, I_m \in \{0.4, 0.6, 0.8\}$. We choose these coverage levels because we assume that it is more difficult to changes people's eating habit through education campaigns. Then to convince them to use a latrine or accept treatment. Mass drug administration is assumed to be distributed over one day once a year. Figure 9.4 shows the numerical solutions for all state variables for each intervention at these different levels of coverage compared to no interventions.

To investigate the impact of the frequency of distribution of mass drug administration, we simulate campaigns distributing drugs every 0.5, 1, 2, 3 and 4 years. Hence, $I_m(t)$ is the proportion of humans who receive a drug against *O. viverrini* in every drug distribution campaign. The influence of the choice of the frequency on the mean worm burden in humans with different levels of coverage is shown in Figure 9.5.

Optimal control

To synchronously optimise the level of coverage of the education campaign (I_e) and the mass drug administration (I_m) in the model, we use the optimal control method. We do not try to optimise the sanitation coverage because we assume that any programme would

try to maximise sanitation for all its additional health benefits. We focus on optimising interventions that are targeted against *O. viverrini*. To fulfil the linearity property of the right-hand side of the model (9.1), we optimise the treatment rate,

$$\gamma(t) = -\frac{\log(1 - I_m(t))}{365},$$

instead of the proportion $I_m(t)$, because $I_m(t)$ and correspondingly $\gamma(t)$ are piecewise constant for a pulsed treatment rate. Since the treatment distribution occurs once a year, we have a rate $\gamma(t)$ of treated people with the properties,

$$\gamma(t) = \begin{cases} \gamma_k, & t \mod 365 = 1, \\ 0, & \text{else}, \end{cases}$$

with the annual rate γ_k for $k = 1, \ldots, n$, $n \in \mathbb{N}$. The first equation of the ODE system (9.1) becomes

$$\frac{\mathrm{d}w_h(t)}{\mathrm{d}t} = \beta_{hf} N_f i_f(t)(1 - I_e) - (\mu_{ph} + \gamma(t))w_h(t). \tag{9.2}$$

Minimising the coverage of the interventions affecting humans leads to the optimal control problem,

$$\min_{I_e,\gamma} \int_0^T w_h^2(t) + \frac{\alpha^2}{2}\left(I_e(t)^2 + \sum_{k=1}^{n} \gamma_k^2\right) \mathrm{d}t,$$

with the weight $\alpha = 0.001$, the time $T = 20 \times 365$ (in days), $n = \frac{T}{365}$, $0 \leq I_e(t) \leq 0.9$ and $0 \leq \gamma_k \leq 0.0016$, which is equivalent to $0 \leq I_m = 1 - \exp(\gamma_k \times 365) \leq 0.8$ for each $k = 1, \ldots, n$. The regularisation parameter α prioritises the minimisation of the mean worm burden instead of the coverage level. The optimal control solutions are robust with respect to this parameter, as the results are similar even with $\alpha = 1$. We assume that it is not possible to reach all people by either campaign, and that the maximum achievable coverage of drug distribution is 80%, while it is 90% of education campaigns.

To simplify the notation, we write $I_e(t) = \bar{I}_e$, $\gamma(t) = \bar{\gamma}$ and $(I_e, \gamma_1 \ldots, \gamma_n) = \bar{I}$. We use the definitions

$$L(t, w_h, \bar{I}) := w_h^2(t) + \frac{\alpha^2}{2}\left(\bar{I}_e^2 + \sum_{k=1}^{n} \gamma_k^2\right)$$

as the integrand; $\frac{\mathrm{d}f}{\mathrm{d}t} = f(x,t)$ with $x = (w_h, w_d, w_c, i_s, i_f)$ as our ODE model (9.1), so $f_i = f(x(i), t)$ for $i = 1, \ldots, 5$;

$$J(\bar{I}) = \int_0^T w_h^2(t) + \frac{\alpha^2}{2}\left(\bar{I}_e^2 + \sum_{k=1}^{n} \gamma_k^2\right) \mathrm{d}t$$

as the integral to minimise and

$$U = \{\bar{I}(t) | \bar{I}(t) \in [0, 0.9] \times [0, 0.0016]^n, t \in [0, T]\}.$$

In order to show that a solution exists to this optimal control problem, we have to prove the following assumptions [31, 64]:

Proposition 1 (Existence)**.** *i) The set of solutions of the ODE system* (9.1) *is not empty and the right-hand side is continuous and bounded.*

ii) U is closed and convex and f can be written as

$$f(t, w_h, \bar{I}_e, \bar{\gamma}) = a(t, w_h) + b(t, w_h)\bar{I}_e + c(t, w_h)\bar{\gamma}.$$

iii) $L(t, w_h, \cdot)$ is convex on U.

Proof. i) The ODE system (9.1) is well-posed in the strip $S \subseteq \mathbb{R}^5$, which is defined by the boundaries of the system's solution for $(w_h, w_d, w_c, i_s, i_f)$:

$$S = \left[0, \beta_{hf}\frac{N_f}{\mu_{ph}}\right] \times \left[0, \frac{\beta_{df}N_f}{\mu_{pd}}\right] \times \left[0, \frac{\beta_{cf}N_f}{\mu_{pc}}\right] \times [0,1]^2.$$

The right-hand side of the system is well-posed and with continuous partial derivatives. The proof of the existence and uniqueness of the solution of the model (9.1) can be found in Section 8.2.

The right-hand side of the ODE system (9.1) is clearly continuous and bounded in the strip $\tilde{S} \subseteq \mathbb{R}^5$, given by

$$\begin{aligned}\tilde{S} = &[-\beta_{hf}N_f, \beta_{hf}N_f] \times [-\beta_{df}N_f, \beta_{df}N_f] \times [-\beta_{cf}N_f, \beta_{cf}N_f] \\ &\times \left[-\mu_s, \frac{\beta_{sh}N_h\beta_{hf}N_f}{\mu_{ph}}\right] \times [-\mu_f, N_s\beta_{fs}].\end{aligned}$$

ii) U is closed and convex because it is a Cartesian product of closed intervals. f can be written as a linear combination of the form

$$f(t, w_h, \bar{I}_e, \bar{\gamma}) = a(t, w_h) + b(t, w_h)\bar{I}_e + c(t, w_h)\bar{\gamma},$$

where

$$f_1(t, w_h, \bar{I}_e, \gamma) = \underbrace{\beta_{hf}N_f i_f - w_h}_{a(t,w_h)} + \underbrace{(-\beta_{hf}N_f i_f)}_{b(t,w_h)}\bar{I}_e + \underbrace{(w_h)}_{c(t,w_h)}\bar{\gamma}.$$

The linear combination for the other system of equations (f_2, f_3, f_4, f_5) looks similar.

iii) To show that $L(t, w_h, \cdot)$ is convex on U, we must have

$$L(t, w_h, (1-\epsilon)\bar{I}_1 + \epsilon\bar{I}_2) \leq (1-\epsilon)L(t, w_h, \bar{I}_1) + \epsilon L(t, w_h, \bar{I}_2)$$

for $\bar{I}_1, \bar{I}_2 \in \bar{I}$. Indeed, it holds

$$\begin{aligned}&L(t, w_h, (1-\epsilon)\bar{I}_1 + \epsilon\bar{I}_2) \\ &= w_h^2 + \frac{\alpha^2}{2}\left(\left((1-\epsilon)\bar{I}_{e,1} + \epsilon\bar{I}_{e,2}\right)^2 + \left((1-\epsilon)\sum_{k=1}^{n}\gamma_{k,1}(t) + \epsilon\sum_{k=1}^{n}\gamma_{k,2}(t)\right)^2\right) \\ &\leq (1-\epsilon)\left(w_h^2 + \frac{\alpha^2}{2}\left(\bar{I}_e^2 + \sum_{k=1}^{n}\gamma_k(t)^2\right)\right) + \epsilon\left(w_h^2 + \frac{\alpha^2}{2}\left(\bar{I}_e^2 + \sum_{k=1}^{n}\gamma_k(t)^2\right)\right).\end{aligned}$$

□

To characterise the optimal solution, we use Pontryagin's maximum principle [66]. The proof can be found in Pontryagin's original text [85].

There exists a piecewise differentiable adjoint variable,

$$\lambda(t) = (\lambda_1(t), \lambda_2(t), \lambda_3(t), \lambda_4(t), \lambda_5(t)),$$

such that

$$\lambda'(t) = \frac{-\partial H(t, x^*(t), \bar{I}^*(t), \lambda(t))}{\partial x},$$

where H denotes the Hamiltonian

$$H(t, w_h, w_d, w_c, i_s, i_f, \bar{I}_e, \bar{\gamma}, \lambda) = L(t, w_h, \bar{I}) + \sum_{l=1}^{5} \lambda_l(t) f_l(x, t)$$

and $x^* = (w_h^*, w_d^*, w_c^*, i_s^*, i_f^*)$ are the corresponding state variables of the optimal control functions $\bar{I}^* = (\bar{I}_e^*, \gamma(t)^*)$.

Proposition 2. *The optimal controls are given by the set*

$$\bar{I}_e^* = \min\left\{\max\left\{0, \frac{\lambda_1 \beta_{hf} N_f i_f}{\alpha^2}\right\}, 1\right\},$$
$$\bar{\gamma}^* = \min\left\{\max\left\{0, \frac{\lambda_1 w_h}{\alpha^2}\right\}, 1\right\}.$$

Proof. Let $\bar{I}^*$ be the optimal control functions to the corresponding state variables $x^* = (w_h^*, w_d^*, w_c^*, i_s^*, i_f^*)$, which minimise our integral function $J(\bar{I})$. It follows with the Pontryagin's maximum principle that adjoint variables $\lambda(t) = (\lambda_1(t), \lambda_2(t), \lambda_3(t), \lambda_4(t), \lambda_5(t))$ exist such that

$$\lambda_1' = -2w_h + \lambda_1(\mu_{ph} + \gamma) - \lambda_4 \beta_{sh} N_h (1 - I_d)(1 - i_s), \tag{9.3a}$$
$$\lambda_2' = \lambda_2 \mu_{pd} - \lambda_4 \beta_{sd} N_d (1 - i_s), \tag{9.3b}$$
$$\lambda_3' = \lambda_3 \mu_{pc} - \lambda_4 \beta_{sc} N_c (1 - i_s), \tag{9.3c}$$
$$\lambda_4' = \lambda_4(\beta_{sh} N_h w_h (1 - I_d) + \beta_{sd} N_d w_d + \beta_{sc} N_c w_c + \mu_s) - \lambda_5 \beta_{fs} N_s (1 - i_f), \tag{9.3d}$$
$$\lambda_5' = \lambda_5(\beta_{fs} N_s i_s + \mu_f) - \lambda_1 \beta_{hf} N_f (1 - I_e) - \lambda_2 \beta_{df} N_f - \lambda_3 \beta_{cf} N_f, \tag{9.3e}$$

with transversality conditions $\lambda_i(t_1) = 0$ for $i = 1, \ldots, 5$. Considering the optimality condition $\frac{\partial H(t, x^*(t), \bar{I}^*(t), \lambda(t))}{\partial I} = 0$, we get the solutions

$$\bar{I}_e^* = \frac{\lambda_1 \beta_{hf} N_f i_f}{\alpha^2}, \tag{9.4a}$$
$$\bar{\gamma}^* = \frac{\lambda_1 w_h}{\alpha^2}. \tag{9.4b}$$

It follows with the characteristics of the control set U that the proposition holds (compare [64]). □

We use the forward-backward sweep method with the Runge-Kutta 4 method to calculate the solution of the optimal control [66]. We calculate the optimal control solution for three different, but fixed, coverage levels of I_d: 0.4, 0.6, and 0.8. We start with the end value of the MLE solution in Figure 9.1 as initial value of the state variables,

$$(w_h(0), w_d(0), w_c(0), i_s(0), i_f(0)) = (47.107, 0.815, 5.120, 0.002, 0.323).$$

We choose the weight $\alpha = 0.001$ and numerically solve the ODE system (9.1) with the MLE parameters given in Table 9.2 forward in time with 1,000 iterations, followed by the simulation of the ODE system of the adjoint functions (9.3) backward in time with likewise 1,000 iterations. With the new solution of the adjoint functions, we can update the solution of the intervention I in accordance with to the equations (9.4). We repeat these steps until the relative error of the interventions is smaller than δ,

$$\left\| I - \tilde{I} \right\| \leq \delta \left\| I \right\|,$$

with $\tilde{I}$ being the previous solution. To account for the possibility of $\|I\| = 0$, we transform it to the condition

$$\delta \left\| I \right\| - \left\| I - \tilde{I} \right\| \geq 0.$$

The parameter δ is set to $\delta = 0.001$ [66].

The solution of the the treatment rate $\gamma(t)$ is transformed back to the proportion $I_m(\gamma) = 1 - \exp(\gamma(t) \times 365)$. The minimisation of the interventions I_e and $I_m(\gamma)$ is shown in Figure 9.6(a) – it is the same solution for all three assumption of $I_d \in \{0.4, 0.6, 0.8\}$. The mean worm burden in the definitive hosts and the prevalence in the intermediate hosts depends on the coverage of improved sanitation, I_d, as shown in Figures 9.6(b)–(f).

The solution of the optimal control problem shows that the optimal coverage for treatment is 44% if it is done on a yearly basis. The coverage of people that should stop eating raw or undercooked fish is set to the maximum of 90% over the whole time period.

Elimination

We define the elimination of *O. viverrini* as in Definition 4 when there is less than one worm per person ($w_h \leq 1$) or less than one infected fish ($i_f \times N_f \leq 1$) or snail ($i_s \times N_s \leq 1$).

Definition 4 (Elimination)**.** *Elimination of* O. viverrini *is reached if at least one of the following statements holds true within a default time frame of 20 years:*

(i) $w_h \leq 1$,

(ii) $i_f \times N_f \leq 1$,

(iii) $i_s \times N_s \leq 1$.

Figure 9.7 shows the time to elimination and the probability of elimination at varying frequencies of mass treatment and at varying levels of coverage for all three interventions. We estimate the time to elimination for MLE parameter values (see Table 9.2) by assuming that interventions are deployed at time $t = 0$ with the endemic equilibrium in the absence of interventions as the initial condition. Figure 9.7(a) shows the time to elimination at different frequencies of mass treatment at coverage levels of $I_m \in \{0.4, 0.5, 0.6, 0.7, 0.8\}$. Figure 9.7(b) shows the time to elimination for all interventions as the coverage of each intervention increases. We estimate the probability of reaching elimination as the proportion of the 500 resampled parameter sets that achieve the definition of elimination above. The probability of elimination as a function of treatment frequency is shown in Figure 9.7(c) and as a function of intervention coverage is shown in Figure 9.7(d). The results show that mass treatment, even at very low frequencies, is more effective and faster in achieving elimination than improved sanitation or education campaigns. In particular, relatively low coverage of treatment at a high frequency is as effective if not even more, than high coverage of the other interventions or of treatment at low frequencies.

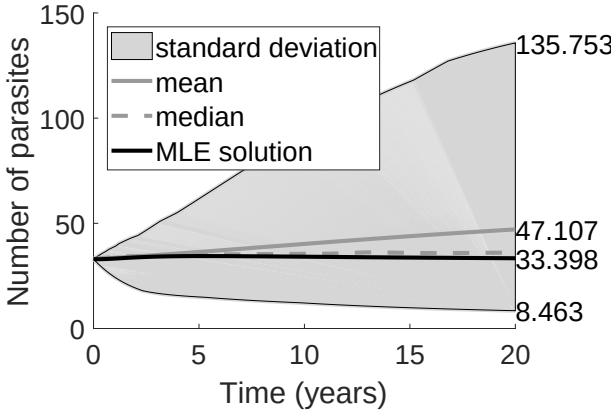

(a) Mean worm burden in humans w_h.

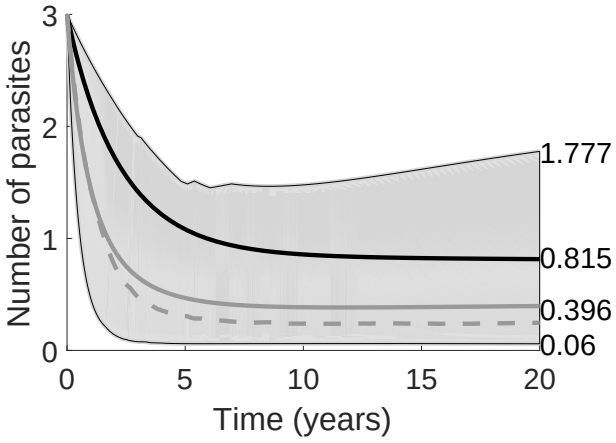

(b) Mean worm burden in dogs w_d.

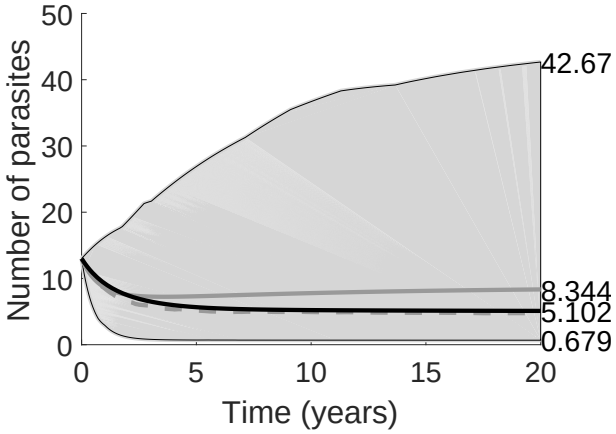

(c) Mean worm burden in cats w_c.

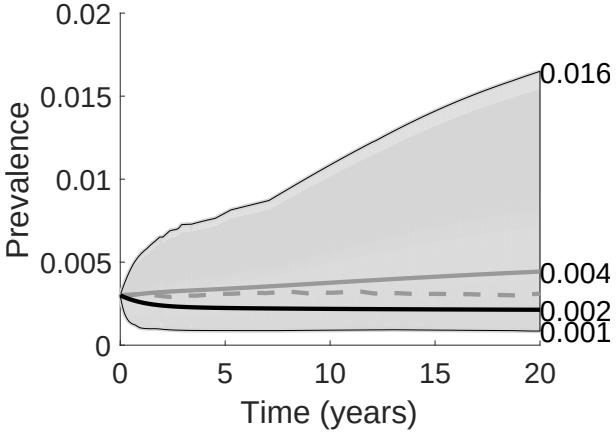

(d) Prevalence of infection in snails i_s.

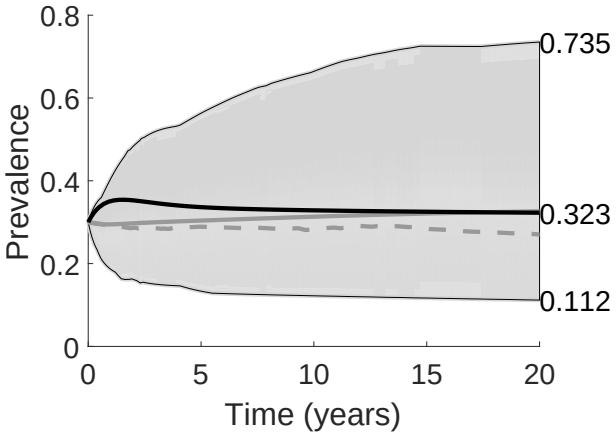

(e) Prevalence of infection in fish i_f.

Figure 9.1: Numerical simulation of the *O. viverrini* model (9.1) with parameter values selected using MLE (black line) and with the 500 parameter sets chosen with the Bayesian sampling-resampling without any interventions ($I_e = I_d = I_m = 0$) the mean (grey line), median (grey dashed line) and standard deviation (grey area).

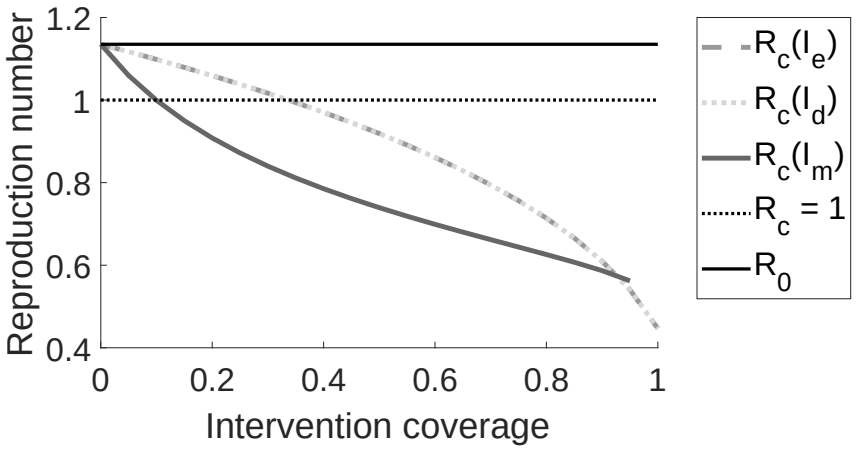

Figure 9.2: Control reproduction number as a function of the coverage level for various intervention applied singly and the basic reproduction number, calculated with the parameters from the MLE solution in Table 9.2.

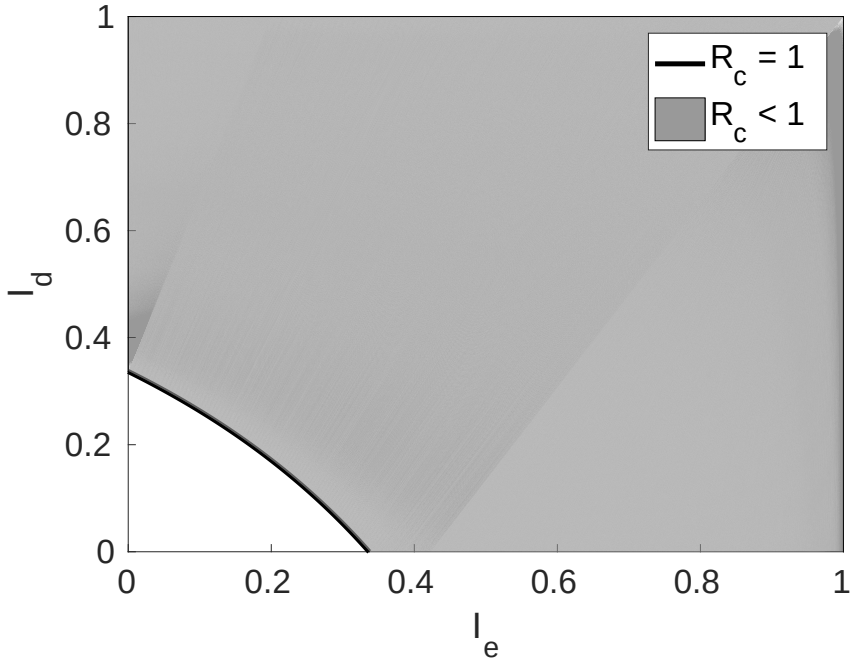

Figure 9.3: Combinations of I_e and I_d such that $R_c < 1$ in absence of I_m ($I_m = 0$). The other parameters are set to their MLE solution in Table 9.2.

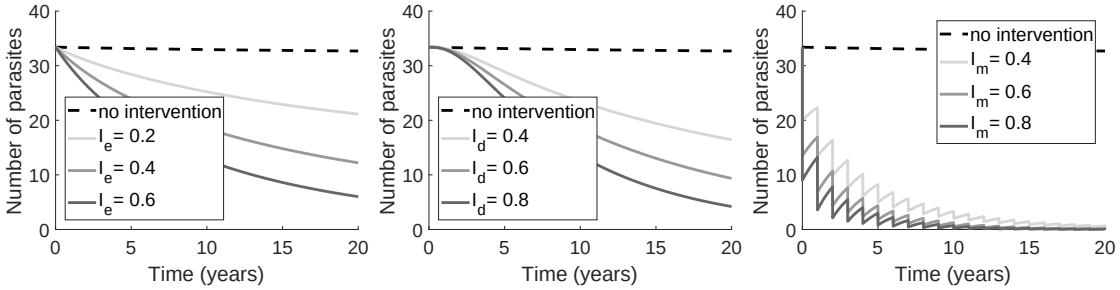

(a) w_h regulated by I_e.

(f) w_h regulated by I_d.

(k) w_h regulated by I_m.

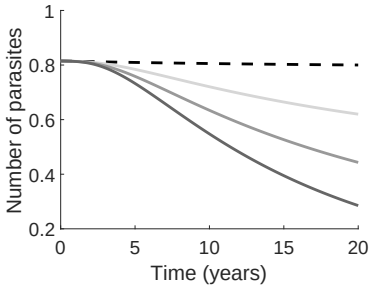

(b) w_d regulated by I_e.

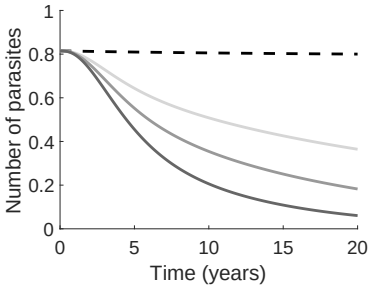

(g) w_d regulated by I_d.

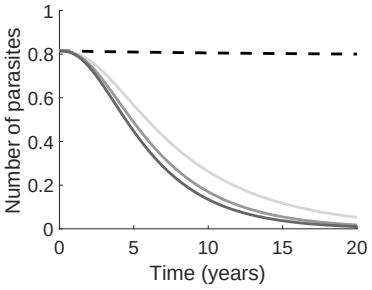

(l) w_d regulated by I_m.

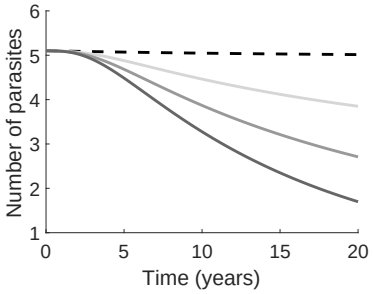

(c) w_c regulated by I_e.

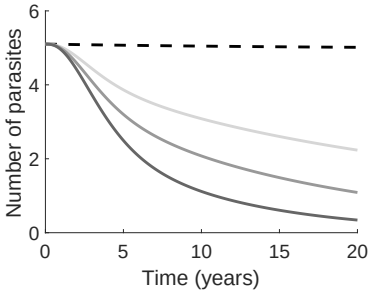

(h) w_c regulated by I_d.

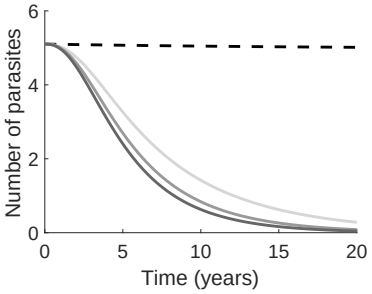

(m) w_c regulated by I_m.

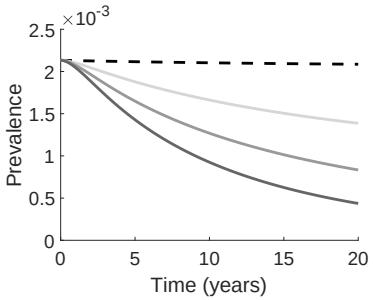

(d) i_s regulated by I_e.

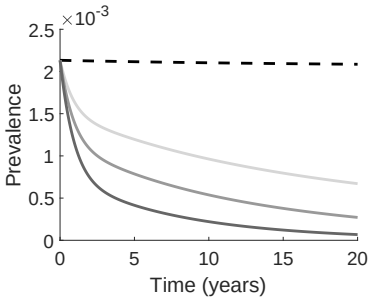

(i) i_s regulated by I_d.

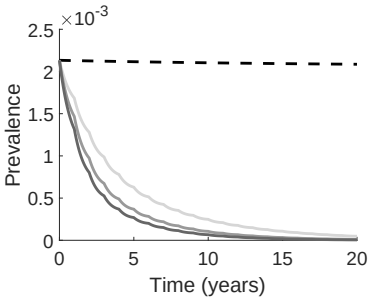

(n) i_s regulated by I_m.

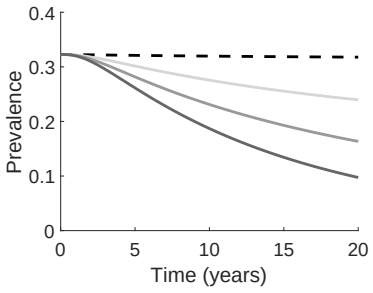

(e) i_f regulated by I_e.

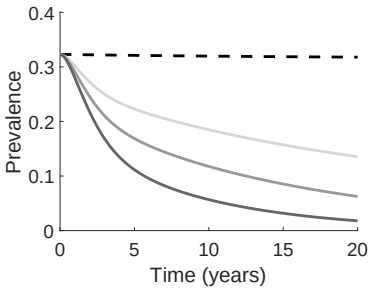

(j) i_f regulated by I_d.

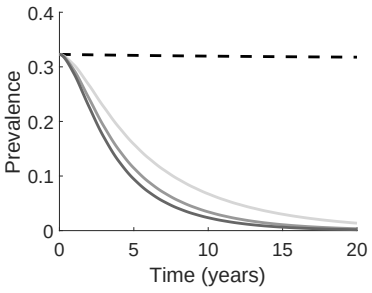

(o) i_f regulated by I_m.

Figure 9.4: Numerical simulations of the model (9.1) with different coverage levels of the interventions compared to the baseline scenarios with no intervention. The parameters are set to the MLE solution in Table 9.2.

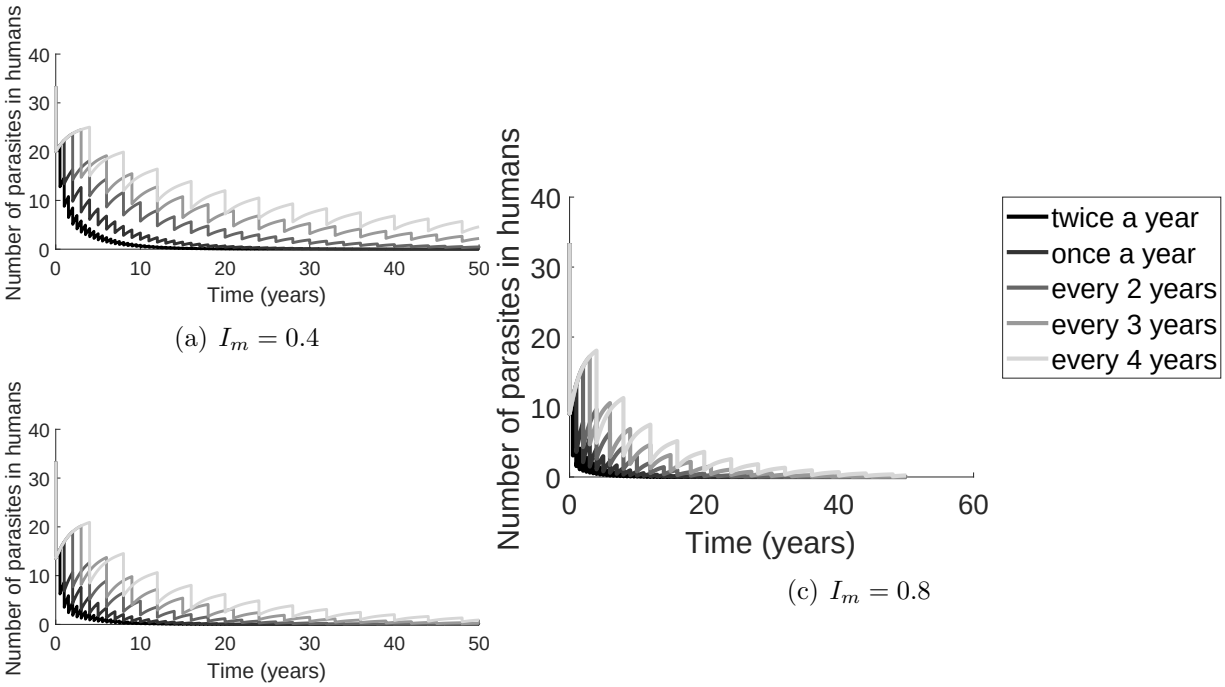

(a) $I_m = 0.4$

(b) $I_m = 0.6$

(c) $I_m = 0.8$

Figure 9.5: Numerical simulations of the frequency of treatment every 0.5, 1, 2, 3 and 4 years and its effect on the mean worm burden in humans. The parameters of the MLE solution in Table 9.2 are used for the calculation.

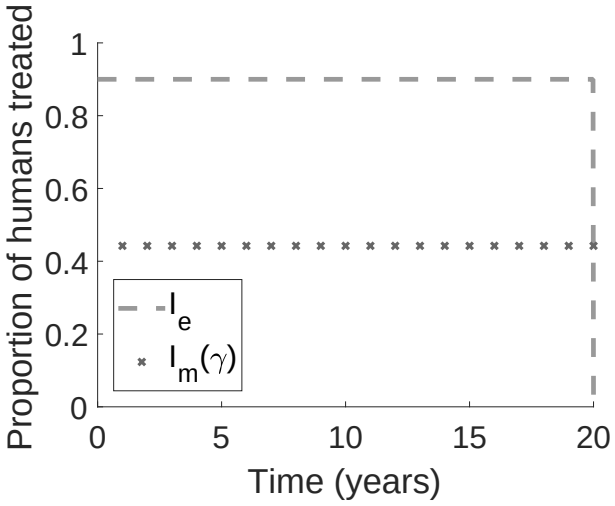

(a) Interventions.

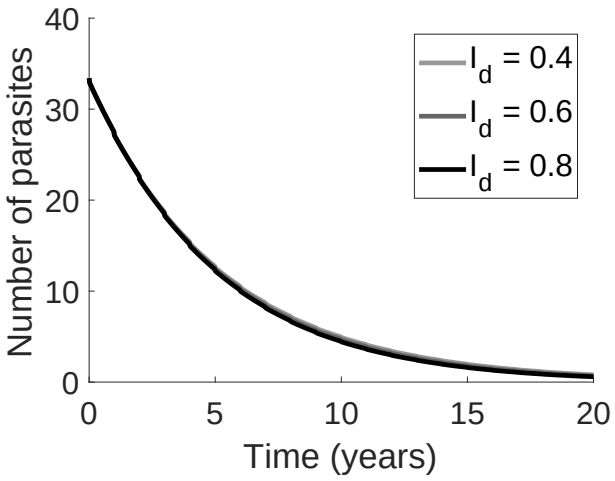

(b) Mean worm burden in humans w_h.

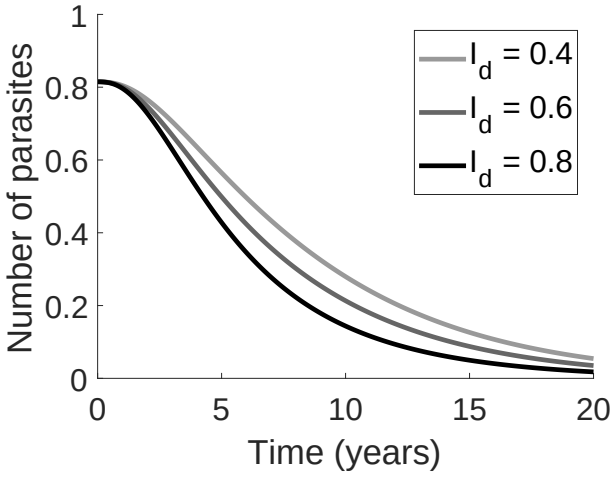

(c) Mean worm burden in dogs w_d.

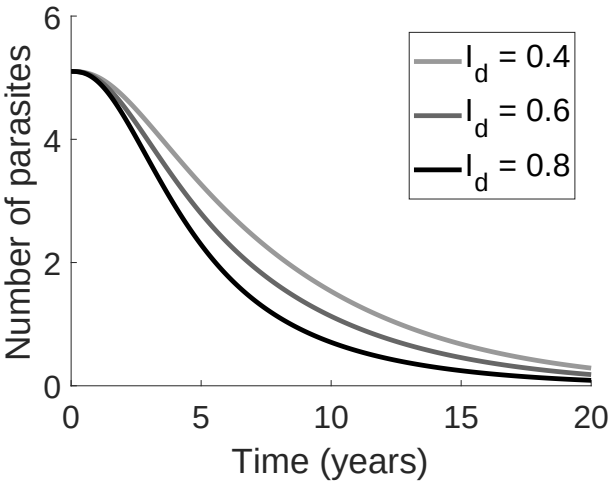

(d) Mean worm burden in cats w_c.

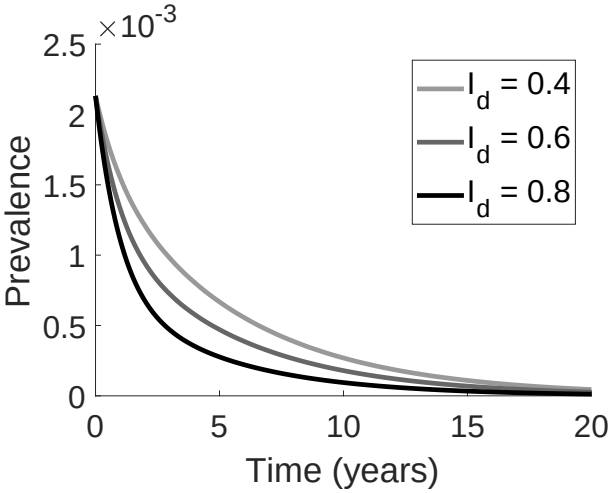

(e) Prevalence of infection in snails i_s.

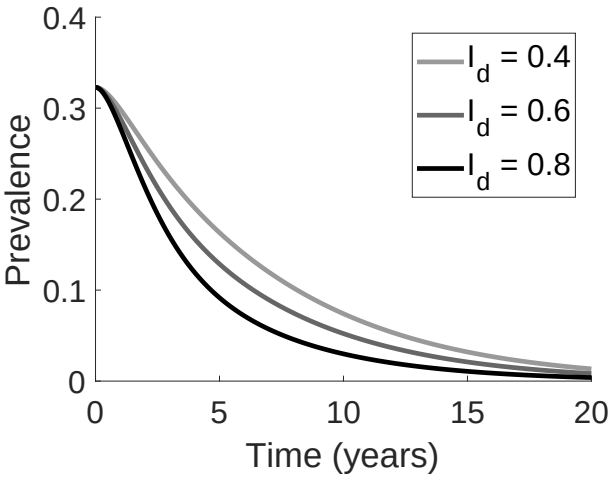

(f) Prevalence of infection in fish I_f.

Figure 9.6: Optimal control results of the interventions and the solution of the model calculated with the Forward-Backward Sweep method for the different assumptions on I_d. The MLE solution parameters (Table 9.2) are used for the calculations.

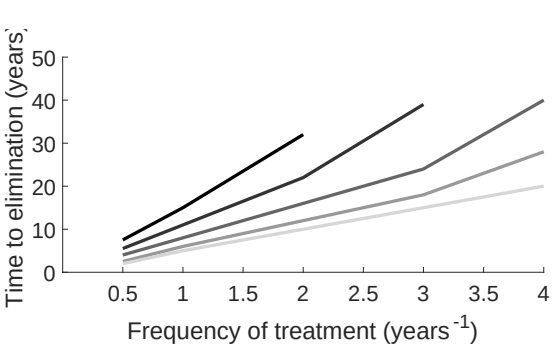

(a) Time to elimination depending on treatment interval.

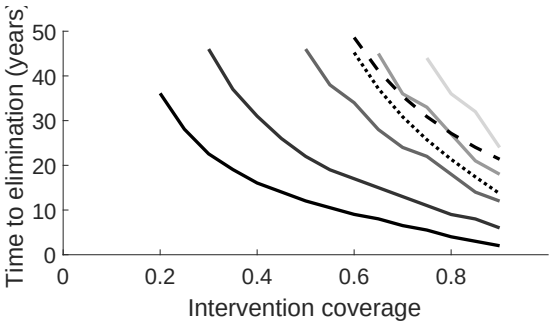

(b) Time to elimination depending on intervention coverage.

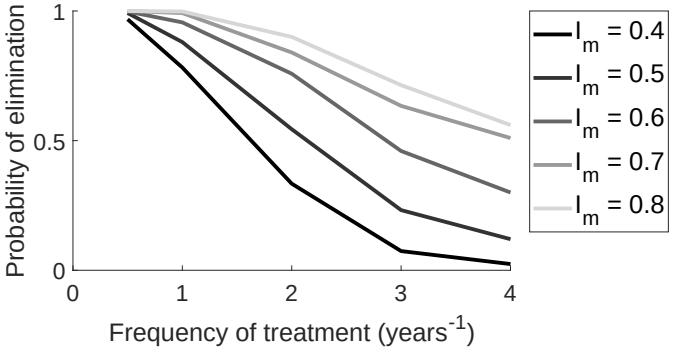

(c) Probability of elimination depending on treatment interval.

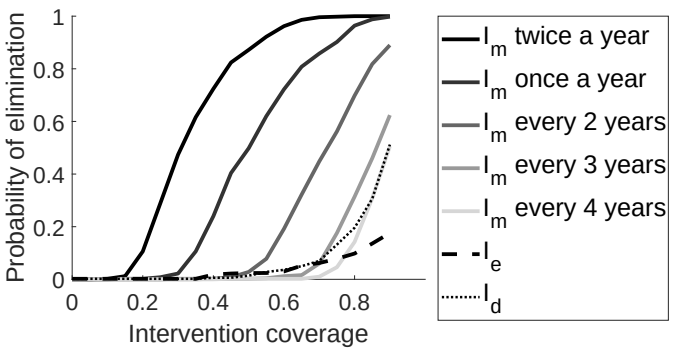

(d) Probability of elimination depending on intervention coverage.

Figure 9.7: Time to elimination and probability of elimination of the different interventions with different settings. I use the parameter of the MLE solution in Table 9.2 for the calculation of the time to elimination and the resampled parameter sets to determine the probability of elimination.

10. Model with age-dependency

The model with age-dependency allows the mean worm burden in humans to depend on the host age. We use a Bayesian sampling approach to estimate the parameters analogous to Section 8.3. The steady state solution is derived by a fixed point iteration. We optimise the coverage level of MDA in an adapted model of five age groups to compare varying coverages across age groups.

10.1 Mathematical model

We extend the model with reservoir hosts (8.4) to include the dependence of mean worm burden in humans on the host age. We model human age continuously by transforming the system of ODEs to a partial differential equation, where the mean worm burden in humans depends on age and time ($w_h(a,t)$). The number of humans also depends on age ($N_h(a)$) and the additional parameter $\phi(a)$ denotes the proportion of people of age a eating raw or undercooked fish for a $a > 0$. This model of *O. viverrini* including age of human is given by the equations:

$$\frac{\partial w_h(a,t)}{\partial t} + \frac{\partial w_h(a,t)}{\partial a} = \phi(a)\beta_{hf} N_f i_f(t) - \mu_{ph} w_h(a,t), \tag{10.1a}$$

$$\frac{\mathrm{d}w_d(t)}{\mathrm{d}t} = \beta_{df} N_f i_f(t) - \mu_{pd} w_d(t), \tag{10.1b}$$

$$\frac{\mathrm{d}w_c(t)}{\mathrm{d}t} = \beta_{cf} N_f i_f(t) - \mu_{pc} w_c(t), \tag{10.1c}$$

$$\frac{\mathrm{d}i_s(t)}{\mathrm{d}t} = \left(\beta_{sh} \int_0^{a_{\max}} N_h(a) w_h(a,t) \mathrm{d}a + \beta_{sd} N_d w_d(t) + \beta_{sc} N_c w_c(t) \right) (1 - i_s(t)) - \mu_s i_s(t), \tag{10.1d}$$

$$\frac{\mathrm{d}i_f(t)}{\mathrm{d}t} = \beta_{fs} N_s i_s(t)(1 - i_f(t)) - \mu_f i_f(t). \tag{10.1e}$$

where, $a_{\max}$ is the maximum age of humans. All state variables are described in Table 8.1 and parameters in Table 8.2 with the additional parameters in Table 9.1 and 10.1.

The parameter μ_{ph} is the death rate of the parasite in humans excluding mortality due to the death of humans (since the mortality of humans is explicitly included with an exponential distribution for the human population).

The integral over age of the mean worm burden in humans $w_h(a,t)$ weighted by the number of humans $N_h(a)$ yields the total number of worms in humans. The total human

population size is given by the integral over age

$$\bar{N_h} = \int_0^{a_{\max}} N_h(a)\mathrm{d}a.$$

We assume that the number of humans follows a truncated exponential distribution with the following equation

$$N_h(a) = \begin{cases} \frac{c}{\lambda}\exp\left(-\frac{a}{\lambda}\right), & \text{if } a \leq a_{\max}, \\ 0, & \text{if } a > a_{\max}, \end{cases}, \tag{10.2}$$

where λ is the average life span of a human and c is a scaling factor defined as

$$c = \frac{\bar{N_h} \cdot \lambda}{\int_0^{a_{\max}} \exp\left(-\frac{a}{\lambda}\right)\mathrm{d}a},$$

where we can estimate the total human population, $\bar{N_h}$, and λ from data.

Parameter	Description	Dimension
$N_h(a)$	Population size of humans dependent on age a	Animals
$\phi(a)$	proportion of humans of age a eating raw or undercooked fish	1/Animals
λ	Mean life span of humans	Time
c	Constant of human population size	Dimensionless

Table 10.1: Additional parameters of the opisthorchiasis model with age-dependency.

10.2 Data and numerical simulation

As Figure 10.1 shows, the distribution is flat between the ages of 0 and 20 years and then decays exponentially after 20 years. We make the simplifying assumption that the distribution is exponential for all ages until a maximum age, $a_{\max}$, which we set to 95 years. We fit a truncated exponential distribution for the number of humans, $N_h(a)$, to the Lao population data to estimate an average life span of humans of $\lambda = 9628$ days $\approx$ 26.37 years using the MLE[1] (see Figure 10.1. By assuming an exponential distribution, we overestimate the population sizes of children and adults under 20, and we underestimate the human life span. However, since the infection rates in children are relatively low and the mortality rates of parasites is still substantially shorter than the estimated human life span, this assumption does not affect our results. We truncate the age distribution to simplify the numerical integration. However since the population size of people over 95

[1]Matlab R2017a: Distribution Fitting App

in Lao PDR is minimal, the effect on our results is negligible. We assume that the total number of humans living on the two islands is $\bar{N}_h = 14541$ [126], leading to the constant $c = 1.5318 \times 10^4$ in the exponential distribution. The distribution is shown in Figure 10.1.

The age-dependent proportion of people who eat raw or undercooked fish, $\phi(a)$, is fitted to a truncated Gaussian distribution in the interval [0, 89] based on the data from the study in Champasack province Southern Lao PDR [126]. Figure 10.2 shows the absolute number of humans eating raw or undercooked fish as well as the proportion of people who eat raw or undercooked fish increases with age since young children rarely eat raw fish, until a peak and then decreases. This decrease is presumably due to decreasing dental health with age, which makes it more difficult to chew undercooked fish.

We need a distribution of the mean worm burden of humans over age for the initial condition for the numerical simulation. We fit the distribution of eggs per gram (epg) of stool in humans over age to a truncated Gaussian distribution in the interval [0, 89] as shown in Figure 7.5. We use the data from Lao PDR on epg in stool, see Chapter 7, and transform it into the number of worms per person using purging data from a study in Thailand [28]. We assume the same trend in the number of worms per human as a function of age as in the proportion of people eating raw or undercooked fish.

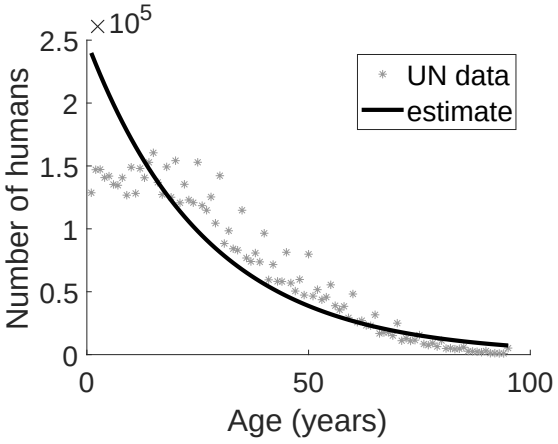

Figure 10.1: Number of humans as a function of age (in years) from the UN data maximum likelihodd estimate of an exponential distribution: $f(\text{age}) = \frac{c}{\lambda} \exp\left(-\frac{\text{age}}{\lambda}\right)$ with $\lambda = 26$ years.

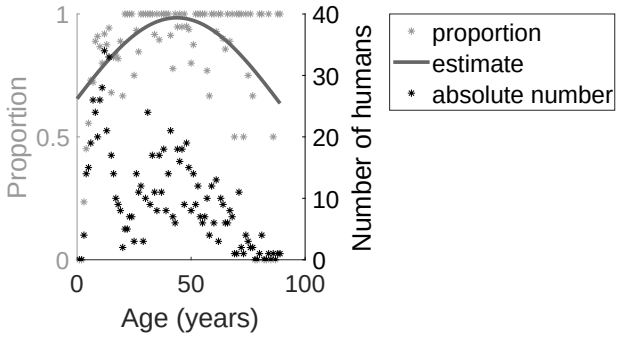

Figure 10.2: Estimate of the proportion of humans eating raw or undercooked fish depending on age fitted to a Gaussian distribution using the data set from Lao PDR: $f(\text{age}) = 0.9844 \cdot \exp\left(-\left(\frac{\text{age}-43.73}{68.51}\right)^2\right)$.

We estimate the population sizes of five hosts and the mortality rates of fish and snails, and worms in humans, cats and dogs by sampling from a prior distribution. We estimate the transmission rates, $\beta = (\beta_{hf}, \beta_{df}, \beta_{cf}, \beta_{sh}, \beta_{sd}, \beta_{sc}, \beta_{fs})$, using the maximum likelihood method.

The likelihood function L is given by the product of the likelihood functions for the intensity of infection in humans and the prevalence of infection in dogs, cats, snails and fish,

$$L = L_h L_d L_c L_s L_f,$$

where we assume a negative binomial distribution for the worm (and the egg) burden,

$$L_h = \prod_{i=1}^{\bar{N}_h} \frac{(\text{epg}_i + r - 1)!}{\text{epg}_i!(r-1)!} \left(\frac{r}{\text{epg}^* + r}\right)^r \left(\frac{\text{epg}^*}{\text{epg}^* + r}\right)^{\text{epg}_i}$$

with n_h the number of human tested in the data set from Lao PDR (see Table 7.1) [126], epg_i the eggs per gram of each person, epg^* the steady state solution of the mean worm burden transformed into the mean egg per gram burden (with data from [28]) and $r > 0$ a real value that we estimate. L_d, L_c, L_s and L_f are given in equation (8.5a). We sample 5,000 sets of parameter values from a triangular distribution with mod and ranges provided in Table 10.2 and choose the set with the highest likelihood as the baseline parametrisation for the maximum likelihood optimisation, where we fit the transmission rates, β. The parameter set with the maximum likelihood is shown in Table Table 10.2.

Variable	Mode	Range	MLE	Unit
N_h	15705	$[1571, 23557]$	8679	Animals
N_d	8437	$[844, 12656]$	7991	Animals
N_c	6098	$[610, 9147]$	2552	Animals
N_s	31019	$[3102, 46529]$	33068	Animals
N_f	9701	$[970, 14552]$	12433	Animals
μ_{ph}	$\frac{1}{4.8\times365}$	$\left[\frac{1}{9.6\times365}, \frac{1}{2.2\times365}\right]$	$\frac{1}{3.7\times365}$	1/Days
μ_{pd}	$\frac{1}{2.2\times365}$	$\left[\frac{1}{4.4\times365}, \frac{1}{1.1\times365}\right]$	$\frac{1}{2.9\times365}$	1/Days
μ_{pc}	$\frac{1}{1.5\times365}$	$\left[\frac{1}{3\times365}, \frac{1}{0.8\times365}\right]$	$\frac{1}{1.7\times365}$	1/Days
μ_s	$\frac{1}{1\times365}$	$\left[\frac{1}{2\times365}, \frac{1}{0.5\times365}\right]$	$\frac{1}{1.1\times365}$	1/Days
μ_f	$\frac{1}{1.5\times365}$	$\left[\frac{1}{3\times30}, \frac{1}{0.8\times365}\right]$	$\frac{1}{2.0\times365}$	1/Days
β_{hf}	5.9785×10^{-6}	$[5.9785 \times 10^{-7}, 1.1957 \times 10^{-5}]$	5.1266×10^{-6}	1/(Animal x Day)
β_{df}	3.2337×10^{-7}	$[3.2337 \times 10^{-8}, 6.4674 \times 10^{-7}]$	5.3964×10^{-7}	1/(Animal x Day)
β_{cf}	2.9608×10^{-6}	$[2.9608 \times 10^{-7}, 5.9216 \times 10^{-6}]$	4.2211×10^{-6}	1/(Animal x Day)
β_{sh}	1.0210×10^{-11}	$[1.0210 \times 10^{-12}, 2.0420 \times 10^{-11}]$	1.3490×10^{-11}	1/(Animal x Day)
β_{sd}	2.8635×10^{-11}	$[2.8635 \times 10^{-12}, 5.7270 \times 10^{-11}]$	2.8636×10^{-11}	1/(Animal x Day)
β_{sc}	4.7734×10^{-12}	$[4.7734 \times 10^{-12}, 9.5468 \times 10^{-11}]$	3.8561×10^{-11}	1/(Animal x Day)
β_{fs}	1.2900×10^{-5}	$[1.2900 \times 10^{-6}, 2.5800 \times 10^{-5}]$	2.1769×10^{-5}	1/(Animal x Day)

Table 10.2: Mode and ranges for the triangular distribution used as prior distribution and the maximum likelihood estimate of the parameter values. The mode is chosen as the maximum likelihood estimate for the reservoir host model, see Table Tab:ranges. The MLE solution is the data set of the highest likelihood and the β's estimated by the MLE method.

We run numerical simulations of the model (10.1) with this MLE parameter set.. We use the method of characteristics [40] to convert the PDE to a system of ODEs, along the

characteristic lines $a = \zeta + t$. We numerically integrate the ODEs by using the tourth order Runge-Kutta method with a time step of one day.

We use the following initial values at time t_0: $w_h(a, t_0)$ is the mean worm burden for every age a as shown in Figure 7.5 and $(w_d(t_0), w_c(t_0), i_s(t_0), i_f(t_0)) = (1, 13, 0.003, 0.3)$ as calculated from Table 7.1 and equation (8.6).

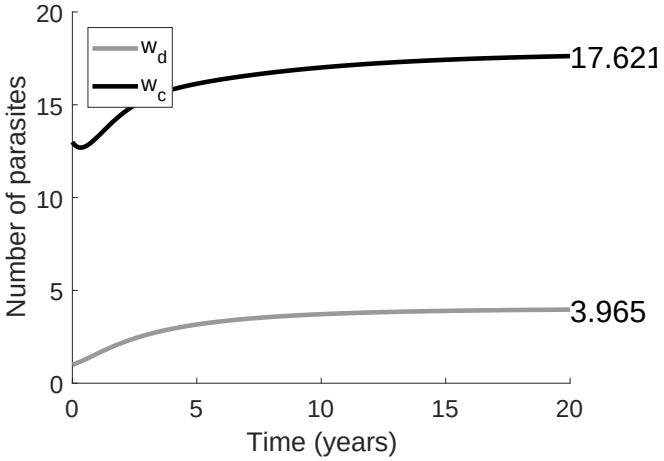

(a) Mean worm burden in dogs w_d and cats w_c.

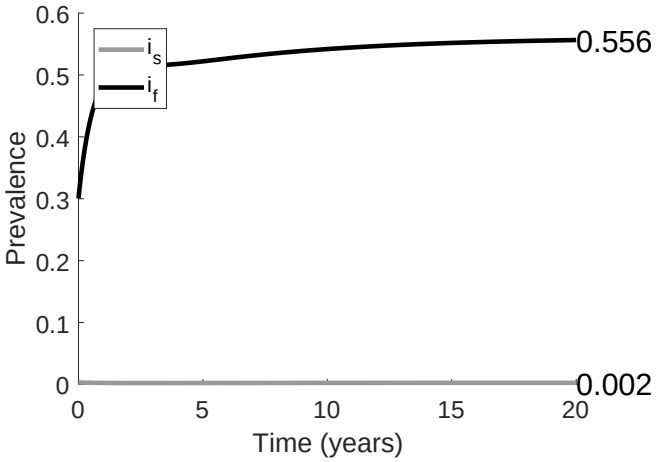

(b) Prevalence of infection in snails i_s and fish i_f.

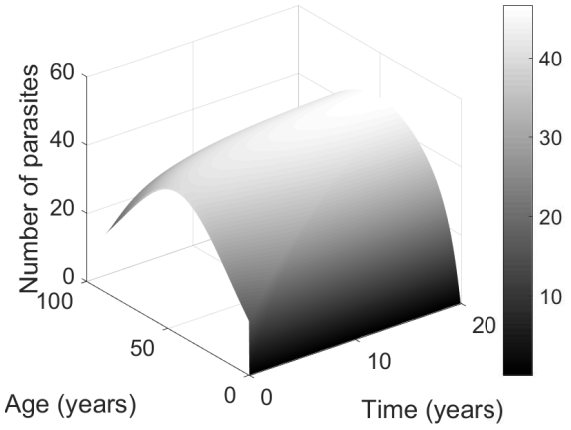

(c) Mean worm burden in humans $w_h(a, t)$ over time and age.

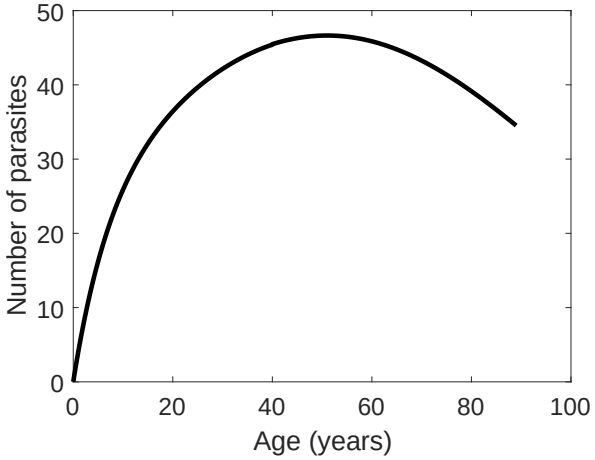

(d) Mean worm burden in humans $w_h(a, 20)$ over age after 20 years.

Figure 10.3: Numerical simulation of the model (10.1) with the parameter values chosen using MLE from Table 10.2 calculated with the Runge Kutta 4 method.

10.3 Steady state solution

Definition 5 (Steady state)**.** *The steady state of a system is a solution that does not change with time; this means that the partial derivative with respect to time is zero [98].*

There is the trivial steady state solution $S_0(a) = (w_h^*(a), w_d^*, w_c^*, i_s^*, i_f^*) = (0, 0, 0, 0, 0)$ for all ages $a \in [0, a_{\max}]$. We calculate the endemic steady state solution $S_e(a) =$

$(w_h^*(a), w_d^*, w_c^*, i_s^*, i_f^*)$ by solving the following system:

$$\frac{\partial w_h^*(a)}{\partial a} = \phi(a)\beta_{hf}N_f i_f^* - \mu_{ph} w_h^*(a), \tag{10.3a}$$

$$0 = \beta_{df}N_f i_f^* - \mu_{pd} w_d^*, \tag{10.3b}$$

$$0 = \beta_{cf}N_f i_f^* - \mu_{pc} w_c^*, \tag{10.3c}$$

$$0 = \left(\beta_{sh} \int_0^{a_{\max}} N_h(a) w_h^*(a) \mathrm{d}a + \beta_{sd}N_d w_d^* + \beta_{sc}N_c w_c^*\right)(1 - i_s^*) - \mu_s i_s^*, \tag{10.3d}$$

$$0 = \beta_{fs}N_s i_s^*(1 - i_f^*) - \mu_f i_f^*. \tag{10.3e}$$

Solving equation (10.3b), (10.3c) and (10.3e) for w_c^*, w_d^* and i_s^*, respectively, leads to

$$w_d^* = \frac{\beta_{df}N_f i_f^*}{\mu_{pd}}, \tag{10.4a}$$

$$w_c^* = \frac{\beta_{cf}N_f i_f^*}{\mu_{pc}}, \tag{10.4b}$$

$$i_s^* = \frac{\mu_f i_f^*}{\beta_{fs}N_s - \beta_{fs}N_s i_f^*}. \tag{10.4c}$$

We rewrite equation (10.3d) in terms of i_f^* and $w_h^*(a)$:

$$0 = \left(\beta_{sh} \int_0^{a_{\max}} N_h(a) w_h^*(a) \mathrm{d}a + \beta_{sd}N_d \frac{\beta_{df}N_f i_f^*}{\mu_{pd}} + \beta_{sc}N_c \frac{\beta_{cf}N_f i_f^*}{\mu_{pc}}\right) \times \left(1 - \frac{\mu_f i_f^*}{\beta_{fs}N_s - \beta_{fs}N_s i_f^*}\right) - \mu_s \frac{\mu_f i_f^*}{\beta_{fs}N_s - \beta_{fs}N_s i_f^*}.$$

This yields to a quadratic equation with two solutions of i_f^* depending on $w_h^*(a)$. The two solutions are of the form

$$i_{f,1} = \frac{\sqrt{f_1} + f_2 + f_3 - f_4 - f_5}{f_6},$$

$$i_{f,2} = -\frac{\sqrt{f_1} - f_2 - f_3 + f_4 + f_5}{f_6}.$$

The f_i terms stand from parameters as factors, where $f_i > 0$ for $i = 1, \ldots, 6$ since all parameters are positive. It follows that one solution is positive and one is negative.

We discretise our differential equation by dividing the human population into groups with size of one day $[w_h^*(a_i)]_{i=0}^{a_{\max}}$. We rewrite equation (10.3a) to calculate $w_h^*(a)$

$$\begin{aligned}\frac{\partial w_h^*(a_i)}{\partial a} &= \frac{w_h^*(a_{i+1}) - w_h^*(a_i)}{\Delta a} \\ &= \phi(a_i)\beta_{hf}N_f i_f^*(w_h^*(a_i)) - \mu_{ph} w_h^*(a_i)\end{aligned}$$

where $\Delta a = 1$ day, for $i = 0 \dots a_{\max}$ and define the function

$$\Phi : \left[0, \frac{N_f \beta_{hf}}{\mu_{ph}}\right] \longrightarrow \left[0, \frac{N_f \beta_{hf}}{\mu_{ph}}\right]$$

with

$$\Phi(w_h^*(a_i)) = -\phi(a_i)\beta_{hf} N_f i_f^* \Delta a + \mu_{ph} w_h^*(a_i)\Delta a + w_h^*(a_{i+1}).$$

We use the function Φ for the fixed point iteration

$$w_h^*(a_i)^{k+1} = \Phi(w_h^*(a_i)^k),$$

with k as iteration index. We set the threshold of $\epsilon = 0.001$ for

$$\left| w_h^*(a_i)^{k+1} - w_h^*(a_i)^k \right| < \epsilon$$

to estimate the steady state solution. If the iteration reaches the limit $k > 100$, we consider the steady state solution not to be calculable.

We next discretise the integral by using the Riemann definition

$$\int_0^{a_{\max}} N_h(a) w_h^*(a) \mathrm{d}a = \sum_{i=0}^{a_{\max}} N_h(a_i) w_h^*(a_i).$$

We take the value of $w_h(a)$ at $t = 20$ from the numerical simulation of (10.3) (as shown in Figure 10.3(c)) as the initial value of $[w_h^*(a_i)]_{i=0}^{a_{\max}}$ for the fixed point iteration. The steady state solution $w_h^*(a)$ is shown in Figure 10.4 and $S_e(a) = (w_h^*(a), 4.0029, 17.7187, 0.0025, 0.5582)$ for all $a \in [0, a_{\max}]$.

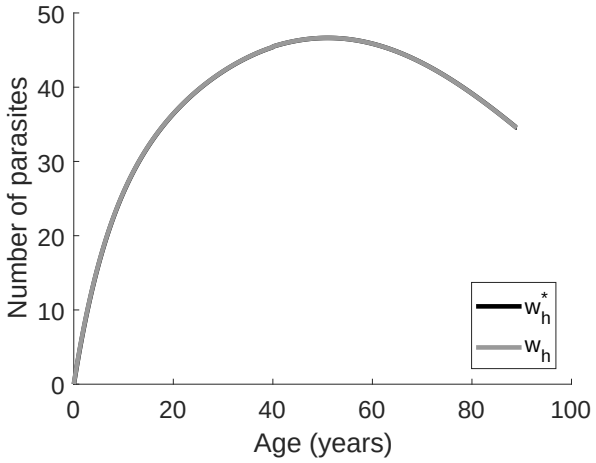

Figure 10.4: Steady state solution of the mean worm burden in humans w_h^* calculated by the fixed point iteration and numerical simulation after 20 years.

10.4 Basic reproduction number

The basic reproduction number is the expected number of offspring from one (hermaphrodite) worm in the absence of density dependence (assuming fully susceptible snail and fish populations). It is mathematically defined as the spectral radius of the next generation matrix $\mathbf{K}$ [27].

For the sake of simplicity, we divide humans into n age groups and rewrite the model (10.1) with ODEs. Here, $for i = 1, 2 \ldots, n$, $w_{h,i}$ is the mean worm burden per human host in the age group i; $N_{h,i}$ is the number of humans in age group i; and ϕ_i the proportion of people in age group i who consume raw or undercooked fish. ζ_i is the rate of movement of worms from the age group i to $i+1$, which is equal to the rate of movement of humans to the next age group, $\zeta_i = \frac{1}{\text{Duration of age group } i}$ for $i = 1, 2, \ldots, n-1$. This leads to the following model:

$$
\begin{aligned}
\frac{\mathrm{d}w_{h,1}}{\mathrm{d}t} &= \phi_1 \beta_{hf} N_f i_f - (\mu_{ph} + \zeta_1)\, w_{h,1}, \\
&\vdots \\
\frac{\mathrm{d}w_{h,i}}{\mathrm{d}t} &= \phi_i \beta_{hf} N_f i_f - (\mu_{ph} + \zeta_i)\, w_{h,i} + \frac{\zeta_{i-1} N_{h,i-1}}{N_{h,i}} w_{h,i-1}, \\
&\vdots \\
\frac{\mathrm{d}w_{h,n}}{\mathrm{d}t} &= \phi_n \beta_{hf} N_f i_f - \mu_{ph} w_{h,n} + \frac{\zeta_{n-1} N_{h,n-1}}{N_{h,n}} w_{h,n-1}, \\
\frac{\mathrm{d}w_d}{\mathrm{d}t} &= \beta_{df} N_f i_f - \mu_{pd} w_d, \\
\frac{\mathrm{d}w_c}{\mathrm{d}t} &= \beta_{cf} N_f i_f - \mu_{pc} w_c, \\
\frac{\mathrm{d}i_s}{\mathrm{d}t} &= \left(\beta_{sh} \sum_{k=1}^{n} N_{h,k} w_{h,k} + \beta_{sd} N_d w_d + \beta_{sc} N_c w_c \right) (1 - i_s) - \mu_s i_s, \\
\frac{\mathrm{d}i_f}{\mathrm{d}t} &= \beta_{fs} N_s i_s (1 - i_f) - \mu_f i_f.
\end{aligned}
\tag{10.5}
$$

The next-generation matrix of this model is

$$
\mathbf{K} = \begin{bmatrix}
0 & \ldots & 0 & \cdots & 0 & 0 & 0 & 0 & 0 & \frac{\phi_1 \beta_{hf} N_f}{\mu_{ph}} \\
\vdots & \ldots & \vdots & \cdots & \vdots & \vdots & \vdots & \vdots & \vdots & \vdots \\
0 & \ldots & 0 & \cdots & 0 & 0 & 0 & 0 & 0 & \frac{\phi_i \beta_{hf} N_f}{\mu_{ph}} \\
\vdots & \ldots & \vdots & \cdots & \vdots & \vdots & \vdots & \vdots & \vdots & \vdots \\
0 & \ldots & 0 & \cdots & 0 & 0 & 0 & 0 & 0 & \frac{\phi_n \beta_{hf} N_f}{\mu_{ph}} \\
0 & \ldots & 0 & \cdots & 0 & 0 & 0 & 0 & 0 & \frac{\beta_{df} N_f}{\mu_{pd}} \\
0 & \ldots & 0 & \cdots & 0 & 0 & 0 & 0 & 0 & \frac{\beta_{cf} N_f}{\mu_{pc}} \\
\frac{N_{h,1} \beta_{sh}}{\mu_{ph}} & \ldots & \frac{N_{h,i} \beta_{sh}}{\mu_{ph}} & \ldots & \frac{\beta_{sh} N_{h,n}}{\mu_{ph}} & \frac{\beta_{sh} N_{h,n}}{\mu_{ph}} & \frac{\beta_{sd} N_d}{\mu_{pd}} & \frac{\beta_{sc} N_c}{\mu_{pc}} & 0 & 0 \\
0 & \ldots & 0 & \ldots & 0 & 0 & 0 & 0 & \frac{\beta_f N_s}{\mu_{ph}} & 0
\end{bmatrix}.
$$

We compute its spectral radius for different numbers of age groups starting with three age groups ($n = 3$) and going up to 1000 age groups ($n = 1000$).

The median of the basic reproduction number is 1.38603 and the range of the oscillation for different numbers n of age groups is 1.4856×10^{-2}, so we conclude $\mathcal{R}_0 = 1.39$ for the adapted model (10.5) with age groups. To evaluate the basic reproduction number of the continuous age model (10.1), we let n tend to ∞.

Claim 1. *The basic reproduction number of the model with age groups* (10.5) *for* $n \to \infty$ *is equal to the basic reproduction number of the continuous age model* (10.1).

Proof. Let h be the length of the age interval of the age groups. We define $\zeta_i = \frac{1}{h}$ for $2 \leq i \leq n-1$. Thus, the system of ODEs for the worm burden in humans for age groups 2 to $n-1$ becomes

$$\begin{aligned} \frac{\mathrm{d}w_{h,i}}{\mathrm{d}t} &= \phi_i \beta_{hf} N_f i_f - \left(\mu_{ph} + \frac{1}{h}\right) w_{h,i} + \frac{1}{h} \frac{N_{h,i-1}}{N_{h,i}} w_{h,i-1} \\ &= \phi_i \beta_{hf} N_f i_f - \mu_{ph} w_{h,i} - \frac{1}{h} \left(w_{h,i} - \frac{N_{h,i-1}}{N_{h,i}} w_{h,i-1} \right). \end{aligned} \tag{10.6}$$

We still assume that the human population is exponentially distributed, so $N_{h,i-1} = \int_{k-h}^{k} N_h(a)\,\mathrm{d}a$ is the number of humans between age $k-h$ and k, $N_{h,i} = \int_{k}^{k+h} N_h(a)\,\mathrm{d}a$ for $k = \frac{a_{\max}}{n}(i-1)$ and all $i = 1, 2, \ldots, n$. Instead of $n \to \infty$, we can also let $h \to 0$. In the last term of the ODE (10.6)

$$\lim_{h \to 0} \frac{1}{h} \left(w_{h,i} - \frac{N_{h,i-1}}{N_{h,i}} w_{h,i-1} \right) = \frac{\partial w_h}{\partial a}.$$

Then

$$\lim_{h \to 0} \frac{N_{h,i-1}}{N_{h,i}} = \lim_{h \to 0} \frac{\int_{k-h}^{k} N_h(a)\,\mathrm{d}a}{\int_{k}^{ik+h} N_h(a)\,\mathrm{d}a} = 1$$

and therefore it follows

$$\frac{\partial w_h}{\partial t} + \frac{\partial w_h}{\partial a} = \phi(a) \beta_{hf} N_f i_f - \mu_{ph} w_h.$$

For $i = 1$ and $i = n$, the terms

$$\lim_{h \to 0} \frac{1}{h} w_{h,1}$$

and

$$\lim_{h \to 0} \frac{1}{h} \frac{N_{h,n-1}}{N_{h,n}} w_{h,n-1} = \lim_{h \to 0} \frac{1}{h} w_{h,n-1},$$

are equal to $\frac{\partial w_h}{\partial a}$ since they are the derivative with respect to age of the first and last age groups in the ODEs. We hence obtain exactly the PDE (10.1a).

It is left to show that the ODE

$$\frac{\mathrm{d}i_s}{\mathrm{d}t} = \left(\beta_{sh}\sum_{k=1}^{n} N_{h,k}w_{h,k} + \beta_{sd}N_d w_d + \beta_{sc}N_c w_c\right)(1-i_s) - \mu_s i_s$$

is equal to the ODE (10.1d) for $n \to \infty$. We thus look at the limits of the ODE

$$\begin{aligned}
\frac{\mathrm{d}i_s}{\mathrm{d}t} &= \lim_{n\to\infty}\left(\beta_{sh}\sum_{k=1}^{n} N_{h,k}w_{h,k} + \beta_{sd}N_d w_d + \beta_{sc}N_c w_c\right)(1-i_s) - \mu_s i_s \\
&= \left(\beta_{sh}\lim_{n\to\infty}\left(\sum_{k=1}^{n} N_{h,k}w_{h,k} + \beta_{sd}N_d w_d + \beta_{sc}N_c w_c\right)(1-i_s)\right) - \mu_s i_s \\
&= \left(\beta_{sh}\int_0^{a_{\max}} N_h(a)w_h(a)\mathrm{d}a + \beta_{sd}N_d w_d + \beta_{sc}N_c w_c\right)(1-i_s) - \mu_s i_s
\end{aligned}$$

with $a_{\max}$ as maximal age, as justified by the Riemann definition of the integral. □

10.5 Effectiveness of mass drug administration

We simulate the impact of mass drug administration (MDA), using praziquantel, which is efficacious against all human trematode infections endemic in Lao PDR [95], in reducing the mean worm burden in humans. We split the human population into five age groups and extend the model with age groups (10.5) to include MDA, as done previously in Chapter 9. We assume the number of humans in each age group follows an the exponential distribution. We model annual treatment that occurs over one day every year with an age-group dependent coverage, where $I_{m,i}$ humans of age group i are treated for $i \in \{1,\ldots,5\}$. The treatment rate of humans is $\gamma(t) = -\frac{\log(1-I_m(t))}{T_\gamma}$ for the day of treatment, where

$T_\gamma = 1$; and $\gamma(t) = 0$ for the rest of the year.

$$\frac{\mathrm{d}w_{h,1}(t)}{\mathrm{d}t} = \phi_1\beta_{hf}N_f i_f(t)(1-I_e(t)) - \left(\mu_{ph} + \zeta_1 - \frac{\log(1-I_{m,1}(t))}{T_\gamma} + \gamma(t)\right)w_{h,1}(t), \tag{10.7a}$$

$$\frac{\mathrm{d}w_{h,2}(t)}{\mathrm{d}t} = \phi_2\beta_{hf}N_f i_f(t)(1-I_e(t)) - \left(\mu_{ph} + \zeta_2 - \frac{\log(1-I_{m,2}(t))}{T_\gamma} + \gamma(t)\right)w_{h,2}(t) + \frac{\zeta_1 N_{h,1}}{N_{h,2}}w_{h,1}(t), \tag{10.7b}$$

$$\frac{\mathrm{d}w_{h,3}(t)}{\mathrm{d}t} = \phi_3\beta_{hf}N_f i_f(t)(1-I_e(t)) - \left(\mu_{ph} + \zeta_3 - \frac{\log(1-I_{m,3}(t))}{T_\gamma} + \gamma(t)\right)w_{h,3}(t) + \frac{\zeta_2 N_{h,2}}{N_{h,3}}w_{h,2}(t), \tag{10.7c}$$

$$\frac{\mathrm{d}w_{h,4}(t)}{\mathrm{d}t} = \phi_4\beta_{hf}N_f i_f(t)(1-I_e(t)) - \left(\mu_{ph} + \zeta_4 - \frac{\log(1-I_{m,4}(t))}{T_\gamma} + \gamma(t)\right)w_{h,4}(t) + \frac{\zeta_3 N_{h,3}}{N_{h,4}}w_{h,3}(t), \tag{10.7d}$$

$$\frac{\mathrm{d}w_{h,5}(t)}{\mathrm{d}t} = \phi_5\beta_{hf}N_f i_f(t)(1-I_e(t)) - \left(\mu_{ph} - \frac{\log(1-I_{m,5}(t))}{T_\gamma} + \gamma(t)\right)w_{h,5}(t) + \frac{\zeta_4 N_{h,4}}{N_{h,5}}w_{h,4}(t), \tag{10.7e}$$

$$\frac{\mathrm{d}w_d(t)}{\mathrm{d}t} = \beta_{df}N_f i_f(t) - \mu_{pd}w_d(t), \tag{10.7f}$$

$$\frac{\mathrm{d}w_c(t)}{\mathrm{d}t} = \beta_{cf}N_f i_f(t) - \mu_{pc}w_c(t), \tag{10.7g}$$

$$\frac{\mathrm{d}i_s(t)}{\mathrm{d}t} = \left(\beta_{sh}\sum_{k=1}^{5} w_{h,k}(t)(1-I_d)N_{h,k} + \beta_{sd}N_d w_d(t) + \beta_{sc}N_c w_c(t)\right)(1-i_s(t)) - \mu_s i_s(t), \tag{10.7h}$$

$$\frac{\mathrm{d}i_f(t)}{\mathrm{d}t} = \beta_{fs}N_s i_s(t)(1-i_f(t)) - \mu_f i_f(t), \tag{10.7i}$$

with the age groups described in Table 10.3.

Group	Age (years)
1	<6
2	6–16
3	17–36
4	37–50
5	>50

Table 10.3: Age groups of the age-stratified model (10.7).

We run thirteen different scenarios to identify the age groups that should be targeted by MDA campaigns. The first three scenarios consider an ideal campaign where all groups are targeted equally with 70% coverage (I), a school-based campaign focusing on children with 80% coverage (II) and a realistic campaign with lower coverage of working-age adults (50%) and 70% of other age groups (III). Strategies IV–$VIII$ consider MDA with equal

coverage of four age groups and 0% of one age group (to determine the impact of not reducing transmission from that age group) with an overall coverage of 70% (to account for the fact that not all age groups have the same population size). Strategies IX–$XIII$ consider campaigns with 70% coverage of each age group singly to determine the impact of transmission from that age group. The strategies are described in Tables 10.4–10.6 and the simulation results of the mean worm burden of each age gourp after 10 years are shown in Figure 10.5.

Applying the annual MDA strategies to the population for 10 years shows that strategies I and III are much more effective in lowering the overall worm burden. The mean worm burden after 10 years is between 15 and 20 worms per person in strategy I and III. Whereas focusing on school children keeps the mean worm burden high at around 40 worms per person on average. The same pattern is seen when looking at the mean worm burden in each age group. Strategy II does not affect the high mean worm burden of the young and old age group, as we assume the school children do not take place in any education campaigns and so do not change their behaviour of eating raw or undercooked fish, and reducing the worm burden of school children, does not sufficiently reduce onward transmission.

In strategies IV–VII we focus on 4 age groups out of the 5, so one age group does not get any treatment. The overall coverage is held at 70% of the human population. Neglecting the youngest age group has the best effect of strategies IV–VII and neglecting the fourth age group 37–50 years has the worst effect. Strategies IX–XII focus on one age group with a coverage level of 70%. The mean worm burden over all age groups shows that focusing on the third, 17–36, or fourth age group, 37–50, years has the highest positive effect and focusing on the youngest age group has the least.

Strategy		Age group				
		<6	6–16	17–36	37–50	>50
I:	ideal MDA	0.7	0.7	0.7	0.7	0.7
II:	school-based treatment	0	0.8	0	0	0
III:	realistic MDA	0.7	0.7	0.5	0.5	0.7

Table 10.4: Coverage of MDA of the age groups for each strategy I, II and III.

We compare each strategy with the MDA strategy I of 70% coverage of all age groups. We calculate the ratio of the mean worm burden of strategy K and the mean worm burden of the baseline strategy I; $r = \frac{w_{h,K}}{w_{h,I}}$ for $K = II, \ldots, XIII$ [142]. The ratio r helps to describe the additional reduction or increase of this strategy in comparison with the baseline strategy I; the additional reduction or increase is calculated by $1 - r$. The results are shown in Figure 10.6. Overall the strategy II has 2.44 times more worms per person than strategy I. Strategy III has only 1.18 times more worms than the baseline strategy. In comparison with the baseline strategy I, strategy IV even has 8% less worms

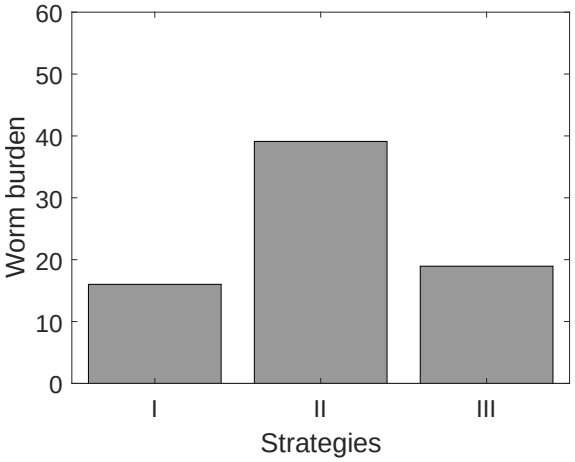

(a) Mean worm burden in humans over all age groups of each strategy.

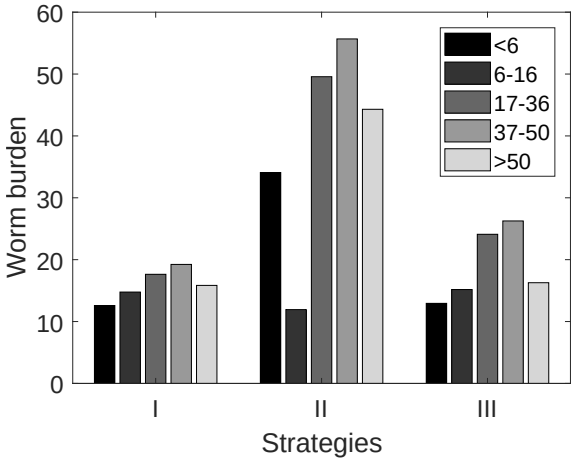

(d) Mean worm burden in humans for each age group and strategy.

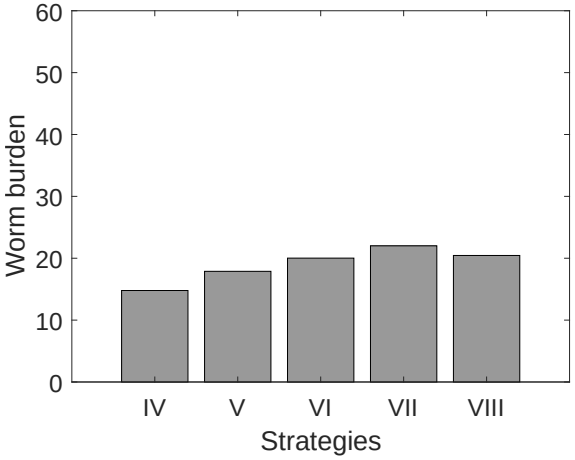

(b) Mean worm burden in humans over all age groups of each strategy.

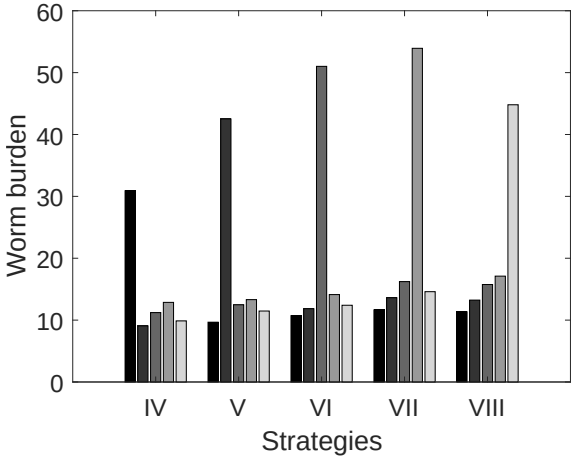

(e) Mean worm burden in humans for each age group and strategy.

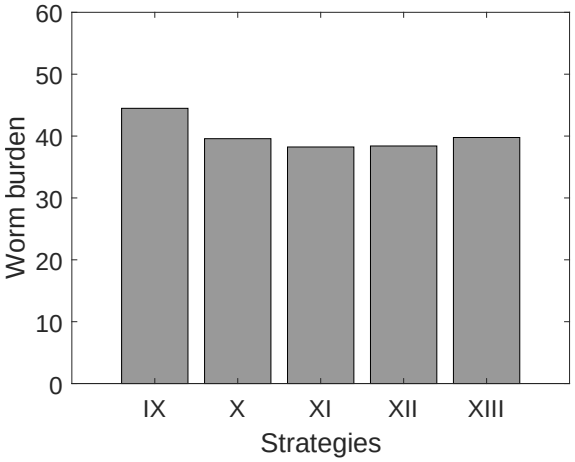

(c) Mean worm burden in humans over all age groups of each strategy.

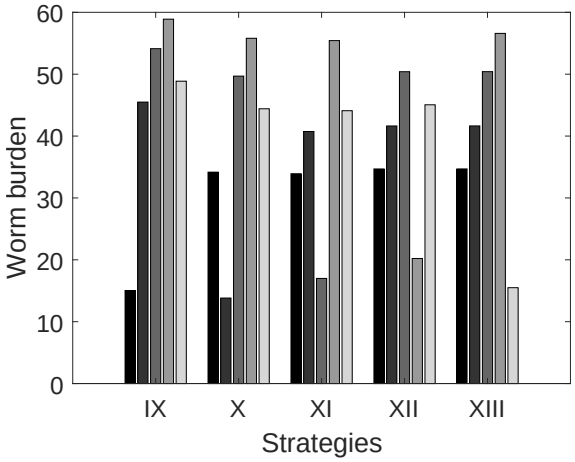

(f) Mean worm burden in humans for each age group and strategy.

Figure 10.5: Intervention strategies (Table 10.4–10.6) applied annually for 10 years. The effect of the intervention on the mean worm burden of each age group and overall population.

Strategy		Age group <6	6–16	17–36	37–50	>50
IV:	ignoring age group <6	0	0.8867	0.8867	0.8867	0.8867
V:	ignoring age group 6–16	0.9739	0	0.9739	0.9739	0.9739
VI:	ignoring age group 17–36	0.9844	0.9844	0	0.9844	0.9844
VII:	ignoring age group 37–50	0.7770	0.7770	0.7770	0	0.7770
$VIII$:	ignoring age group >50	0.7956	0.7956	0.7956	0.7956	0

Table 10.5: Coverage of MDA of the age groups for each strategy $IV - VIII$.

Strategy		Age group <6	6–16	17–36	37–50	>50
IX:	focusing on age group <6	0.7	0	0	0	0
X:	focusing on age group 6–16	0	0.7	0	0	0
XI:	focusing on age group 17–36	0	0	0.7	0	0
XII:	focusing on age group 37–50	0	0	0	0.7	0
$XIII$:	focusing on age group >50	0	0	0	0	0.7

Table 10.6: Coverage of MDA of the age groups for each strategy $IX - XIII$.

and strategy VII has 1.37 times more worms than the baseline strategy. Focusing on only one age group as in strategies IX–XII increases the mean worm burden between 2.39–2.78 times more than the baseline strategy.

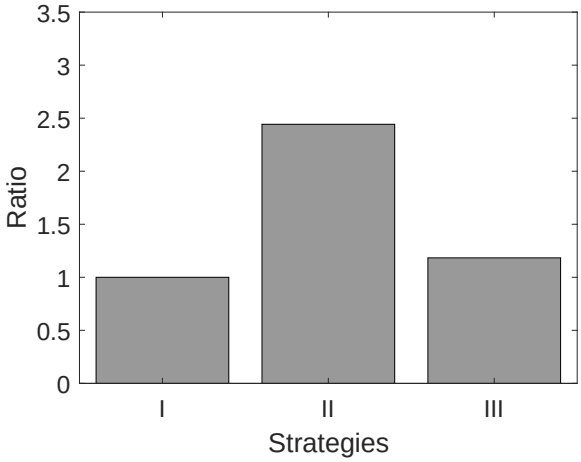

(a) Ratio of the mean worm burden of each strategy to the baseline strategy.

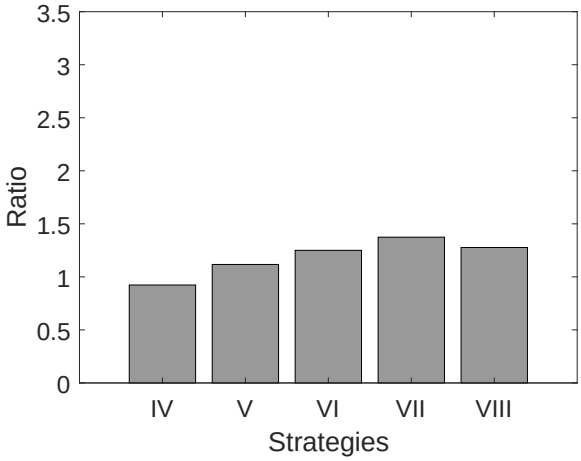

(b) Ratio of the mean worm burden of each strategy to the baseline strategy.

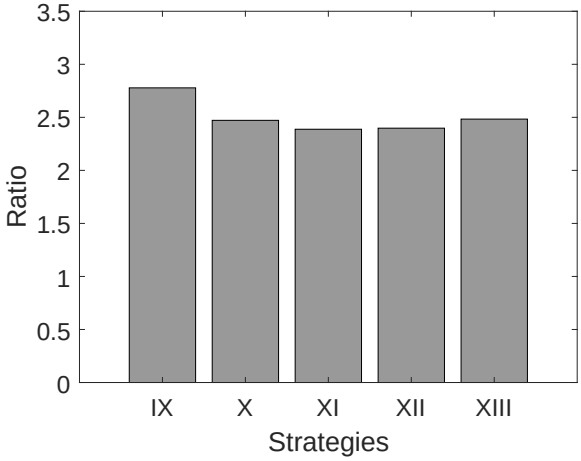

(c) Ratio of the mean worm burden of each strategy to the baseline strategy.

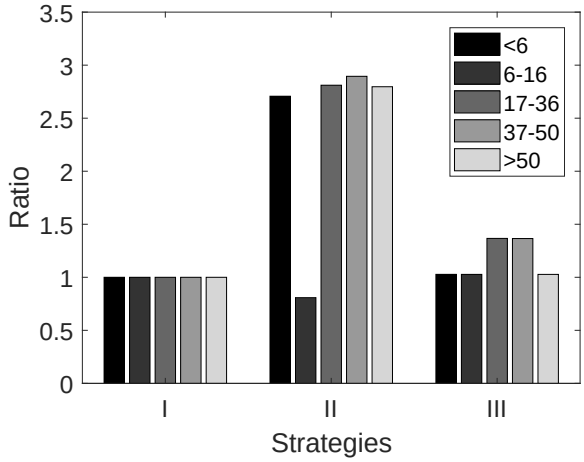

(d) Ratio of the mean worm burden in each age group to the baseline strategy.

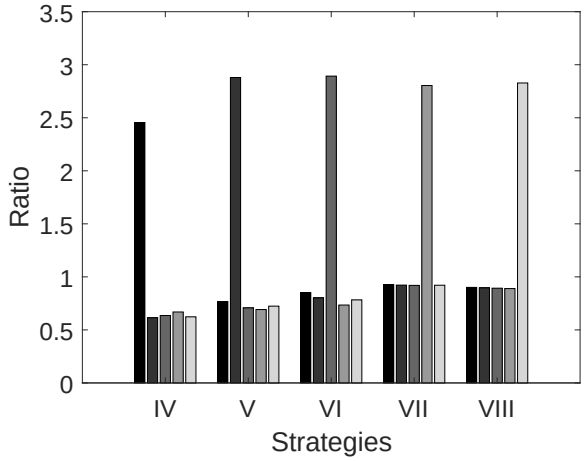

(e) Ratio of the mean worm burden in each age group to the baseline strategy.

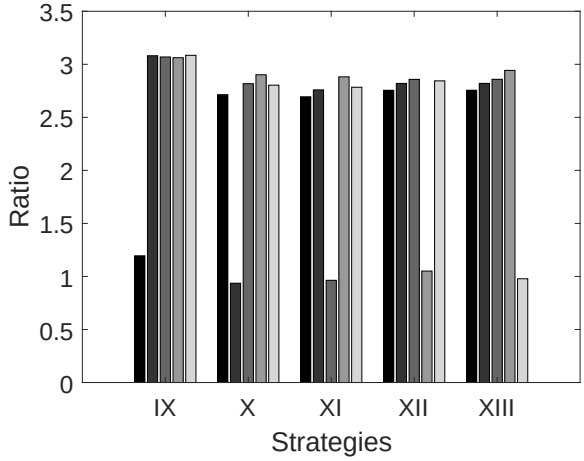

(f) Ratio of the mean worm burden in each age group to the baseline strategy.

Figure 10.6: The ratio of the mean worm burden compared to the baseline strategy I.

11. Individual-based model

We develop an individual-based model that simulates the worm burden in each human separately depending on gender, age and eating habits, this allows us to better determine the impact of worm burden on morbidity and mortality. The worm burden of the reservoir hosts dogs and cats is modelled as a pool of worm burden. I add interventions with different coverage levels and analyse their effect on the mean worm burden in the definitive hosts and on the prevalence of the intermediate hosts. I calculate the odds ratio of deaths of the different intervention strategies to compare their effect on mortality.

11.1 Methods

General outline of the model

We develop an individual-based model of *O. viverrini* to simulate its transmission dynamics and the impact of different strategies of interventions. We model the definitive host human individually with a certain number of worms in each person and the prevalence of the intermediate hosts snails and fish as groups of susceptible and infected hosts. We further model the mammalian definitive hosts dogs and cats as a pool of worms in each set of hosts. Figure 11.1 illustrates the individual-based model of *O. viverrini*. We provide an outline of the model here, but details are shown in Appendix B.

Human demography

The size of the human population is fixed. Each person has the different characteristics: sex and age; and a fixed probability to eat raw or undercooked fish. The sex is chosen randomly with a binomial distribution and a given probability to be male. The distribution of humans over age is shown in Figure 11.2 and the distribution of a fixed probability to eat raw or undercooked fish in Figure 11.3.

People die in a stochastically with the mean rate dependent on their age and worm burden. The probability to die is shown in Figure 11.4, the maximum age is set to 85 years. They are replaced by a newborn person. A fixed number of newborns in every time step keeps the age distribution stable over time by replacing the deceased population. When not enough people die in one time step, the missing number is randomly selected out of the people most likely in order to die accordingly to the mortality, and replaced by newborns.

Human infection

Worms in humans die stochastically and are added to the population with a transmission probability depending on human behaviour of eating raw or undercooked fish and the number of infected fish.

Reservoir hosts demography and infection

The reservoir hosts are represented by a pool of the worm burden in dogs and cats. We have a fixed number of dogs and cats in the model, which have each a certain amount of worms at the beginning. The number of worms in the pool of cats and dogs is calculated from the data from Lao PDR in Table 7.2, multiplied by their population sizes in Table 11.1, which have been estimated in Table 9.2. The pool of worms in dogs and cats is simulated separately. The worms in the pool die and join in the same random way as in humans.

Intermediate hosts demography

Snails and fish are simulated as two populations with a group of infected animals and a group of susceptible animals. The susceptible snails get infected randomly depending on the number of worms in humans, dogs, cats, and the susceptible fish depending on the number of infected snails. Fish and snails die individually in a stochastically way. If the total number of snails or fish decreases below the value, the number of susceptible snails

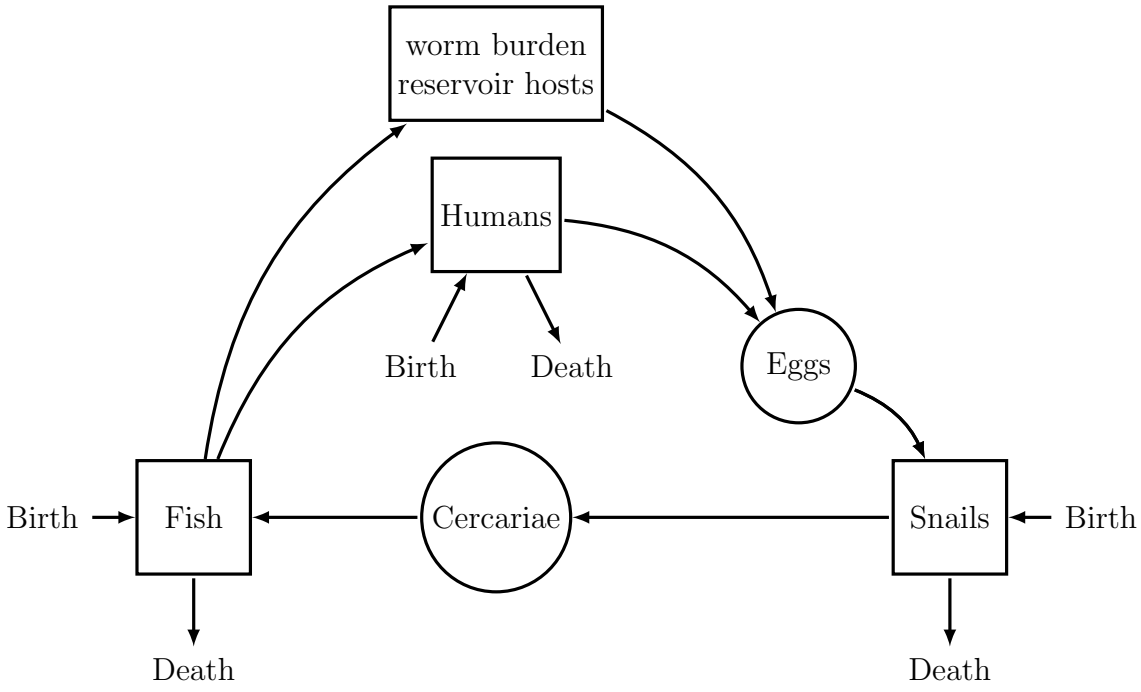

Figure 11.1: Schematic representation of the individual based model of *O. viverrini* with the non-human definitive hosts as a pool of worm burden.

Figure 11.2: Distribution of humans over age.

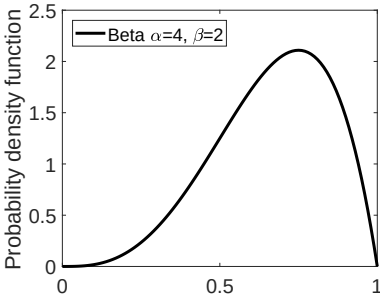

Figure 11.3: Distribution of the probability to eat raw fish given at birth.

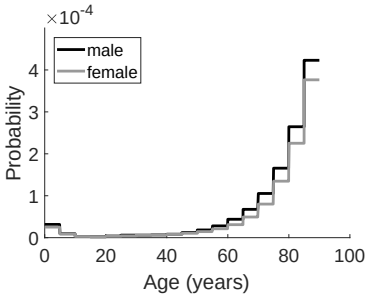

Figure 11.4: Distribution of the probability of humans to die depending on age.

Variable	Description	Value	Units
N_h	Number of humans	15,000	animals
N_d	Number of dogs	8,058	animals
N_c	Number of cats	5,824	animals
N_s	Number of snails	29,627	animals
N_f	Number of fish	9,266	animals
μ_{ph}	Per capita death rate of adult parasites in humans	$\frac{1}{4.8\times365}$	1/Time
μ_{pd}	Per capita death rate of adult parasites in dogs	$\frac{1}{2.2\times365}$	1/Time
μ_{pc}	Per capita death rate of adult parasites in cats	$\frac{1}{1.5\times365}$	1/Time
μ_s	Per capita death rate of snails	$\frac{1}{1\times365}$	1/Time
μ_f	Per capita death rate of fish including mortality through fishing by humans	$\frac{1}{1.5\times365}$	1/Time

Table 11.1: Population sizes and parameters used in the simulations.

and fish is increased to keep the population constant. The construction of the algorithm ensures that it is not possible to have more snails or fish. The constant values are provided in Table 11.1.

Drug treatment

If we assume that the given drug has an efficacy of 100%, it follows that treated humans are free of worms after treatment. Only humans who are infected get treatment. There exits a fraction of the human population that do not take part in any treatment programme because of chronic hypertension, hepatitis, diabetes, chronic kidney failure, or chronic cardiovascular diseases [95, 96]. In addition to this fraction, all pregnant women do not take part in any treatment programme. People who take part in a MDA campaign several times after reinfection are more likely to die as they have a higher risk of getting cancer. This higher risk comes from the damage to the liver which persists even after treatment. This situation combined with reinfection and repeated drug treatment correlates with the frequency of treatment as a risk factor for CCA. We use the odds ratio in Table 11.2 [103].

Number of worms	Odds ratio	Number of treatments	Odds ratio
0	1	0	1
< 38	1.67	1	3.4
< 76	3.23	2–4	4.6
> 76	14.08		

Table 11.2: Odds ratio of getting cancer dependant on worm burden and number of past treatments [103]. We transformed the eggs per gram into the mean worm burden by the formula in [28].

Education campaigns

Education campaigns have an effect on people's behaviour of eating raw or undercooked fish. We assume that these campaigns change people's eating behaviour to no longer eat raw or undercooked fish. Consequently, in the model, education campaigns change the fixed probability of eating raw or undercooked fish to zero.

Improved sanitation

There is a certain probability that each human has a latrine available. On the two islands in Lao PDR, 44.06% of the people had a latrine (in 2012) [126]. In accordance with this percentage, it is randomly decided if a person has a latrine available or not. We have a probability dependent on age and sex for the use of a latrine, since not all people who have a latrine available use it. The probability to use the latrine, if it is available, is shown in Figure 7.4. The people who use the latrine are assumed to not transmit any parasites to snails.

Simulations

We use 1 day time steps and simulate transmission for 20 years. Humans choose their eating habits monthly. If they choose to eat raw or undercooked fish, they eat it every fourth day. They also decide if they take part in regularly conducted treatment programmes. The transmission of worms to the definitive hosts and the prevalence in the intermediate hosts is calculated on a daily basis while the death of worms in humans is calculated on a monthly basis.

We simulate a fixed population size of 15,000 humans. We use the odds ratio of the human population size to the population size of the other hosts from Table 9.2 and define the population sizes in Table 11.1. The transmission and death rates are taken from Chapter 9.

The initial number of worms in humans is taken from the distribution found in Figure 7.6, fitted to the data from Lao PDR. The initial number of worms in the pool of cats and dogs is taken from Table 7.2, see Chapter 7.

11.2 Data and parameter values

The data we use in the model are based on the study done from October 2011 until August 2012 on the two islands Done Khon and Done Som in the Champasack province in Lao PDR. We have data on the intensity of infection in humans, their age, gender, and habits of eating raw or undercooked fish. We have data on the intensity of infection and prevalence of the reservoir hosts cats and dogs and the prevalence of infection in snails and fish. [126]. The human distribution over age is fitted from the United Nations Data on Lao PDR from 2015 [120], while the number of newborns is equal to the death rate of Lao PDR from 2015 [117]. The number of animals and death rates, found in Table 11.1, are based on estimates from Table 9.2 as found in Table.

Parameter fitting

The transmission rates from one host to the next host are unknown. We estimate these parameters by creating prior distributions and redefining posterior distributions with the help of a distance measure. We use the estimates from Table 9.2 as the mode of the prior triangular distribution.

We sample 5000 parameter sets from this triangular distributions with the modes and ranges as seen in Table 11.3. The simulations of all 5000 data sets are run for a time span of 20 years.

We define the distance measure

$$\rho(m_{i,j}, D) = \sqrt{\sum_j \left(\frac{m_{i,j} - D_j}{\mathrm{sd}(m_j)} \right)^2} \tag{11.1}$$

with $m_{i,j}$ being the output from run i ($i \in \{1, \ldots, 5000\}$) and animal j ($j \in \{h, d, c, s, f\}$) and D_j being the data we have from the Lao PDR data set, cf. Table 7.2. The output $m_{i,j}$ is the mean worm burden in the definitive hosts and the prevalence of infection in the intermediate hosts. We scale the results and the data by dividing by the standard deviation of all results of the simulations and calculate the distance between the model runs and the data by equation (11.1). We create a posterior distribution with the 100 runs that minimize the distance the most [125].

To test if there is a difference in the prior and posterior distribution of the transmission rate, we apply a variance test. We test the variance from the distribution of all 5000 data sets and the variance of the 100 best data sets with a two sample F-test[1] with a significance level of 5% shown in Figure 11.5 [125].

[1] MatlabR2017a: vartest2

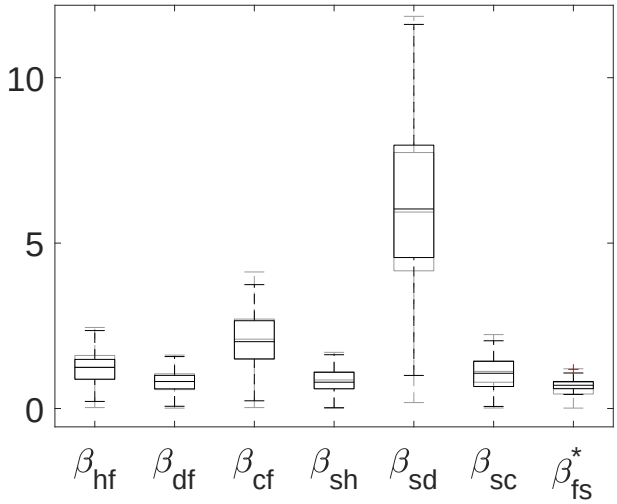

Figure 11.5: Box plot of the transmission rates, scaled by the best fit as in Table 11.3. The grey box plots are the prior distributions and the black box plots are the posterior distributions. The transmission rates marked by a star are significantly narrower distributed in the posterior than in the prior with a significance level of 5%.

Parameter	Description	Dimension	Mode	Ranges	Best solution
β_{hf}	Transmission rate from infectious fish to humans per person per fish	1/(Time × Animals)	1.4946×10^{-7}	$[1.4946 \times 10^{-10}, 2.9893 \times 10^{-7}]$	1.2070×10^{-7}
β_{df}	Transmission rate from infectious fish to dogs per dog per fish	1/(Time × Animals)	1.7785×10^{-6}	$[1.7785 \times 10^{-9}, 3.5571 \times 10^{-6}]$	2.1760×10^{-6}
β_{cf}	Transmission rate from infectious fish to cats per cat per fish	1/(Time × Animals)	7.4020×10^{-6}	$[7.4020 \times 10^{-9}, 1.4804 \times 10^{-5}]$	3.5269×10^{-6}
β_{sh}	Infection rate of snails per parasite in a human host	1/(Time × Animals)	3.0630×10^{-11}	$[3.0630 \times 10^{-14}, 6.1260 \times 10^{-11}]$	3.5762×10^{-11}
β_{sd}	Infection rate of snails per parasite in a dog host	1/(Time × Animals)	8.5905×10^{-11}	$[8.5905 \times 10^{-14}, 1.7181 \times 10^{-10}]$	1.4328×10^{-11}
β_{sc}	Infection rate of snails per parasite in a cat host	1/(Time × Animals)	1.4320×10^{-10}	$[1.4320 \times 10^{-13}, 2.8640 \times 10^{-10}]$	1.2768×10^{-10}
β_{fs}	Infection rate of fish per snail	1/(Time × Animals)	6.4500×10^{-6}	$[6.4500 \times 10^{-9}, 1.2900 \times 10^{-5}]$	1.0701×10^{-5}

Table 11.3: Description of transmission rates used in the model with the initial values, the ranges of the triangular distribution, and its best fit. The initial value are adapted from the estimates in Table 9.2.

11.3 Results

We plot the simulation runs of the posterior distribution and showing the mean as well as the median and depict the standard deviation of the these parameter sets.

The median and the mean of posterior parameter sets from dogs, cats, snails and fish are close to the numbers of the data from Lao PDR. The number of worms in humans is too low but acceptable as it is still increasing after 20 years. We conclude that the model indeed describes important parts of the transmission of the life cycle of *O. viverrini*, see Figure 11.6.

Impact of interventions

We simulate the nine different strategies of combination of interventions shown in Tables 11.4 and 11.5 with the posterior distribution parameter sets. We define strategy I as the baseline strategy with no intervention as control strategy. We count the number of deaths over the 20 years simulated and compare them to the baseline strategy.

Strategy	MDA coverage	education campaign coverage	MDA Time interval
I - baseline	0	0	0
II	0.4	0	6 months
III	0.4	0	yearly
IV	0.4	0	every 2 years
V	0.4	0	every 4 years

Table 11.4: Description of the intervention strategies with different time intervals of the MDA. The level of coverage of improved sanitation is fixed at 0.4406 for all simulations [126].

Strategy	MDA coverage	education campaign coverage	MDA Time interval
I- baseline	0	0	0
VI	0.4	0.2	yearly
VII	0.4	0.4	yearly
$VIII$	0.4	0.6	yearly
IX	0.4	0.8	yearly

Table 11.5: Description of the intervention strategies. The level of coverage of improved sanitation is fixed at 0.4406 for all simulations [126].

We analyse the influence of the frequency of drug treatment on the number of deaths compared to the simulation without any interventions. We calculate the odds ratio of the number of deaths of strategies $II - V$ to strategy I and present the results of the 100 best parameter sets in a box plot in Figure 11.7.

The following numbers represent the median of the simulations of the 100 parameter sets in the box plot. If MDA is done every six months, then 1.2373 times more people die if they do not change their eating habits in comparison with when there is no MDA.

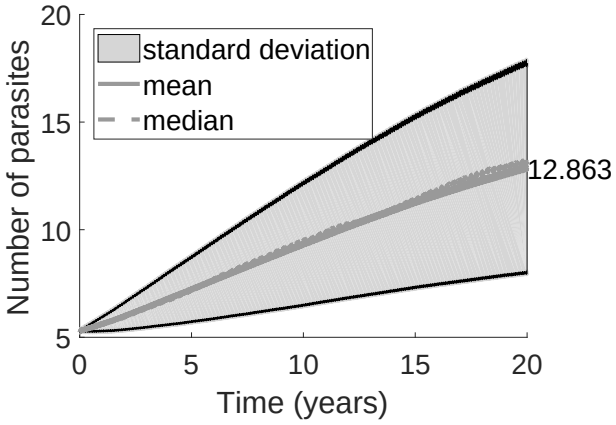

(a) Mean worm burden in humans.

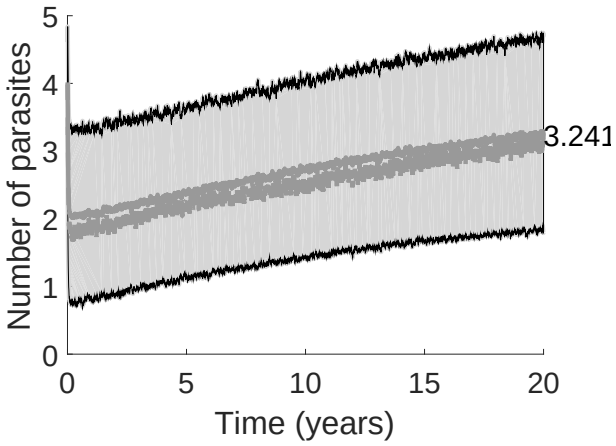

(b) Mean worm burden in dogs.

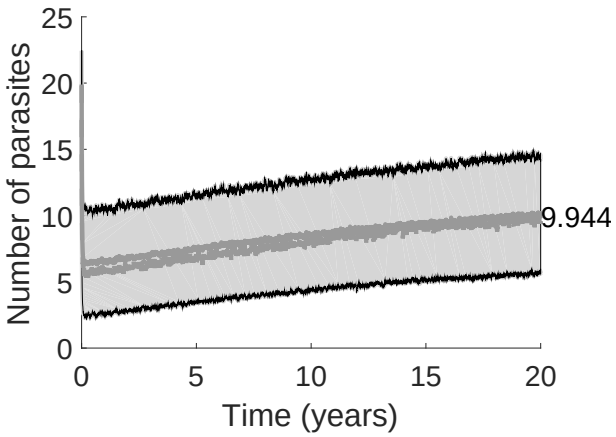

(c) Mean worm burden in cats.

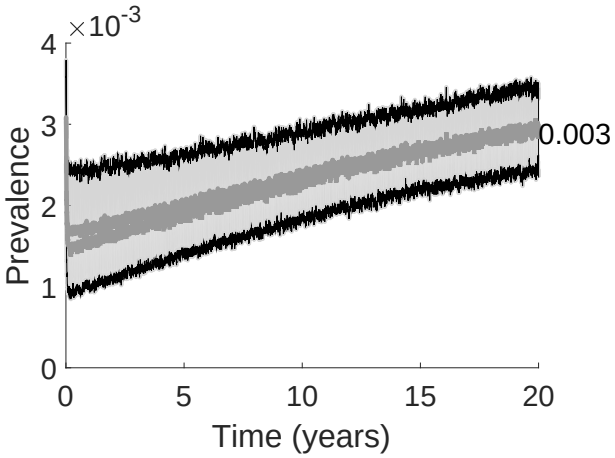

(d) Prevalence of infection in snails.

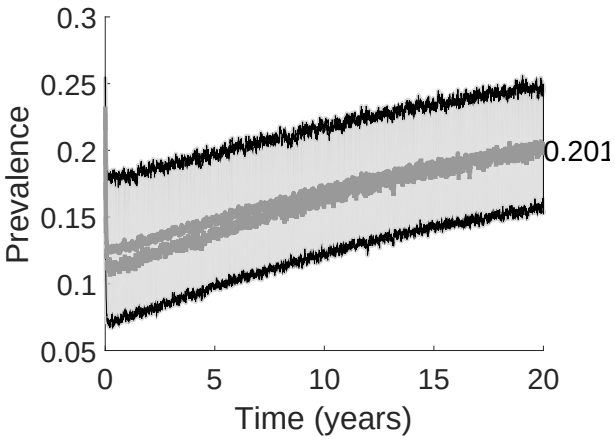

(e) Prevalence of infection in fish.

Figure 11.6: Numerical simulation of the mean, median and standard deviation of the posterior distribution. There are no interventions in these simulations.

This number increases 1.3884 when MDA campaigns are conducted every year, due to 1.4490 times when MDA campaigns are conducted every two year. We expect that this increase is due to the time between the treatments where people have more opportunity to get infected again. When treatment only occurs every fourth year, the odds ratio goes down to 1.3413 times more deaths because the relatively rare treatment does not have as stronger influence on the number of deaths as the other strategies.

As we recommend an annual MDA, we now look at the coverage level of the education campaign. With a coverage level of 20% and MDA of 40%, 1.1381 times more people die than without any intervention. If we increase the coverage of the education campaign to 40%, then still more people die than without any intervention (1.0241 times). If the coverage reaches 60%, the intervention can prevent more deaths with 0.9953 times deaths in 20 years. With a coverage level of 80%, it is 0.9115 times the level without the interventions.

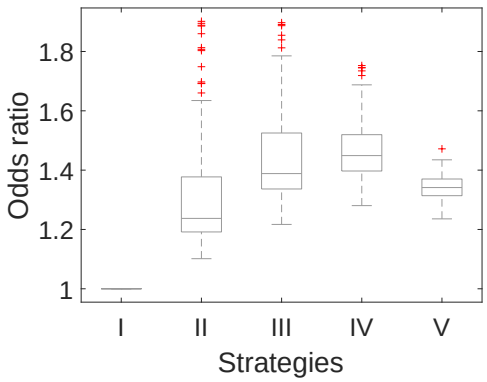

(a) Odds ratio of deaths depending on different time intervals of MDA.

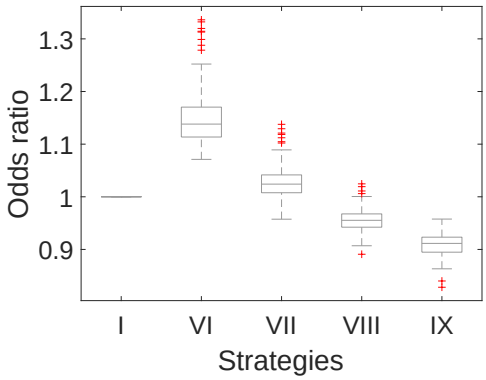

(b) Odds ratio of deaths depending on different coverage levels of education campaigns.

Figure 11.7: Box plot of the odds ratio of the number of deaths from the simulations with the 100 best parameter sets with strategies $II - IX$ compared to the baseline strategy I in Table 11.4.

11.4 Outlook

This individual-based model lays a foundation to model *O. viverrini* on an individual basis. To improve the model the following points should be considered:

- **Age distribution:** The average age increases during the simulations. We tried to keep the age distribution by a minimum number of newborns every day. A possible solution would be to include birth and deaths rates as well as model a growing population.

- **Mortality:** The number of deaths per time step is too high which leads back to the problem of the age distribution. The odds ratio of number of worms to getting cancer is given in large intervals, the same holds for the odds ratio of number of treatment to getting cancer. We could improve the probability to die with more precise data.

- **Worm burden distribution:** The worm burden follows a negative binomial distribution. Even when we start with this assumption, the peak of the worm burden

shifts up with the simulations. This peak has been shifted and flattened including the odds ratio of getting cancer depending on the worm burden in humans.

- **Fitting:** The numerical simulation of the mean worm burden in the definitive hosts and the prevalence of infection in the intermediate hosts increases over time. We would expect that it reaches a steady state solution after a certain time. The model output is very sensitive to the infections rates. To get a better fit of the infection rate a algorithm is needed, that searches for the best solution in a very tiny range.
- **Modelling morbidity:** Morbidity due to infection with *O. viverrini* can be measured with this model. As we model the mean worm burden individual, we can calculate the morbidity of each human and express it in DALYS.
- **Additional data on treatment:** There is new data available. The data includes treatment rates and prevalence of infection from sequential years. With these data the model fitting could be done over time.

12. Discussion

The World Health Organization (WHO) published a roadmap for implementation to overcome the impact of neglected tropical diseases (NTDs) [141]. The roadmap evolved from a goal of the medium-term strategic plan 2008-2013

> to provide access for all populations to interventions for the prevention, control, elimination and eradication of neglected tropical diseases [140].

The 2020 targets for food-borne trematodes (FBT), including *O. viverrini*, are:

- 75% of population at risk of food-borne trematode infections are reached by preventive chemotherapy [141].
- Morbidity due to food-borne trematode infections controlled in all endemic countries [141].

WHO recommends carrying out community diagnosis and preventive chemotherapy at the district level, and complementary interventions such as safe food practices, improved sanitation, and veterinary public health measures [135]. Praziquantel is the recommended treatment for patients with *O. viverrini* infections. It has been used for treatment for decades because of its high efficiency, large safety margin and reasonable price. Other alternative drugs are studied, the best candidate which is tribendimidine [93]. Unlike praziquantel, which is taken in two doses, tribendimidine is a single dose and has fewer adverse effects [95]. Reducing cholangiocarcinoma (CCA) with preventive chemotherapy leads to a reduction the *O. viverrini* worm burden, but there remains a high prevalence of *O. viverrini* infections [113].

Thailand developed the cholangiocarcinoma screening and care program (CASCAP), which involves a package with different levels of prevention activities. The primary prevention activity aims to block the transmission and rise a fluke-free generation. The secondary prevention activity aims to detect early cases of CCA using ultrasound screening. These detected cases get treatment and care in the tertiary prevention. It also has the goal of raising social and public awareness of *O. viverrini* and CCA to ensure that these cases receive treatment and care through the Cholangiocarcinoma Foundation [61].

In the province Khon Kaen, in the Northeast Thailand, a project was started called the Lawa model. In communities around the Lawa lake, a new research-based strategy for integrative control was launched. Starting in 2007 the programme runs including chemotherapy, novel intensive health education methods in the communities and schools, ecosystem monitoring, and active community participation. The successful programme shows a decrease in the prevalence of infection in fish, from a maximum of 70% during

the baseline study to under 1%. The integrated opisthorchis control includes treatment of infected individuals and school children, community-based activities, school-based control activities, monitoring and evaluation of all key activities to improve the model; and sustainability development with an intensive community participatory approach. The community-based activities are (i) the distribution of brochures about the liver fluke infection and liver cancer, (ii) health education by lectures and events at night, (iii) door-to-door education with the help of volunteers, (iv) folk songs about liver flukes and (v) big billboard posters [112].

The question arises: what are the most effective interventions without increasing the incidence rate of CCA? To answer this complex question, there are many aspects of *O. viverrini* that need to be looked at. It is important to understand the life cycle of *O. viverrini* and the roles of the hosts, especially of the reservoir hosts. Analysis of the life cycle shows the weakest point to target with interventions. Further aspects consider the role of interventions, including question such as which intervention has the highest impact and how many people need to be targeted. If we look closer at MDA, we investigate which age group should be targeted and how often so as to not increase the morbidity caused by reinfection.

To answer all these questions we have developed different models. We started with a basic population-based model, and a slight modification to this model to include reservoir hosts. Using these models we defined the role of each host and weakest points in the life cycle. We added interventions to the model to understand the effects of education campaigns, improved sanitation and MDA. We included age dependency of the worm burden in humans in order to simulate the application of MDA to certain age groups. Lastly, we created an individual-based model to analyse the dependence of mortality on frequency of treatment, and the coverage level of education campaigns.

12.1 Mathematical models

We started with two simple population-based models to analyse the role of all hosts and the sensitivity of the basic reproduction number $\mathcal{R}_0$ and the endemic equilibrium point to parameters. The first of the two population-based models of the transmission dynamics of *O. viverrini* is the basic model (8.1) which includes the intermediate hosts snails and fish, and humans as definitive hosts. The second model, which has reservoir hosts (8.4), also includes cats and dogs as additional definitive hosts. The models are mathematically and epidemiologically well-posed. We obtained an explicit expression for the basic reproduction number $\mathcal{R}_0$, and the disease-free and the endemic equilibrium points. The existence of the equilibrium points was proven, and we investigated their stability with respect to $\mathcal{R}_0$. The parameter values were constructed by using a sampling-resampling approach with data from two islands in Lao PDR. The models simulate the

mean worm burden in the definitive hosts, and the prevalence in the intermediate hosts over time.

The host-specific type-reproduction number defines the number of new infections from one infected individual when certain types of hosts are excluded from the model. It identifies the reservoir community and their maintenance hosts. We showed that humans, snails, and fish are maintenance-hosts, because they can sustain transmission on their own. Furthermore, transmission is not possible if any of these species are removed from the cycle, so that they are also reservoir hosts. This implies that it is possible to interrupt transmission with interventions that only target humans and ignore cats and dogs. For example, improving sanitation to a high enough level could be sufficient to eliminate opisthorchis transmission in Lao PDR. Targeting cats and dogs can reduce the mean worm burden in humans – but not eliminate it.

The basic model could not differentiate between the sensitivity of the basic reproduction number, $\mathcal{R}_0$ to the parameters. Sensitivity analysis of the model with reservoir hosts showed that $\mathcal{R}_0$ depends mostly on the death rate of parasites in humans (μ_{ph}), of snails (μ_s), and of fish (μ_f), and the population sizes of snails (N_s) and fish (N_f). Increasing the death rate of parasites in humans (μ_{ph}) is possible through regular treatment of humans with praziquantel. Increasing the death rates of snails (μ_s) and fish (μ_f) is more difficult, but reducing the number of snails is possible through snail control. Improved sanitation (which lowers β_{sh}) and safe fish production (which lowers β_{hf}) have a moderate effect on reducing $\mathcal{R}_0$.

There are some differences in the sensitivity indices of the equilibrium mean worm burden in humans (w_h^*) between the basic model and the model with reservoir hosts, and between the local and global analysis compare Figure 8.5. However, the death rate of parasites in humans (μ_{ph}), the transmission rate from fish to humans (β_{hf}), and the number of fish (N_f) most often have a high sensitivity index. This suggests that regular treatment of humans and safe fish production are the most effective interventions for reducing the parasite burden in humans. Sensitivity analysis of the model with reservoir hosts (8.4) showed that the cats have more influence on the worm burden in humans than dogs. Including interventions in the model with reservoir hosts (8.4) led to the third model which inlcudes interventions (9.1).

We defined the basic reproduction number and the control reproduction number of the model with continuous treatment (9.1). Education campaigns (I_e) and improved sanitation (I_d) show a similar relationship between coverage and the control reproduction number, with a sharper decrease as coverage increases. Since increasing coverage leads to larger gains, if these interventions are deployed, high coverage should be targeted. In contrast to that MDA get decreasing gains with increasing coverage. The coverage of mass treatment (I_m) has a stronger influence on the reproduction number, and a lower coverage is sufficient to reach the threshold of $\mathcal{R}_0 = 1$. The minimal coverage of successfully targeted humans with education campaigns is $I_e \approx 0.34$. The same is true

for the coverage of improved sanitation, $I_d \approx 0.34$. The coverage of continuous treatment has to reach $I_m \approx 0.10$ within at least a year in order to eventually lead to elimination.

Including age so the mean worm burden depends on time and humans age provides the opportunity to simulate the effect of intervention strategies targeting certain age groups. We developed two deterministic models of *O. viverrini* transmission that included age dependence in the worm burden of humans (10.1). This allowed us to capture the phenomenon that the worm burden typically increases with age since older individuals have had more time to accumulate worms and, on average adults eat more raw fish than children, until a peak of around 50 years. The average worm burden of humans does not saturate, but decreases with age after 50, possibly because deteriorating dental health (in particular due to the high prevalence of betel nut consumption), makes chewing raw fish more difficult. This has been modelled through the parameter, $\phi(a)$, which denotes the proportion of people eating raw or undercooked fish at age a. The steady state solution of the model for mean worm burden in humans replicates these dynamics in line with the data for the age distribution of eggs per gram in stool.

We defined the basic reproduction number, R_0, for the model with age-dependency (10.1). The value of R_0 is not very large, so the elimination of transmission may be feasible with sufficient control interventions.

Population-based models cannot capture morbidity or mortality of *O. viverrini* infection, well, so we proposed an individual-based model of *O. viverrini* in Chapter 11, which takes into account certain characteristics of humans such as age, gender, eating behaviour, behaviour of using improved sanitation, and their mortality. The reservoir hosts are modelled as a pool of worms in cats and dogs and the intermediate hosts as groups of susceptible and infected animals.

12.2 Interventions

Interventions which target the mean worm burden in humans are: education campaigns, improved sanitation and MDA. From the model, the decrease of worm burden in humans due to MDA, with pulsed treatment, also depends on the frequency of the distribution. The more often the distribution takes place, the faster the mean worm burden decreases. The decrease in mean worm burden in humans is much steeper with distributions once or twice a year, than every second, third, or fourth years. However, as the coverage of mass drug administration increases, the impact of the frequency of distribution decreases.

The optimal control calculation suggests an annual MDA coverage of $I_m \approx 0.44$ to achieve elimination of *O. viverrini* in 20 years, and that education campaigns should target 90% of the humans to stop eating raw or undercooked fish. Varying the underlying coverage of improved sanitation, $I_d \in \{0.4, 0.6, 0.8\}$, does not a strong influence on the optimal control calculations of the coverage of mass treatment or education campaigns.

According to our simulation results, MDA has to take place once or twice a year to achieve the elimination of *O. viverrini* within 20 years. About 97% of the 500 resampled parameter sets reach elimination with a mass treatment coverage of the optimal control solution of 44% administered twice a year. A treatment once a year with the same coverage of 44% still leads to an elimination in about 78% of the parameter sets. The other two interventions, education campaigns (I_e) and improved sanitation (I_d), require a very high coverage (over 60%) to reach an elimination within 49 and 45 years respectively. Also, the probability of elimination of these two interventions within 20 years is below 18% and 51% respectively even with a high coverage level. Therefore, education campaigns and improved sanitation alone are not enough to reach the elimination goal, and mass treatment of humans is necessary.

However, high coverage of education campaigns reduces the reinfection of treated humans, and improved sanitation reduces transmission to snails and brings additional health benefits. Hence, we should seek a coverage as high as possible of these interventions. In this analysis, we have defined the coverage of the education campaigns as the proportion of humans who stop eating raw or undercooked fish and consequently do not reinfect themselves. We have similarly defined the coverage of improved sanitation as the proportion of defecations that occur with improved sanitation. Neither of these definitions of coverage are easy to measure in the field, but may only be approximated through questionnaires.

School-based mass treatment has been a common strategy for reducing transmission and morbidity of the related trematode disease, schistosomiasis, with mixed results [42, 65]. Mathematical models of schistosomiasis have suggested that school-based programmes can be successful if the pre-treatment prevalence is low, but are unlikely to achieve global control targets if pre-treatment prevalence is high [127]. My results show that school-based treatment campaigns, even if they are able to achieve very high coverage, do not have a large impact on reducing the worm burden of the overall population, although they can have a substantial reduction in the burden of school-aged children. Therefore, control efforts should focus on community-wide campaigns. The realistic MDA (strategy III) has a lower coverage of the age groups $17-36$ years and $37-50$ years but after 10 years of annual treatment the mean worm burden is not much higher across all age groups than the ideal MDA (strategy I). Looking at each age group the mean worm burden in the less noticed group is much higher than in the other ones. Although campaigns should aim at a coverage which is as high as possible in all age groups. An exceptional effort to reach the same coverage across all age groups is unlikely to be necessary.

We also considered the impact that each age group had on maintaining transmission by simulating MDA campaigns in only one age group, or by excluding only one age group. The simulations for excluding a group allows on increased treatment coverage of the other groups, so that the overall population coverage was 70% which accounts for the fact that not all groups had same the population size. The simulations targeting only one group assumed a fixed coverage in that age group of 80%. Hence, the results also depend on

the population size of that age group. As expected, treating only children (< 6 years old) had the least impact, and excluding children was even better than the baseline strategy, since on average humans with more worms were treated. Excluding any other age group resulted in a worse outcome than the baseline strategy, suggesting that all age groups play an above-average role in maintaining transmission. Excluding the middle aged adults (37–50 years old) results in the worst outcome, suggesting that on a per capita basis, they play the biggest role in maintaining transmission. Treating only the young adult and middle age group (17–50 years old) had the best outcomes. However, the differences between the impact of treating adults of different ages was relatively small.

The individual-based model allows us to determine mortality in the population, such that the effects of interventions on mortality can be measured. The odds ratio of mortality with MDA and education campaigns to simulations with no interventions shows that, without a sustainable education campaign, MDA could do more harm than help. With a yearly treatment of at least 40% of humans, at least 60% should also receive an education campaign to change their eating behaviour. Otherwise mortality can be increase due to an increased risk of cancer from repeated treatment and reinfection

12.3 Assumptions

All models ignored seasonality in the infection dynamics in fish, and the latency period in snails and fish. Transmission of *O. viverrini* follows a seasonal pattern because of an increase of the amount of snails and fish in the rainy season. This implies that the effectiveness of interventions is dependent on the season it is implemented. Additionally, it may also be possible that cats or dogs could sustain transmission in the rainy season.

The dynamics of *O. viverrini* infection in fish is more similar to that of the parasites in humans than in snails, because fish can be superinfected, and the number of metacercariae in fish correspond to the number of potential adult worms in humans. However, little data is available on the intensity of infection in fish, so based on available prevalence data. Therefore, we make the simplifying assumption of susceptible-infectious dynamics for fish.

The sensitivity analysis depends on the data used to fit the models. This data was collected in 2011–2012 from a cross-sectional survey in two islands. Hence, in the absence of any time-series data, we made the parsimonious assumption that the system was at an endemic equilibrium, and that the coverage of any interventions (such as improved sanitation) was constant, with their effects included in the model parameters. There have been intermittent MDA campaigns in the past, as part of schistosomiasis control programme.

In the first three models we assumed all humans are identical and ignored the fact that babies are born without infection, and children have a lower worm burden than adults. Since humans accumulate parasites over their life times, heterogeneity in the

distribution of worms in humans may lead to sustained transmission, even at lower mean worm burdens. At high parasite density there are likely to be effects of density-dependence such as competition and immune regulation, but we ignore these effects in our simple model.

O. viverrini is a hermaphrodite – it has both male and female reproductive organs – so any two worms in one definitive host can reproduce and Allee effects at low worm densities are less relevant for this species [35] (although they can be relatively easy included in an individual-based model). Assortative mixing between species is unlikely because cats and dogs are domestic pets, so all definitive hosts live in the same households, eat the same fish, and are likely to the infect the same fish.

Fish trading can help the disease to spread into new areas. As we assume closed local transmission we neglected that infected fish could be transported to other areas or infected fish could be imported from else where.

The infection rate from fish to the definitive hosts ($\beta_{hf}, \beta_{df}, \beta_{cf}$) depends on the intensity of infection in fish. We ignore the intensity of infection in fish, but model the prevalence of infected fish. Similar to the heterogeneity in humans, the heterogeneity of intensity of infection in fish could lead to higher transmission. Infected snails and fish are not infectious immediately, but need some time for the parasite to develop. This latent period could lead to a lower prevalence of infectious snails and fish, because infected snails and fish can die before becoming infectious.

The worms are not only unequally distributed over age but are generally heterogeneous, with an overdispersed distribution over the population (that is, a few people have an extremely high number of worms while the majority have zero to a few worms). We modelled this by assuming a negative binomial distribution for the worm burden in the human population, but ignored the secondary impacts – such as the impact of worm burden on morbidity; the nonlinear relationship between treatment and worm burden on morbidity; and the impact of targeted interventions – of this overdispersion.

We also did not consider the sustainability of the interventions. It has been shown that governmental control programmes are often only successful during the implementation [101]. We assume here that the interventions will continue to be active and equally efficacious over the simulation period; that is the human population will maintain the behaviour change of not eating raw fish and that the improved sanitation will be maintained.

We assumed perfect efficaciousness of all interventions at the given coverage level – although in our models this would be equivalent to imperfect interventions at higher coverage levels. We also assumed no decay in the use of improved sanitation and behavioural change. Sustaining the effectiveness of such interventions is possible but would require sustained efforts by national control programmes.

We also only considered the impact of interventions in reducing transmission, and not on reducing disease burden. This may have a substantial impact on the results because,

while differently treating particular age groups may have a minor impact on transmission, they have a substantial impact on consequent disease burden. The effect of interventions as education campaigns and improved sanitation are difficult to measure. We assume that a person who takes part in an education campaign changes its eating habit definitely to not eating raw or undercooked fish. Data on sustainability of these interventions would be needed to analyse their impact. However, the relationship between worm burden and morbidity for opisthorchiasis is complicated, as field studies have shown that repeated treatment of high intensity infections may increase the risk of cancer [103].

12.4 Outlook

This work lays a basis to model transmission dynamics of *O. viverrini*. There are still many unanswered questions concerning:

- **Interventions:** What does improve the sustainability of interventions, is it the coverage level, the frequency of application or something else? When is the best time to implement an intervention concerning the seasonality of snails and fish?
- **Morbidity and mortality:** Which effect do *O. viverrini* infections and treatment campaigns have on morbidity and mortality? What are the options to measure morbidity and mortality?
- **Spreading:** How far does the infection of *O. viverrini* spread through traded fish and fish movement in the water? What favours the new settlement of *Bythnia* snails and how could it be prevented?

13. Conclusion

Targeting humans as a first priority is common in all the current interventions programmes. Intervention analysis in the models shows that MDA cannot be omitted if elimination of *O. viverrini* should be achieved as fast as possible. MDA is only successful against the disease if it is done in combination with an education campaigns. People have to change their eating habits or MDA could do more harm than help. Reinfection of *O. viverrini* and frequent treatment leads to a higher risk of getting CCA and reduced health status. Improved sanitation reduces the infection of snails, and also stops the transmission of other food-borne trematodes. Building and using improved toilets is also important because of the additional benefits of improved hygiene.

Targeting the intermediate hosts with interventions is much more difficult. It is known that rice fields are the preferred living habitats for the *Bythnia* snails, but they can survive the burning or drying of the field. They can also be reintroduced from a pond nearby when the farmers floods the fields again [128]. It is easier to target the transmission from fish to humans than from snails to fish. To stop the transmission from snails to fish, safe fish production could be implemented, but many people live from fishing, so we may create another problem, while solving one. Education campaigns include not only the knowledge about the diseases and the parasite, but also the prevention measures. Cooking the fish kills the parasite by heat, but this requires changes in the cultural habit of eating raw or undercooked fish. Moreover it is not only humans who eat infected fish, but also their pets eat leftovers and get infected.

In this setting, it is unlikely that cats and dogs are necessary to maintain transmission. This means it could be possible to eliminate *O. viverrini* by only targeting humans by effective interventions such as regular treatment, safe fish production and improved sanitation. Whether or no this is generalisable to other geographical areas would require similar analysis of models parametrised to data from those settings. MDA campaigns can be effective in reducing transmission, especially when combined with improved sanitation and eating behaviour change campaigns. Specifically, elimination of *O. viverrini* in these islands may be feasible within 20 years, if a reasonable coverage of at least 40% of annual MDA campaigns are maintained, alongside efforts to change the population's eating habits, and improved sanitation. Since treating adults has the most impact on reducing transmission, campaigns should target adults, if such targeting is operationally infeasible. Otherwise, achieving moderate coverage levels in all age groups can still have a substantial impact on reducing worm burden. Education campaigns and improved sanitation coverage should be as high as possible due to their additional benefits. The coverage of education campaigns should be at least 60% and sustainable.

The WHO roadmap for NTDs focuses on preventive chemotherapy, but the models show that sustainable education campaigns are as important as MDA on these two islands in the Mekong river in Lao PDR. Using mathematical models could help to choose suitable intervention for each region of Lao PDR. Given more data across the country, the suitability of intervention can be further refined by region.

A. Appendix

Proposition 3 (Routh-Horwitz criterion, see [63])**.** *For a polynomial*

$$f(x) = a_0x^3 + a_1x^2 + a_2x + a_3 = 0 \tag{A.1}$$

with $a_i \in \mathbb{R}$ for $i = 0, 1, 2, 3$, the number of roots with positive real parts is equal to the number of sign changes in either one of the sequences

$$T_0, T_1, \frac{T_2}{T_1}$$

or

$$T_0, T_1, T_1T_2,$$

where

$$T_0 = a_0 > 0, \quad T_1 = a_1, \quad T_2 = \det \begin{bmatrix} a_1 & a_0 \\ a_3 & a_2 \end{bmatrix}.$$

Given $a_0 > 0$, all roots have negative real parts if and only if T_0, T_1 and T_2 are all positive.

B. Appendix

Construction of the individual-based model

We transform β and μ from rates to probabilities ($\tilde{\beta} = 1 - \exp(-\beta \cdot t)$, $\tilde{\mu} = 1 - \exp(-\mu \cdot t)$) [32] with time t, for the daily applied $t = 365$, and the monthly applied $t = 30$.

Creating population of humans

1. We assume a population size of $N_h = 15,000$ and have the number of newborns of 6.754 per 1,000 people per year [117]. We hence have $N_h \cdot 6.754/1000/365$ newborns in minimum every day.

2. Every human has a gender, taken form the binomial distribution with the probability $p = 0.5012$ of being male [120].

3. The age of humans is taken from an exponential distribution in days. The distribution is fitted separately for women and men with $\mu_m = 9518.49$ days for men and $\mu_f = 9726.2$ days for women [120].

4. Each human has a fixed probability of eating raw fish given by birth. This probability is randomly chosen out of a beta distribution Beta$(4, 2)$ as seen in Figure 11.3.

5. The worm burden is randomly distributed to each human who has chosen to eat raw fish. The number of worms is Poisson distributed with $\lambda = a_i \cdot \log(\text{age in yrs}) + b_i$ for $i \in \{m, f\}$. We fitted the data [126] for men $a_m = 5.503$, $b_m = 0.3164$ and for women $a_f = 8.2843$, $b_f = -7.2013$ to the Poisson distribution as shown in Figure 7.6.

Creating population of reservoir hosts

1. The initial number of worms in all cats and dogs is the number of cats and dogs multiplied by the mean worm burden in cats and dogs from Lao PDR [126]. This is $N_d \cdot 3.7905$ for dogs and $N_c \cdot 25.9234$ for cats as seen in Table 7.1 and the number of reservoir hosts as seen in Table 11.1.

Creating population of intermediate hosts

1. The total number of the intermediate hosts fish ($N_f = 9266$) and snails ($N_s = 29627$) are the population sizes, calculated using the odds ratio from the human populations to the population size of the other hosts from Table 9.2.

2. The number of infected fish (f_i) is calculated as $N_f \cdot 0.2691$ with 0.2691 being the prevalence of fish from [126], see Table 7.1.

3. The number of susceptible fish (f_s) is $N_f \cdot (1 - 0.2961)$, see Table 7.1.

4. The number of infected snails (s_f) is calculated as $N_s \cdot 0.0029$ with 0.0029 being the prevalence of snails from [126].

5. The number of susceptible snails (s_s) is $N_s \cdot (1 - 0.0029)$.

Simulation in time

One time step represents one day.

1. **Humans.**

   a) Humans choose their temporary probability of eating raw fish. The data [126] are fitted to an exponential distribution $a_i \cdot \exp\left(-\left(\frac{\text{age in yrs}-b_i}{c_i}\right)^2\right) \cdot 0.6$ fir $i \in \{m, f\}$ separately for men and women, shown in Figure 7.3. Men have parameters $a_m = 0.9884$, $b_m = 44.1$, $c_m = 75.15$ and women have $a_f = 0.9813$, $b_f = 43.59$, $c_m = 63.32$. The distribution is multiplied by 0.6 according to the data [126] to give the proportion of people eating raw or undercooked fish. With their individual probability of eating raw fish, it is decided with a binomial distribution if they are going to eat fish or not. All children below 2 years do not eat raw fish. This probability is multiplied with the fixed probability to eat raw or undercooked fish given by birth. Humans have the same eating habit for one month. When they choose to eat raw or undercooked fish, they do it only every fourth day, so approximately two times a week.

   b) The death of a worm in a human being is decided individually by a binomial distribution with the probability of the worm to die of $p = \tilde{\mu}_{ph}$ on a monthly base.

   c) The number of new worms in humans is randomly taken from a Poisson distribution with $\lambda = f_i \beta_{fh}$. Only the humans eating raw or undercooked fish are getting new worms and only on the days they are eating fish.

   d) Each human gets one day older.

   e) The probability of each person to die depends on age, gender, number of worms and number of treatments [136, 103]. We take the odds ratio in Table 11.2 of getting CCA and multiply it with the probability to die as the cancer is usually fatal.

   f) We have a maximum age of 85 years.

   g) As we have a fixed population size i.e. dead people are replaced by newborns.

h) The number of newborns is counted and compared to the minimum number of newborns. When this minimum is not reached, some additional humans are chosen with the same probability of mortality to be replaced by newborns. This is done to keep the age distribution stable.

2. **Reservoir hosts: dogs and cats.**

   a) For each worm in a dog or cat, it is individually decided by a binomial distribution if it dies with the probability $p_d = \tilde{\mu}_{pd}$ in case of dogs and the probability $p_c = \tilde{\mu}_{pc}$ in case of cats.

   b) The worms of all dogs are summed up and the worms of all cats are summed up. The number of new worms in the pool of worm burden dogs/cats is randomly chosen by a Poisson distribution with $\lambda_d = f_i \beta_{df} N_d$ for dogs and $\lambda_c = f_i \beta_{cf} N_c$ for cats.

3. **Intermediate hosts: snails and fish.**

   a) The number of new infected snails and fish is taken randomly from a Poisson distribution with

$$\begin{aligned}\lambda_s = (\sum &(\text{number of worms in humans}) \cdot \beta_{sh} \\ &+ (\text{number of worms in pool (dogs)}) \cdot \beta_{sd} \\ &+ (\text{number of worms in pool (cats)}) \cdot \beta_{sc}) s_s\end{aligned}$$

   for snails and

$$\lambda_f = s_i f_s \beta_{fs}$$

   for fish.

   b) Snails and fish die individually determined with a binomial distribution with the probability $p_s = \tilde{\mu}_s$ to die for snails and $p_f = \tilde{\mu}_f$ to die for fish.

   c) The number of snails and fish is fixed (N_s, N_f). If the number of snails and fish is smaller then the fixed population size, new snails and fish are added to the susceptible population.

Interventions

1. **Drug treatment.**

   a) Drug treatment is done over a certain time interval, for example annually, i.e., every 365^{th} time step.

   b) Each drug treatment has a defined coverage.

c) The humans receiving treatment are randomly chosen. The number of chosen humans is given by the coverage.

d) There exists a fraction of humans who never take part in a drug treatment campaign because of health issues. Therefore, each person decides from a binomial distribution with the probability 1–0.0587 to take part in the treatment. We calculate this fraction with the help of the study from 2018 [95, 96].

e) Pregnant women do not receive any drugs and do not part in the MDA. Each woman has a probability dependent on her age to be pregnant and thus a probability of not taking part. We use ay a binomial distribution to decide if the woman takes part or not shown in Figure B.1 [119].

f) Humans without worms are not taking part in the MDA.

g) All worms in the humans, who take part in the treatment program, die as we assume perfect efficacy.

2. **Education campaign.**

a) The education campaigns are conducted over a certain time interval, e.g. once per year, so every 365^{th} time step.

b) The humans are randomly chosen accordingly to the predefined coverage level to take part in the education campaign.

c) The eating habit of the humans taking part in the education campaign changes to not eating raw or undercooked fish, i.e., the respective probability is set to zero.

3. **Improved sanitation.**

a) Since not all humans have a latrine available, we have a certain coverage of latrines, using a value of 0.4406 from [126].

b) Each human has a probability to use the latrine dependent on gender and age $a_i \cdot \log(\text{age in yrs}) + b_i$ for $i \in \{m, f\}$, where $a_m = -0.02674$ and $b_m = 0.1417$ for men and $a_f = 0.007993$ and $b_f = 0.04745$ for women [126]. It is binomially decided, depending on this probability, if they use the latrine or not in case of having one available. They decide this once a month and have the same habit the whole month.

c) The humans using the latrine cannot transmit any eggs to snails. This means, the number of worms of these humans is not taken into account when calculating the new number of infected snails, but they keep their worm burden.

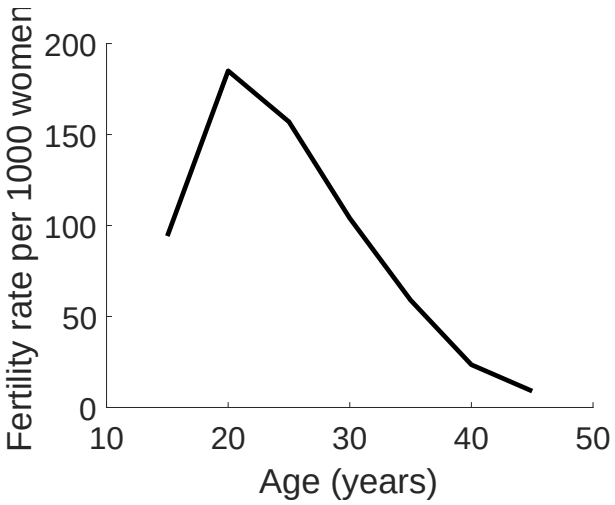

Figure B.1: Fertility rate per age group per 1000 women[119].

Bibliography

[1] Lahsen Ababouch. Assuring fish safety and quality in international fish trade. *Marine Pollution Bulletin*, 53(10):561–568, 2006.

[2] E.J. Allen and H.D. Victory. Modelling and simulation of a schistosomiasis infection with biological control. *Acta Tropica*, 87(2):251–267, 2003.

[3] Ross H. Andrews, Paiboon Sithithaworn, and Trevor N. Petney. *Opisthorchis viverrini*: an underestimated parasite in world health. *Trends in Parasitology*, 24(11):497–501, 2008.

[4] Vuong Tuan Anh, Nguyen Thuy Tram, Lise Tønner Klank, Phung Dac Cam, and Anders Dalsgaard. Faecal and protozoan parasite contamination of water spinach (Ipomoea aquatica) cultivated in urban wastewater in Phnom Penh, Cambodia. *Tropical Medicine & International Health*, 12(s2):73–81, 2007.

[5] Surasit Aunpromma, Prasarn Tangkawattana, Pittaya Papirom, Prapan Kanjampa, Smarn Tesana, Banchob Sripa, and Sirikachorn Tangkawattana. High prevalence of *Opisthorchis viverrini* infection in reservoir hosts in four districts of Khon Kaen Province, an opisthorchiasis endemic area of Thailand. *Parasitology International*, 61(1):60–64, 2012.

[6] AD Barbour. Macdonald's model and the transmission of bilharzia. *Transactions of the Royal Society of Tropical Medicine and Hygiene*, 72(1):6–15, 1978.

[7] Vicente Y. Belizario, Francis Isidore G. Totañes, Winifreda U. de Leon, Yvonne F. Lumampao, and Raezelle Nadine T. Ciro. Soil-transmitted helminth and other intestinal parasitic infections among school children in indigenous people communities in Davao del Norte, Philippines. *Acta Tropica*, 120:S12–S18, 2011.

[8] Robert Bergquist and Sara Lustigman. Chapter 10 - control of important helminthic infections: Vaccinedevelopment as part of the solution. In Xiao-Nong Zhou, Robert Bergquist, Remigio Olveda, and Jürg Utzinger, editors, *Important Helminth Infections in Southeast Asia: Diversity and Potential for Control and Elimination, Part B*, volume 73 of *Advances in Parasitology*, pages 297–326. Academic Press, Oxford, United Kindgom, 2010.

[9] David Blair, Takeshi Agatsuma, and Wenlin Wang. Paragonimiasis. In *Food-Borne Parasitic Zoonoses: Fish and Plant-Borne Parasites*, pages 117–150. Springer US, Boston, MA, 2007.

[10] Philipp J. Bless, Fabian Schär, Virak Khieu, Stefanie Kramme, Sinuon Muth, Hanspeter Marti, and Peter Odermatt. High prevalence of large trematode eggs in schoolchildren in Cambodia. *Acta Tropica*, 141:295–302, 2015.

[11] Melba G. Bondad-Reantaso, Rohana P. Subasinghe, J. Richard Arthur, Kazuo Ogawa, Supranee Chinabut, Robert Adlard, Zilong Tan, and Mohamed Shariff. Disease and health management in Asian aquaculture. *Veterinary Parasitology*, 132(3):249–272, 2005.

[12] Fred Brauer, Pauline van den Driessche, and Jianhong Wu, editors. *Mathematical Epidemiology*. Springer, Berlin-Heidelberg, 2008.

[13] Warren Y. Brockelman, E.Suchart Upatham, Vithoon Viyanant, Suraphol Ardsungnoen, and Raat Chantanawat. Field studies on the transmission of the human liver fluke, *Opisthorchis viverrini*, in northeast Thailand: population changes of the snail intermediate host. *International Journal for Parasitology*, 16(5):545–552, 1986.

[14] Kanitta Bundhamcharoen, Patarapan Odton, Sirinya Phulkerd, and Viroj Tangcharoensathien. Burden of disease in Thailand: changes in health gap between 1999 and 2004. *BMC Public Health*, 11(1):53, 2011.

[15] Christine Bürli, Helmut Harbrecht, Peter Odermatt, Somphou Sayasone, and Nakul Chitnis. Age dependency in the transmission dynamics of the liver fluke, *Opisthorchis viverrini* and the effectiveness of interventions. In preparation.

[16] Christine Bürli, Helmut Harbrecht, Peter Odermatt, Somphou Sayasone, and Nakul Chitnis. Individual-based model of the liver fluke, *Opisthorchis viverrini*. In preparation.

[17] Christine Bürli, Helmut Harbrecht, Peter Odermatt, Somphou Sayasone, and Nakul Chitnis. The liver fluke *Opisthorchis viverrini* and the impact on public health in Lao PDR. In preparation.

[18] Christine Bürli, Helmut Harbrecht, Peter Odermatt, Somphou Sayasone, and Nakul Chitnis. Analysis of interventions against the liver fluke, *Opisthorchis viverrini*. *Mathematical Biosciences*, 303:115–125, 2018.

[19] Christine Bürli, Helmut Harbrecht, Peter Odermatt, Somphou Sayasone, and Nakul Chitnis. Mathematical analysis of the transmission dynamics of the liver fluke, *Opisthorchis viverrini*. *Journal of Theoretical Biology*, 439:181–194, 2018.

[20] Jean C. Buzby and Tanya Roberts. The economics of enteric infections: Human foodborne disease costs. *Gastroenterology*, 136(6):1851–1862, 2009.

[21] Hal Caswell. *Matrix Population Models, Second Edition (Paperback)*. Sinauer Associates, Inc., Sunderland, United States of America, 2001.

[22] Jong-Yil Chai. Intestinal flukes. In *Food-Borne Parasitic Zoonoses: Fish and Plant-Borne Parasites*, pages 53–115. Springer US, Boston, MA, 2007.

[23] Nakul Chitnis, James M. Hyman, and Jim M. Cushing. Determining important parameters in the spread of malaria through the sensitivity analysis of a mathematical model. *Bulletin of Mathematical Biology*, 70(5):1272–1296, 2008.

[24] Min-Ho Choi, Sue K. Park, Zhimin Li, Zhuo Ji, Gui Yu, Zheng Feng, Longqi Xu, Seung-Yull Cho, Han-Jong Rim, Soon-Hyung Lee, and Sung-Tae Hong. Effect of Control Strategies on Prevalence, Incidence and Re-infection of Clonorchiasis in Endemic Areas of China. *PLOS Neglected Tropical Diseases*, 4(2):1–9, 2010.

[25] MS Choi, D Choi, MH Choi, Z Ji, Z Li, SY Cho, KS Hong, HJ Rim, and ST Hong. Correlation between sonographic findings and infection intensity in clonorchiasis. *American Journal of Tropical Medicine and Hygiene*, 73(6):1139–44, 2005.

[26] Jesper Hedegaard Clausen, Henry Madsen, K. Darwin Murrell, Phan Thi Van, Ha Nguyen Thi Thu, Dung Trung Do, Lan Anh Nguyen Thi, Hung Nguyen Manh, and Anders Dalsgaard. Prevention and Control of Fish-borne Zoonotic Trematodes in Fish Nurseries, Vietnam. *Emerging Infectious Diseases*, 18(9):1438–1445, 2012.

[27] O. Diekmann, J. A. P. Heesterbeek, and M. G. Roberts. The construction of next-generation matrices for compartmental epidemic models. *Journal of The Royal Society Interface*, 7(47):873–885, 2010.

[28] D. B. Elkins, P. Sithithaworn, M. Haswell-Elkins, S. Kaewkes, P. Awacharagan, and S. Wongratanacheewin. *Opisthorchis viverrini*: relationships between egg counts, worms recovered and antibody levels within an endemic community in northeast thailand. *Parasitology*, 102(2):283–288, 1991.

[29] DB Elkins, E Mairiang, P Sithithaworn, P Mairiang, J Chaiyakum, N Chamadol, V Loapaiboon, and MR Haswell-Elkins. Cross-sectional patterns of hepatobiliary abnormalities and possible precursor conditions of cholangiocarcinoma associated with *Opisthorchis viverrini* infection in humans. *American Journal of Tropical Medicine and Hygiene*, 55(3):295–301, 1996.

[30] Ian Fairweather. Reducing the future threat from (liver) fluke: realistic prospect or quixotic fantasy? *Veterinary Parasitology*, 180(1):133–143, 2011.

[31] Wendell H. Fleming and Raymond W. Rishel. *Deterministic and Stochastic Optimal Control*. Springer, New York, 1975.

[32] Rachael L. Fleurence and Christopher S. Hollenbeak. Rates and probabilities in economic modelling. *Pharmaco Economics*, 25(1):3–6, 2007.

[33] Armelle Forrer, Somphou, Penelope Vounatsou, Youthanavanh Vonghachack, Dalouny Bouakhasith, Steffen Vogt, Rüdiger Glaser, Jürg Utzinger, Kongsap Akkhavong, and Peter Odermatt. Spatial Distribution of, and Risk Factors for, *Opisthorchis viverrini* Infection in Southern Lao PDR. *PLoS Neglected Tropical Diseases*, 6(2):e1481, 2012.

[34] Bernard Fried, Thaddeus K. Graczyk, and Leena Tamang. Food-borne intestinal trematodiases in humans. *Parasitology Research*, 93(2):159–170, 2004.

[35] T. Fürst, S. Sayasone, P. Odermatt, J. Keiser, and J. Utzinger. Manifestation, diagnosis, and management of foodborne trematodiasis. *BMJ*, 344:e4093–e4093, 2012.

[36] Thomas Fürst, Urs Duthaler, Banchop Sripa, Jürg Utzinger, and Jennifer Keiser. Trematode Infections: Liver and Lung Flukes. *Infectious Disease Clinics of North America*, 26(2):399–419, 2012.

[37] Thomas Fürst, Jennifer Keiser, and Jürg Utzinger. Global burden of human food-borne trematodiasis: A systematic review and meta-analysis. *The Lancet Infectious Diseases*, 12(3):210–221, 2012.

[38] Thomas Fürst, Puangrat Yongvanit, Narong Khuntikeo, Zhao-Rong Lun, Juanita A. Haagsma, Paul R. Torgerson, Peter Odermatt, Christine Bürli, Nakul Chitnis, and Paiboon Sithithaworn. Foodborne trematodiases in East Asia: epidemiology and burden. In Jürg Utzinger, Peiling Yap, Peter Steinmann, and Martin Bratschi, editors, *Neglected Tropical Diseases — East Asia*, Neglected Tropical Diseases. Springer, 2019.

[39] Global Burden of Disease 2016 DALYs and HALE Collaborators. Global, regional, and national disability-adjusted life-years (DALYs) for 333 diseases and injuries and healthy life expectancy (HALE) for 195 countries and territories, 1990–2016: A systematic analysis for the Global Burden of Disease Study 2016. *The Lancet*, 390(10100):1260–1344, 2017.

[40] Mark S. Gockenbach. *Partial differential equations*. SIAM, Society for Industrial and Applied Mathematics, Philadelphia, United States of America, 2nd edition, 2011.

[41] Thaddeus K. Graczyk and Bernard Fried. Human waterborne trematode and protozoan infections. volume 64 of *Advances in Parasitology*, pages 111–160. Academic Press, 2007.

[42] H. L. Guyatt, S Brooker, C. M. Kihamia, A Hall, and D. A. Bundy. Evaluation of efficacy of school-based anthelmintic treatments against anaemia in children in the

United Republic of Tanzania. *Bulletin of the World Health Organization*, 79(8):695–703, 2001.

[43] H. L. Guyatt, T. Smith, B. Gryseels, C. Lengeler, H. Mshinda, S. Siziya, B. Salanave, N. Mohome, J. Makwala, K. P. Ngimbi, and M. Tanner. Aggregation in schistosomiasis: comparison of the relationships between prevalence and intensity in different endemic areas. *Parasitology*, 109(01):45–55, 1994.

[44] J. D. F. Habbema, S. J. De Vlas, A. P. Plaisier, and G.J. Van Oortmarsen. The mircosimulation approach to epidemiologic modeling of helminth infections, with special reference to schistosomiasis. *The American Journal of Tropical Medicine and Hygiene*, 55(5):165–169, 1996.

[45] Melissa R. Haswell-Elkins, Soisungwan Satarug, Mitsuhiro Tsuda, Eimorn Mairiang, Hiroyasu Esumi, Paiboon Sithithaworn, Pisain Mairiang, Minoru Saitoh, Puangrat Yongvanit, and David B. Elkins. Liver fluke infection and cholangiocarcinoma: model of endogenous nitric oxide and extragastric nitrosation in human carcinogenesis. *Mutation Research/Fundamental and Molecular Mechanisms of Mutagenesis*, 305(2):241–252, 1994.

[46] H. Hethcote. The mathematics of infectious diseases. *SIAM Review*, 42(4):599–653, 2000.

[47] Naoto Hisakane, Masashi Kirinoki, Yuichi Chigusa, Muth Sinuon, Duong Socheat, Hajime Matsuda, and Hirofumi Ishikawa. The evaluation of control measures against *Schistosoma mekongi* in Cambodia by a mathematical model. *Parasitology International*, 57(3):379–385, 2008.

[48] Sung-Tae Hong and Yueyi Fang. *Clonorchis sinensis* and clonorchiasis, an update. *Parasitology International*, 61(1):17–24, 2012. Opisthorchiasis and clonorchiasis: Major neglected tropical diseases in Eurasia.

[49] Peter J. Hotez and John P. Ehrenberg. Chapter 2 - escalating the global fight against neglected tropical diseases through interventions in the asia pacific region. In Xiao-Nong Zhou, Robert Bergquist, Remigio Olveda, and Jürg Utzinger, editors, *Important Helminth Infections in Southeast Asia: Diversity and Potential for Control and Elimination, Part A*, volume 72 of *Advances in Parasitology*, pages 31–53. Academic Press, 2010.

[50] Institute for Health Metrics and Evaluation. Gbd compare. `http://vizhub.helathdata.org/gbd-compare`, 2017. Accessed: 2017-11-24.

[51] Maria Vang Johansen, Tore Lier, and Paiboon Sithithaworn. Towards improved diagnosis of neglected zoonotic trematodes using a one health approach. *Acta Trop-*

ica, 141:161–169, 2015. Progress in research and control of helminth infections in Asia.

[52] Maria Vang Johansen, Paiboon Sithithaworn, Robert Bergquist, and Jürg Utzinger. Chapter 7 - Towards Improved Diagnosis of Zoonotic Trematode Infections in Southeast Asia. In Xiao-Nong Zhou, Robert Bergquist, Remigio Olveda, and Jürg Utzinger, editors, *Important Helminth Infections in Southeast Asia: Diversity and Potential for Control and Elimination, Part B*, volume 73 of *Advances in Parasitology*, pages 171–195. Academic Press, 2010.

[53] S Kaewkes, DB Elkins, P Sithithaworn, and MR Haswell-Elkins. Comparative studies on the morphology of the eggs of *Opisthorchis viverrini* and lecithodendriid trematodes. *Southeast Asian Journal of Tropical Medicine and Public Health*, 22(4):623–30, 1991.

[54] Sasithorn Kaewkes. Taxonomy and biology of liver flukes. *Acta Tropica*, 88(3):177–186, 2003.

[55] Natthawut Kaewpitoon, Soraya J Kaewpitoon, and Prasit Pengsaa. Opisthorchiasis in Thailand: Review and current status. *World Journal of Gastroenterology*, 14(15):2297–302, 2008.

[56] J. Keiser and J. Utzinger. Food-Borne Trematodiases. *Clinical Microbiology Reviews*, 22(3):466–483, 2009.

[57] Jennifer Keiser, Xiao Shu-Hua, Xue Jian, Chang Zhen-San, Peter Odermatt, Smarn Tesana, Marcel Tanner, and Jürg Utzinger. Effect of artesunate and artemether against *Clonorchis sinensis* and *Opisthorchis viverrini* in rodent models. *International Journal of Antimicrobial Agents*, 28(4):370–373, 2006.

[58] Jennifer Keiser and Jürg Utzinger. Chemotherapy for major food-borne trematodes: a review. *Expert Opinion on Pharmacotherapy*, 5(8):1711–1726, 2004.

[59] Jennifer Keiser and Jürg Utzinger. Emerging foodborne trematodiasis. *Emerging Infectious Diseases*, 11(10):1507–1514, 2005.

[60] Shahid A Khan, Brian R Davidson, Robert D Goldin, Nigel Heaton, John Karani, Stephen P Pereira, William M C Rosenberg, Paul Tait, Simon D Taylor-Robinson, Andrew V Thillainayagam, Howard C Thomas, and Harpreet Wasan. Guidelines for the diagnosis and treatment of cholangiocarcinoma: An update. *Gut*, 61(12):1657–1669, 2012.

[61] Narong Khuntikeo, Attapol Titapun, Watcharin Loilome, Puangrat Yongvanit, Bandit Thinkhamrop, Nittaya Chamadol, Thidarat Boonmars, Teerachai Nethanomsak,

Ross H. Andrews, Trevor N. Petney, and Paiboon Sithithaworn. Current Perspectives on Opisthorchiasis Control and Cholangiocarcinoma Detection in Southeast Asia. *Frontiers in Medicine*, 5:117, 2018.

[62] Kulthida Kopolrat, Paiboon Sithithaworn, Smarn Tesana, Ross H. Andrews, and Trevor N. Petney. Susceptibility, metacercarial burden, and mortality of juvenile silver barb, common carp, mrigal, and tilapia following exposure to *Haplorchis taichui*. *Parasitology Research*, 114(4):1433–1442, 2015.

[63] G.A. Korn and T.M. Korn. *Mathematical Handbook for Scientists and Engineers: Definitions, Theorems, and Formulas for Reference and Review*. Dover Civil and Mechanical Engineering Series. Dover Publications, 2000.

[64] Anuj Kumar, Prashant K. Srivastava, and Yasuhiro Takeuchi. Modeling the role of information and limited optimal treatment on disease prevalence. *Journal of Theoretical Biology*, 414:103–119, 2017.

[65] Agola E. Lelo, David N. Mburu, Gabriel N. Magoma, Ben N. Mungai, Jimmy H. Kihara, Ibrahim N. Mwangi, Geoffrey M. Maina, Joseph M. Kinuthia, Martin W. Mutuku, Eric S. Loker, Gerald M. Mkoji, and Michelle L. Steinauer. No Apparent Reduction in Schistosome Burden or Genetic Diversity Following Four Years of School-Based Mass Drug Administration in Mwea, Central Kenya, a Heavy Transmission Area. *PLOS Neglected Tropical Diseases*, 8(10):1–11, 2014.

[66] Suzanne Lenhart and John T. Workmann. *Optimal Control Applied to Biological Models*. Chapman & Hall/CRC, London, 2007.

[67] Tomas M. Leon, Travis C. Porco, Christina S. Kim, Sasithorn Kaewkes, Wanlop Kaewkes, Banchob Sripa, and Robert C. Spear. Modeling liver fluke transmission in northeast thailand: Impacts of development, hydrology, and control. *Acta Tropica*, 188:101–107, 2018.

[68] Ting Li, Shenyi He, Hong Zhao, Guanghui Zhao, and Xing-Quan Zhu. Major trends in human parasitic diseases in China. *Trends in Parasitology*, 26(5):264–270, 2010.

[69] P Loaharanau and S Sornmani. Preliminary estimates of economic impact of liver fluke infection in Thailand and the feasibility of irradiation as a control measure. *Southeast Asian Journal of Tropical Medicine and Public Health*, 22:384–90, 1991.

[70] Zhao-Rong Lun, Robin B Gasser, De-Hua Lai, An-Xing Li, Xing-Quan Zhu, Xing-Bing Yu, and Yue-Yi Fang. Clonorchiasis: a key foodborne zoonosis in China. *The Lancet Infectious Diseases*, 5(1):31–41, 2005.

[71] Eimorn Mairiang, Thewarach Laha, Jeffrey M. Bethony, Bandit Thinkhamrop, Sasithorn Kaewkes, Paiboon Sithithaworn, Smarn Tesana, Alex Loukas, Paul J. Brindley, and Banchob Sripa. Ultrasonography assessment of hepatobiliary abnormalities in 3359 subjects with *Opisthorchis viverrini* infection in endemic areas of Thailand. *Parasitology International*, 61(1):208–211, 2012.

[72] Simeone Marino, Ian B. Hogue, Christian J. Ray, and Denise E. Kirschner. A methodology for performing global uncertainty and sensitivity analysis in systems biology. *Journal of Theoretical Biology*, 254(1):178–196, 2008.

[73] S. Mas-Coma, M.D. Bargues, and M.A. Valero. Fascioliasis and other plant-borne trematode zoonoses. *International Journal for Parasitology*, 35(11):1255–1278, 2005.

[74] Santiago Mas-Coma, Marìa Dolores Bargues, and Marìa Adela Valero. Plant-borne trematode zoonoses: Fascioliasis and fasciolopsiasis. In K. Darwin Murrell and Bernard Fried, editors, *Food-Borne Parasitic Zoonoses: Fish and Plant-Borne Parasites*, pages 293–334. Springer US, Boston, MA, 2007.

[75] Antonio Montresor, Dai Tran Cong, Mouth Sinuon, Reiko Tsuyuoka, Chitsavang Chanthavisouk, Hanne Strandgaard, Raman Velayudhan, Corinne M. Capuano, Tuan Le Anh, and Ah S. Tee Dató. Large-scale preventive chemotherapy for the control of helminth infection in western pacific countries: Six years later. *PLOS Neglected Tropical Diseases*, 2(8):1–7, 2008.

[76] In Jae Myung. Tutorial on maximum likelihood estimation. *Journal of Mathematical Psychology*, 47(1):90–100, 2003.

[77] Jun Nakagawa, John P. Ehrenberg, Joshua Nealon, Thomas Fürst, Padmasiri Aratchige, Glenda Gonzales, Chitsavang Chanthavisouk, Leda M. Hernandez, Tayphasavanh Fengthong, Jürg Utzinger, and Peter Steinmann. Towards effective prevention and control of helminth neglected tropical diseases in the western pacific region through multi-disease and multi-sectoral interventions. *Acta Tropica*, 141:407–418, 2015.

[78] Khuntikeo Narong, Pugkhem Ake, Titapun Attapol, and Bhudhisawasdi Vajarabhongsa. Surgical management of perihilar cholangiocarcinoma: a Khon Kaen experience. *Journal of Hepato-Biliary-Pancreatic Sciences*, 21(8):521–524, 2014.

[79] Ingemar Nåsell and Warren M. Hirsch. The transmission dynamics of schistosomiasis. *Communications on Pure and Applied Mathematics*, 26(4):395–453, 1973.

[80] Hiroshi Nishiura, Bethany Hoye, Marcel Klaassen, Silke Bauer, and Hans Heesterbeek. How to find natural reservoir hosts from endemic prevalence in a multi-host population: A case study of influenza in waterfowl. *Epidemics*, 1(2):118–128, 2009.

[81] Chamadol Nittaya, Pairojkul Chawalit, Khuntikeo Narong, Laopaiboon Vallop, Loilome Watcharin, Sithithaworn Paiboon, and Yongvanit Paungrat. Histological confirmation of periductal fibrosis from ultrasound diagnosis in cholangiocarcinoma patients. *Journal of Hepato-Biliary-Pancreatic Sciences*, 21(5):316–322, 2014.

[82] HJ Over, J Jansen, and PW van Olm. Distribution and impact of helminth diseases of livestock in developing countries. `http://www.fao.org/docrep/004/T0584E/T0584E00.HTM#TOC`, 1992. Accessed: 2017-11-24.

[83] Tushar Patel. New insights into the molecular pathogenesis of intrahepatic cholangiocarcinoma. *Journal of Gastroenterology*, 49(2):165–172, 2014.

[84] Opal Pitaksakulrat, Paiboon Sithithaworn, Nonglak Laoprom, Thewarach Laha, Trevor N. Petney, and Ross H. Andrews. A cross-sectional study on the potential transmission of the carcinogenic liver fluke *Opisthorchis viverrini* and other fish-borne zoonotic trematodes by aquaculture fish. *Foodborne Pathogens and Disease*, 10(1):35–41, 2013.

[85] L. S. Pontryagin, V. G. Boltyanskii, R. V. Gamkrelize, and E. F. Mishchenko. *The Mathematical Theory of Optimal Processes.* Wiley, New York, 1962.

[86] Khanittha Pratumchart, Kulwadee Suwannatrai, Chanisala Sereewong, Kavin Thinkhamrop, Jukkrid Chaiyos, Thidarat Boonmars, and Apiporn T. Suwannatrai. Ecological Niche Model based on Maximum Entropy for mapping distribution of *Bithynia siamensis goniomphalos*, first intermediate host snail of *Opisthorchis viverrini* in Thailand. *Acta Tropica*, 193:183–191, 2019.

[87] S Pungpak, M Riganti, D Bunnag, and T Harinasuta. Clinical features in severe opisthorchiasis viverrini. *Southeast Asian J Trop Med Publi Health*, 16(3):405–9, 1985.

[88] S Pungpak, C Viravan, B Radomyos, K Chalermrut, C Yemput, W Plooksawasdi, M Ho, T Harinasuta, and D Bunnag. *Opisthorchis viverrini* infection in Thailand: studies on the morbidity of the infection and resolution following praziquantel treatment. *The American Journal of Tropical Medicine and Hygiene*, 56(3):311–314, 1997.

[89] H.-J. Rim. Clonorchiasis: an update. *Journal of Helminthology*, 79(3):269–281, 2005.

[90] Han Jong Rim. The current pathobiology and chemotherapy of clonorchiasis. *The Korean Journal of Parasitology*, 24(Suppl):1–141, 1986.

[91] M. G. Roberts and J. A. P. Heesterbeek. A new method for estimating the effort required to control an infectious disease. *Proceedings of the Royal Society B: Biological Sciences*, 270(1522):1359–1364, 2003.

[92] Ronald Ross. The logical basis of the sanitary policy of mosquito reduction. *Science*, 22(570):689–699, 1905.

[93] Weerachai Saijuntha, Kanyarat Duenngai, Sirikachorn Tangkawattana, Trevor N. Petney, Ross H. Andrews, and Paiboon Sithithaworn. Chapter 7 - recent advances in the diagnosis and detection of *Opisthorchis viverrini* sensu lato in human and intermediate hosts for use in control and elimination programs. In Banchob Sripa and Paul J. Brindley, editors, *Asiatic Liver Fluke — From Basic Science to Public Health, Part A*, volume 101 of *Advances in Parasitology*, pages 177–214. Academic Press, 2018.

[94] Weerachai Saijuntha, Paiboon Sithithaworn, Nadda Kaitsopit, Ross H. Andrews, and Trevor N. Petney. *Liver Flukes:* Clonorchis *and* Opisthorchis, pages 153–199. Springer, New York, NY, 2014.

[95] Somphou Sayasone, Jennifer Keiser, Isabel Meister, Youthanavanh Vonghachack, Syda Xayavong, Kanpaseuth Senggnam, Khampheng Phongluxa, Jan Hattendorf, and Peter Odermatt. Efficacy and safety of tribendimidine versus praziquantel against *Opisthorchis viverrini* in Laos: an open-label, randomised, non-inferiority, phase 2 trial. *The Lancet Infectious Diseases*, 18(2):155–161, 2018.

[96] Somphou Sayasone, Isabel Meister, Jason R. Andrews, Peter Odermatt, Youthanavanh Vonghachack, Syda Xayavong, Kanpaseuth Senggnam, Khampheng Phongluxa, Jan Hattendorf, Isaac I. Bogoch, and Jennifer Keiser. Efficacy and safety of praziquantel against light infections of *Opisthorchis viverrini*: A randomized parallel single-blind dose-ranging trial. *Clinical Infectious Diseases*, 64(4):451, 2017.

[97] Alexander Schratz, Martha Fernanda Pineda, Liberty G. Reforma, Nicole M. Fox, Tuan Le Anh, L. Tommaso Cavalli-Sforza, Mackenzie K. Henderson, Raymond Mendoza, Jürg Utzinger, John P. Ehrenberg, and Ah Sian Tee. Chapter 4 - Neglected Diseases and Ethnic Minorities in the Western Pacific Region: Exploring the Links. In Xiao-Nong Zhou, Robert Bergquist, Remigio Olveda, and Jürg Utzinger, editors, *Important Helminth Infections in Southeast Asia: Diversity and Potential for Control and Elimination, Part A*, volume 72 of *Advances in Parasitology*, pages 79–107. Academic Press, 2010.

[98] Bernd S. W. Schröder. *A Workbook for Differential Equations*. Wiley, New Jersey, United States of America, 2010.

[99] P. Sithithaworn, B. Sripa, S. Kaewkes, and MR Haswell-Elkins. Foodborne trematodes. In *Manson's tropical diseases*, pages 1461–1476. WB Saunders, London, 2009.

[100] P. Sithithaworn, S. Tesana, V. Pipitgool, S. Kaewkes, C. Pairojkul, B. Sripa, A. Paupairoj, and K. Thaiklar. Relationship between faecal egg count and worm burden of *Opisthorchis viverrini* in human autopsy cases. *Parasitology*, 102(2):277–281, 1991.

[101] Paiboon Sithithaworn, Ross H. Andrews, Nguyen Van De, Thitima Wongsaroj, Muth Sinuon, Peter Odermatt, Yukifumi Nawa, Song Liang, Paul J. Brindley, and Banchob Sripa. The current status of opisthorchiasis and clonorchiasis in the Mekong Basin. *Parasitology International*, 61(1):10–16, 2012.

[102] Paiboon Sithithaworn and Melissa Haswell-Elkins. Epidemiology of *Opisthorchis viverrini*. *Acta Tropica*, 88(3):187–194, 2003.

[103] Paiboon Sithithaworn, Puangrat Yongvanit, Kunyarat Duenngai, Nadda Kiatsopit, and Chawalit Pairojkul. Roles of liver fluke infection as risk factor for cholangiocarcinoma. *Journal of Hepato-Biliary-Pancreatic Sciences*, 21(5):301–308, 2014.

[104] Paiboon Sithithaworn, Puangrat Yongvanit, Smarn Tesana, and Chawalit Pairojkul. Liver flukes. In *Food-Borne Parasitic Zoonoses: Fish and Plant-Borne Parasites*, pages 3–52. Springer US, Boston, MA, 2007.

[105] A. F. M. Smith and A. E. Gelfand. Bayesian statistics without tears: A sampling–resampling perspective. *The American Statistician*, 46(2):84–88, 1992.

[106] David L. Smith, Katherine E. Battle, Simon I. Hay, Christopher M. Barker, Thomas W. Scott, and F. Ellis McKenzie. Ross, macdonald, and a theory for the dynamics and control of mosquito-transmitted pathogens. *PLOS Pathogens*, 8(4):1–13, 2012.

[107] Ki-Won Song, Shin-Yong Kang, and Soo-Hyung Lee. A mathematical approach to the mode of transmission of clonorchiasis in the inhabitants of Nak-dong and Han River basin. *The Korean Journal of Parasitology*, 17(2):114–120, 1979.

[108] Phonepasong Soukhathammavong, Peter Odermatt, Somphou Sayasone, Youthanavanh Vonghachack, Penelope Vounatsou, Christoph Hatz, Kongsap Akkhavong, and Jennifer Keiser. Efficacy and safety of mefloquine, artesunate, mefloquine–artesunate, tribendimidine, and praziquantel in patients with *Opisthorchis viverrini*: a randomised, exploratory, open-label, phase 2 trial. *The Lancet Infectious Diseases*, 11(2):110–118, 2011.

[109] Banchob Sripa, Jeffrey M. Bethony, Paiboon Sithithaworn, Sasithorn Kaewkes, Eimorn Mairiang, Alex Loukas, Jason Mulvenna, Thewarach Laha, Peter J. Hotez,

and Paul J. Brindley. Opisthorchiasis and Opisthorchis-associated cholangiocarcinoma in Thailand and Laos. *Acta Tropica*, 120:158–168, 2011.

[110] Banchob Sripa, Paul J. Brindley, Jason Mulvenna, Thewarach Laha, Michael J. Smout, Eimorn Mairiang, Jeffrey M. Bethony, and Alex Loukas. The tumorigenic liver fluke *Opisthorchis viverrini* – multiple pathways to cancer. *Trends in Parasitology*, 28(10):395–407, 2012.

[111] Banchob Sripa, Sirikachorn Tangkawattana, Thewarach Laha, Sasithorn Kaewkes, Frank F. Mallory, John F. Smith, and Bruce A. Wilcox. Toward integrated opisthorchiasis control in northeast Thailand: The Lawa project. *Acta Tropica*, 141:361–367, 2015.

[112] Banchob Sripa, Sirikachorn Tangkawattana, and Thinnakorn Sangnikul. The Lawa model: A sustainable, integrated opisthorchiasis control program using the Eco-Health approach in the Lawa Lake region of Thailand. *Parasitology International*, 66(4):346–354, 2017.

[113] Jennifer A. Steele, Carsten H. Richter, Pierre Echaubard, Parichat Saenna, Virginia Stout, Paiboon Sithithaworn, and Bruce A. Wilcox. Thinking beyond *Opisthorchis viverrini* for risk of cholangiocarcinoma in the lower Mekong region: a systematic review and meta-analysis. *Infectious Diseases of Poverty*, 7(1):44, 2018.

[114] Chris M. Stone and Nakul Chitnis. Implications of heterogeneous biting exposure and animal hosts on *Trypanosomiasis brucei gambiense* transmission and control. *PLOS Computational Biology*, 11(10):1–22, 2015.

[115] Apiporn Suwannatrai, Prasert Saichua, and Melissa Haswell. *Chapter 2 — Epidemiology of* Opisthorchis viverrini *Infection*, volume 101 of *Advances in Parasitology*, pages 41–67. Academic Press, 2018.

[116] S Tesana, T Srisawangwonk, S Kaewkes, P Sithithaworn, P Kanla, and C Arunyanart. Eggshell morphology of the small eggs of human trematodes in Thailand. *The Southeast Asian Journal of Tropical Medicine and Public Health*, 22(4):631–6, 1991.

[117] The World Bank. Death rate. `https://data.worldbank.org/indicator/SP.DYN.CDRT.IN?locations=LA`. Accessed: 2018-04-15.

[118] Hop Nguyen Thi, De Nguyen Van, Murrell Darwin, and Dalsgaard Anders. Occurrence and species distribution of fishborne zoonotic trematodes in wastewater-fed aquaculture in northern Vietnam. *Tropical Medicine & International Health*, 12(s2):66–72, 2007.

[119] United Nations. Population division: World fertility data 2015. `http://www.un.org/en/development/desa/population/publications/dataset/fertility/wfd2015.shtml`. Accessed: 2018-04-16.

[120] United Nations. UN data a world of information. `http://data.un.org/Data.aspx?q=area%5bLao+People%27s+Democratic+Republic%5d+datamart%5bPOP%2cWHO%5d&d=POP&f=tableCode%3a22%3bcountryCode%3a418`. Accessed: 2017-04-07.

[121] E.S. Upatham and V. Viyanant. *Opisthorchis viverrini* and opisthorchiasis: a historical review and future perspective. *Acta Tropica*, 88(3):171–176, 2003.

[122] E.S. Upatham, V. Viyanant, W.Y. Brockelman, S. Kurathong, P. Lee, and R. Kraengraeng. Rate of re-infection by *Opisthorchis viverrini* in an endemic Northeast Thai community after chemotherapy. *International Journal for Parasitology*, 18(5):643–649, 1988.

[123] T Uttaravichien, V Bhudhisawasdi, C Pairojkul, and A Pugkhem. Intrahepatic cholangiocarcinoma in Thailand. *Journal of Hepatobiliary Pancreatc Surgery*, 6(2):128–35, 1999.

[124] M. A. Valero, M. De Renzi, M. Panova, M. A. Garcia-Bodelon, M. V. Periago, D. Ordoñez, and S. Mas-Coma. Crowding effect on adult growth, pre-patent period and egg shedding of *Fasciola hepatica*. *Parasitology*, 133(4):453–463, 2006.

[125] Elske van der Vaart, Mark A. Beaumont, Alice S.A. Johnston, and Richard M. Sibly. Calibration and evaluation of individual-based models using approximate bayesian computation. *Ecological Modelling*, 312:182–190, 2015.

[126] Youthanavanh Vonghachack, Peter Odermatt, Keoka Taisayyavong, Souphanh Phounsavath, Kongsap Akkhavong, and Somphou Sayasone. Transmission of *Opisthorchis viverrini*, *Schistosoma mekongi* and soil-transmitted helminthes on the Mekong Islands, Southern Lao PDR. *Infectious Diseases of Poverty*, 6(1):131, 2017.

[127] Xiaoxia Wang, David Gurarie, Peter L. Mungai, Eric M. Muchiri, Uriel Kitron, and Charles H. King. Projecting the long-term impact of school- or community-based mass-treatment interventions for control of schistosoma infection. *PLOS Neglected Tropical Diseases*, 6(11):1–14, 2012.

[128] Yi-Chen Wang, Richard Cheng Yong Ho, Chen-Chieh Feng, Jutamas Namsanor, and Paiboon Sithithaworn. An ecological study of Bithynia snails, the first intermediate host of *Opisthorchis viverrini* in northeast Thailand. *Acta Tropica*, 141:24–252, 2015.

[129] Gail M. Williams, Adrian C. Sleigh, Yuesheng Li, Zheng Feng, George M. Davis, Hongen Chen, Allen G.P. Ross, Robert Bergquist, and Donald P. McManus. Mathematical modelling of *schistosomiasis japonica*: comparison of control strategies in the People's Republic of China. *Acta Tropica*, 82(2):253–262, 2002.

[130] M. E. J. Woolhouse, G. Hasibeder, and S. K. Chandiwana. On estimating the basic reproduction number for *Schistosoma haematobium*. *Tropical Medicine & International Health*, 1(4):456–463, 1996.

[131] M. E. J. Woolhouse, C. H. Watts, and S. K. Chandiwana. Heterogeneities in transmission rates and the epidemiology of schistosome infection. *Proceedings: Biological Sciences*, 245(1313):109–114, 1991.

[132] ME Woolhouse, JF Etard, K Dietz, PD Ndhlovu, and SK Chandiwana. Heterogeneities in schistosome transmission dynamics and control. *Parasitology*, 117:475–82, 1998.

[133] M.E.J. Woolhouse. On the application of mathematical models of schistosome transmission dynamics. i. natural transmission. *Acta Tropica*, 49(4):241–270, 1991.

[134] M.E.J. Woolhouse. On the application of mathematical models of schistosome transmission dynamics. ii. control. *Acta Tropica*, 50(3):189–204, 1992.

[135] World Health Organization. Foodborne trematode infections; *Opisthorchis viverrini*. `https://www.who.int/foodborne_trematode_infections/opisthorchiasis/Opisthorchiasis_viverrini/en/`. Accessed: 2019-04-16.

[136] World Health Organization. Global health observatory data repository. `http://apps.who.int/gho/data/?theme=main&vid=60890`. Accessed: 2018-01-09.

[137] World Health Organization. Control of foodborne trematode infections. *WHO Technical Report Series*, 849:1–157, 1995.

[138] World Health Organization. Wastewater and excreta use in aquaculture. 2006.

[139] World Health Organization and FAO. Foodborne trematode infections in Asia. Report of a joint WHO/FAO workshop. 2004.

[140] World Health Organzation. Medium-term strategic plan 2008-2013. `http://apps.who.int/gb/e/e_amtsp3.html`, 2009. Accessed: 2019-05-06.

[141] World Health Organzation. Accelerating work to overcome the global impact of neglected tropical diseases — a roadmap for implementation. 2012.

[142] Pei Zhang, Zhilan Feng, and Fabio Milner. A schistosomiasis model with an age-structure in human hosts and its application to treatment strategies. *Mathematical Biosciences*, 205(1):8–107, 2007.

[143] Andreas Ziegler. *Generalized Estimating Equations.* Springer, New York, 2011.

Curriculum Vitae

Christine Bürli
Anton-Julius-Eggstein-Gasse 6
CH - 6005 Luzern
+41 (0)79 675 90 48
christine.buerli@gmail.com

Personal Profile

Highly motivated, hardworking, and keen to learn. Good team working skills and organizational qualities through various projects. Excellent programming skills and good knowledge of standard software packages. Fluent in German and English.

Education

11/2015 – 7/2019	**PhD student in Mathematics** Swiss Tropical and Public Health Institute and University of Basel, Switzerland Thesis: Mathematical Modelling of Transmission Dynamics of the Liver Fluke, *Opisthorchis viverrini.*
9/2014 - 2/2017	**Teaching diploma for middle schools (Mathematics)** Fachhochschule Nordwestschweiz, Brugg, Switzerland
2/2013 - 5/2015	**Master of Science in Mathematics** University of Basel, Switzerland Thesis: Mathematical Modelling of Transmission Dynamics of the Liver Fluke, *Opisthorchis viverrini.*
11/2013	**SVEB Certificate (Certificate of the Swiss Federation for Adult Learning SVEB/FSEA) Level 1** The Federal Office for Sport (BASPO), Magglingen, Switzerland
9/2009 - 2/2013	**Bachelor of Science in Mathematics** University of Basel, Switzerland

Work Experience

Since 8/2019	**Teacher of Mathematics** Kantonsschule Reussbühl (middle school), Lucerne, Switzerland
8/2018 - 7/2019	**Teacher of Mathematics** Kantonsschule Alpenquai (middle school), Lucerne, Switzerland
8/2015 - 7/2016	**Teacher of Mathematics** Berufsfachschule für Gesundheit und Soziales (vocational school), Brugg, Switzerland
8/2012-7/2018	**Tutor** Academia Learning, Basel, Switzerland

6/2014 – 7/2014	**Internship** Uri's Financial Management (Finanzdirektion des Kantons Uri), specialist unit for statistics, Altdorf, Switzerland • implement different forecast scenarios of cash management • collect and evaluate data • writing reports
1/2011 – 2/2011	**Internship** SUVA (Swiss accident insurance institution), satistics and actuarial practice unit, Lucerne, Switzerland • data preparation with the software SAS • evaluate data • writing reports

Skills

Languages:	German	native speaker
	English	fluent
	French	basic
IT:	Matlab	very good knowledge
	MS Office	very good knowledge
	R	good knowledge
	Java	basic knowledge
	Python	basic knowledge

Publications

Thomas Fürst, Puangrat Yongvanit, Narong Khuntikeo, Zhao-Rong Lun, Juanita A. Haagsma, Paul R. Torgerson, Peter Odermatt, Christine Bürli, Nakul Chitnis and Paiboon Sithithaworn (2019): **Foodborne trematodiases in East Asia: Epidemiology and burden**. In Jürg Utzinger, Peiling Yap, Peter Steinmann, and Martin Bratschi editors, *Neglected Tropical Diseases - East Asia,* Springer.

Christine Bürli, Helmut Harbrecht, Peter Odermatt, Somphou Sayasone, Nakul Chitnis (2018): **Analysis of interventions against the liver fluke, *Opisthorchis viverrini.*** *Mathematical Biosciences*

Christine Bürli, Helmut Harbrecht, Peter Odermatt, Somphou Sayasone, Nakul Chitnis (2018): **Mathematical analysis of the transmission dynamics of the liver fluke, *Opisthorchis viverrini***. *Journal of Theoretical Biology*

Presentations

7/2018	"Population-based and individual-based modelling of *Opisthorchis viverrini*". Presented at the European Conference on Mathematical and Theoretical Biology in Lisbon, Portugal.
10/2017	„Mathematical modelling of the transmission dynamics of *Opisthorchis viverrini*". Presented at the European Conference of Tropical Medicine and International Health in Antwerp.
3/2017	"Mathematical modelling of the transmission dynamics of *Opisthorchis viverrini*". Presented at the Neglected Tropical Diseases Asia 2017 meeting in Khon Kaen, Thailand

Voluntary activites

2013 - 2019 **Scout Movement Uri**

President of the association (Kantonsleiterin der Pfadi Uri)

- Managing the local umbrella organization of the scout movement
- Responsibility for the finances, annual plan and the recruitment
- Organization and management of meetings
- Attendance of meetings with umbrella organization and representation of our canton

2009 – 2016 **Scout Movement Central Switzerland**

Co-leader of different scout movement training courses (Jugend- und Sportausbildungskurse in Lagersport/Trekking)

- Organization and planning of courses
- Training and support of younger leaders
- Teaching lessons for participants